2022

VOLUNTARY CONTROL OF BREATHING ACCORDING TO THE BREATHING PATTERN DURING LISTENING TO MUSIC AND NON-CONTACT MEASUREMENT OF HEART RATE AND RESPIRATION

Dibyajyoti Biswal
University of Kentucky, dibya.eee@gmail.com
Author ORCID Identifier:
https://orcid.org/0000-0002-8351-1660
Digital Object Identifier: https://doi.org/10.13023/etd.2022.286

STUDENT AGREEMENT:

I represent that my thesis or dissertation and abstract are my original work. Proper attribution has been given to all outside sources. I understand that I am solely responsible for obtaining any needed copyright permissions. I have obtained needed written permission statement(s) from the owner(s) of each third-party copyrighted matter to be included in my work, allowing electronic distribution (if such use is not permitted by the fair use doctrine) which will be submitted to UKnowledge as Additional File.

I hereby grant to The University of Kentucky and its agents the irrevocable, non-exclusive, and royalty-free license to archive and make accessible my work in whole or in part in all forms of media, now or hereafter known. I agree that the document mentioned above may be made available immediately for worldwide access unless an embargo applies.

I retain all other ownership rights to the copyright of my work. I also retain the right to use in future works (such as articles or books) all or part of my work. I understand that I am free to register the copyright to my work.

REVIEW, APPROVAL AND ACCEPTANCE

The document mentioned above has been reviewed and accepted by the student's advisor, on behalf of the advisory committee, and by the Director of Graduate Studies (DGS), on behalf of the program; we verify that this is the final, approved version of the student's thesis including all changes required by the advisory committee. The undersigned agree to abide by the statements above.

Dibyajyoti Biswal, Student

Dr. Abhijit Patwardhan, Major Professor

Dr. Sridhar Sunderam, Director of Graduate Studies

VOLUNTARY CONTROL OF BREATHING ACCORDING TO THE BREATHING PATTERN DURING LISTENING TO MUSIC AND NON-CONTACT MEASUREMENT OF HEART RATE AND RESPIRATION

DISSERTATION

A dissertation submitted in partial fulfillment of the
requirements for the degree of Doctor of Philosophy in the
College of Engineering
at the University of Kentucky

By

Dibyajyoti Biswal

Lexington, Kentucky

Director: Dr. Abhijit Patwardhan, Professor of Biomedical Engineering

Lexington, Kentucky

2022

https://orcid.org/**0000-0002-8351-1660**

ABSTRACT OF DISSERTATION

VOLUNTARY CONTROL OF BREATHING ACCORDING TO THE BREATHING PATTERN DURING LISTENING TO MUSIC AND NON-CONTACT MEASUREMENT OF HEART RATE AND RESPIRATION

We investigated if listening to songs changes breathing pattern which changes autonomic responses such as heart rate (HR) and heart rate variability (HRV) or change in breathing pattern is a byproduct of listening to songs or change in breathing pattern as well as listening to songs causes changes in autonomic responses. Seven subjects (4 males and 3 females) participated in a pilot study where they listened to two types of songs and used a custom developed biofeedback program to control their breathing pattern to match the one recorded during listening to the songs.

Coherencies between EEG, breathing pattern and RR intervals (RRI) were calculated to study the interaction with neural responses. Trends in HRV varied only during listening to songs, suggesting that autonomic response was affected by listening to songs irrespective of control of breathing. Effective coherence during songs while spontaneously breathing was more than during silence and during control of breathing. These results, although preliminary, suggest that listening to songs as well as change in breathing patterns changes the autonomic response but the effect of listening to songs may surpass the effect of changes in breathing.

We explored feasibility of using non-contact measurements of HR and breathing rate (BR) by using recently developed Facemesh and other methods for tracking regions of interests from videos of faces of subjects. Performance was better for BR than HR, and over currently used methods. However, refinement of the approach would be needed to get the precision required for detecting subtle changes.

KEYWORDS: Non-contact measurement, autonomic responses, Control of breathing, EEG, audio, songs

Dibyajyoti Biswal

(Name of Student)

04/18/2022

Date

VOLUNTARY CONTROL OF BREATHING ACCORDING TO THE BREATHING PATTERN DURING LISTENING TO MUSIC AND NON-CONTACT MEASUREMENT OF HEART RATE AND RESPIRATION

By
Dibyajyoti Biswal

Dr. Abhijit Patwardhan
Director of Dissertation

Dr. Sridhar Sunderam
Director of Graduate Studies

04/18/2022
Date

DEDICATION

This work is dedicated to my parents for believing in me and paving my path of growth since my childhood, Kuna for guiding me every step of the way and being a pillar of support in my career, Dada and my sisters-in-laws for their support to my parents during my absence in India, my partner Gabriel for being the source of support and my friends for fueling me with motivation and joyful times.

ACKNOWLEDGMENTS

The following dissertation, while an individual work, benefited from the insights and direction of several people. First, my Dissertation Chair, Dr Abhijit Patwardhan, for providing timely and instructive comments and evaluation at every stage of the dissertation process, allowing me to complete this project on schedule. Next, I wish to thank the complete Dissertation Committee, faculties and lab members, respectively: Dr Guoquiang Yu, Dr Sridhar Sunderam, Dr Himanshu Thapliyal, late Dr. David Randall, Joyce Evans, Dr MohammadJavad Mollakazemi, Brooke Place and Sridevi Thiagarajan. Each individual provided insights that guided and challenged my thinking, substantially improving the finished product].

In addition to the technical and instrumental assistance above, I received equally important assistance from family and friends. My husband, Gabriel Bode-Jimenez, provided on-going support throughout the dissertation process, as well as technical assistance critical for completing the project in a timely manner.

TABLE OF CONTENTS

TABLE OF FIGURES

TABLE OF TABLES

CHAPTER 1: INTRODUCTION

Songs are known to have palliative effects. It is known that listening to songs affect autonomic parameters such as HRV and breathing pattern. Studies have also shown that change in breathing pattern also affects HRV[1], [2]. Because of this reason, it is not yet clear in terms of the cause of the changes in autonomic parameters during listening to songs. Figure 1-1 (a) shows a schematic of the possible role of breathing pattern in mechanisms of autonomic responses while to listening to songs. To further investigate the role of breathing pattern in the autonomic responses observed while listening to songs, we proposed an experiment involving control of breathing patterns. Because of the possibility that the act of control of breathing patterns might also affect the autonomic responses, the study was designed, as shown in the schematic in Figure 1-1 (b), to investigate the effect of control of breathing pattern in comparison to the effect of listening to songs by sub-dividing each song trials (when subjects listen to songs and/or controlling breathing pattern recorded during listening to songs) into three sub-trials. The sub-trials include listening to songs while breathing spontaneously while the breathing pattern was recorded using the program, followed by not listening to songs and controlling breathing pattern to the recorded breathing pattern, followed by listening to songs while controlling the breathing pattern. The expectation was that the inter-comparison of the physiological parameters calculated during the mentioned trials would help in exploring answers to the questions related to whether control of breathing pattern influence on autonomic responses is less than the influence due to listening to songs. We hypothesized that such experiment would be helpful in minimizing the confound of changes in the breathing pattern that also occur while listening to music [1], [3]. Towards this goal, we implemented a visual-feedback based program using a LabVIEW environment for ease of control of breathing. The implementation and testing of the program were conducted using test cases as described in section 3.4.2. This study was primarily designed to determine whether change of breathing is the cause of change in autonomic parameters (HR and HRV) while listening to songs or it is a co-symptom or change of breathing along with listening to songs causes changes in autonomic parameters. We also explored any possible changes in neurological responses, as seen in EEGs, during listening to songs and when control of breathing was used to make

breathing pattern to match that observed during listening to songs. The similarity between changes in EEG and breathing pattern or RR interval (RRI) was calculated to study the

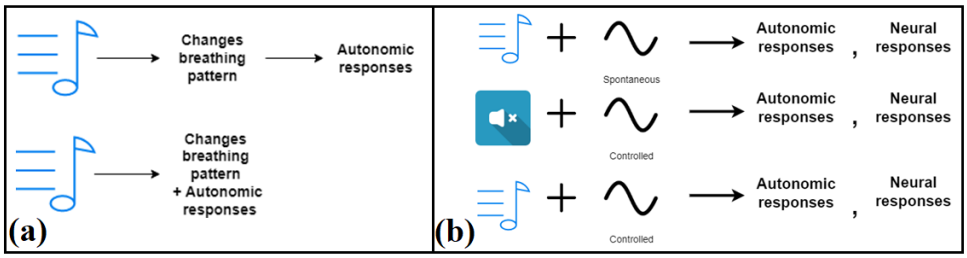

Figure 1-1: Schematic representation of the possible role of breathing in autonomic responses while listening to songs (a) and the study design using control of breathing pattern (b)

interaction of breathing patterns and HR variation with neural responses.

Due to known effect of listening to songs on autonomic responses, in many hospitals and rehabilitation places music therapy is used. However, there is no standardized therapy based on songs. The reason could be that the mechanism of the effect on cardiovascular and neurological health is unknown. To explore the mechanism, we proposed using control of breathing to isolate the effect of listening to song on autonomic and neural responses while the breathing pattern is same throughout the song trials. The act of control of breathing may also have effect on autonomic and neural responses. Hence study was designed in order to isolate the effect of listening to song from that due to changes in breathing pattern.

The non-contact measurement approach was tested during listening to songs and control of breathing experiments to study the performance of non-contact measurement in the environment where stimuli are not expected to cause moderate to large changes in autonomic responses like what happens during other stimuli such as physical activities[4]–[6].

Various stimuli such as audio, video, smell, taste and touch have measurable effects on HR, HRV, BR and breathing rate variability (BRV) like vital measurements [7]–[12]. The research including the aforementioned stimuli includes calculation of HR, HRV, breathing rate and breathing pattern variability. There are certain stimuli that cause significant variation in HR, HRV, BR and BRV and others cause comparatively smaller variation in these physiological parameters. For example, where active singing could

change the physiological parameters significantly, the effect of listening to songs on autonomic and neural responses is not as drastic as prior. Most studies involving human subjects and calculation of HR, HRV, BR and BRV use contact or tethered devices for data acquisition. Contact measurement systems are not portable because of their weight and might need continuous external power source. Use of contact measurement may limit the mobility of the subjects due to the length of the wires and aforementioned physical restrictions. Connected multiple equipment to the body through wires could also make the subject conscious of the environment which in turn may affect the study of the effects of stimuli causing minute changes in physiological parameters or where the effects can be complex. For example, during our prior studies, subjects were sitting on a chair for around 1-2 hours. Because they were connected to the contact measurement devices if they wanted to take a break, then we had to disconnect the wires for the devices and connect them all back again when they are ready. Then as the positioning of the contact measurement devices could be changed, we had to repeat the calibration to get accurate results which could increase the time of study and repetition of events might affect the data. Even though the subjects did not feel any discomfort, this process added more time to the experiment, made the protocol less automated and had possibility to make the subject more conscious of the study environment. Due to above reasons we wanted to test the possibility of using non-contact measurement; which is widely investigated in a variety of settings due to the above stated potential advantages. For these reasons, a method to develop a non-contact measurement of heart rate (HR) and breathing rate (BR) is proposed. In the developed system the areas of framework of non-contact measurement where improvement could be done to increase the accuracy were identified which include region of interest (ROI) detection and tracking, useful color channel derived from the RGB frame of the collected frames and filtering on the extracted color channel. ROI detection and tracking as well as color channels were studied in detail followed by calculation of HR and BR. In the proposed system to find the best method in terms of efficiency and accuracy, two widely used ROI detection and tracking methods (Kanade-Lucas-Tomasi (KLT) and 68-point facial landmark system) were compared against newly developed Facemesh technique which is a 3D facial landmark system based on deep learning concept developed by MediaPipe of Google Research which was developed for implementation of AR

(augmented reality) media features [13]. Furthermore, two-step ROI selection, detection and tracking were used for a comparison between the aforementioned three methods and for accurate non-contact measurement. There has been an interest among researchers to find the best color channel and face location to use for accurate non-contact measurement. For this reason, the comparison between more widely used signals which are proven to be the effective channel to use for non-contact measurement (raw green channel, average of RGB individual frames and plane orthogonal skin (POS)) were conducted. Most of the studies have suggested that cheeks and forehead are the viable regions for implementing non-contact measurement. We did a granular level comparison between the skin of the cheeks (left and right), forehead and whole face to find the best location to consider in our case. While exploring ways to find best location to extract HR and BR, we also attempted to study the viability of lips region which contains glabrous skin which is different from any other region on the face in comparison to cheeks in terms of HR and BR calculation using 68-point landmark technique. Different types of filters were evaluated to denoise and preprocess the signals followed by calculation of HR and BR. The purpose of finding the robust workflow was done to assist any future development in this area. After successful completion of the designed workflow using the most robust (in our case) signal processing algorithm, we called the HR and BR as non-contact HR and BR which was compared to the contact HR and BR. Statistical comparison between non-contact HR and BR against contact HR and BR was conducted. The results of comparison for all the subjects among all the trials are shown in 5.1.3.

To summarize this dissertation, it has two specific aims. Those are,

Does change in breathing pattern that is observed while listening to songs by itself change autonomic response, or listening to songs changes the autonomic response and changes in breathing pattern are a co-symptom, or controlling the breathing pattern and also listening to songs produces responses that are different than just listening to songs or controlling breathing pattern but not listening to songs? To find the answer to the aforementioned question, a visual feedback based breathing follower program was developed using LabVIEW and tested in order to implement control of breathing to the breathing pattern recorded during listening to songs. During the trials ECG, breathing pattern, EEG (locations: F3, F4, T3, T4, P3, P4, O1, O2) were recorded. From the collected

data the parameters calculated were HRV, HR and BR. From HRV high-frequency power (HF), low-frequency power (LF) and HF/LF power ratio were calculated. Coherence between RRI and breathing pattern, RRI and EEG signals and breathing pattern with EEG signals were calculated to find the interaction between aforementioned signals. EEG signal was used to study the variation in neurological response due to listening to songs and control of breathing patterns. From the calculated parameters the similarity between spontaneous breathing (without intention of control) and control of breathing (controlling the breathing to spontaneous breathing pattern) trials while listening to and not listening to songs was investigated to help us determine whether the autonomic effect seen due to the act of control of breathing is of lesser extent than what is seen during listening to songs. The non-contact measurement system developed was tested in these experiments to determine its performance in a research environment with listening to songs and control of breathing pattern as stimuli.

There are several instances where investigation of the effects of stimuli on physiological responses are expected to be subtle, such as effects of listening to songs on autonomic function. Use of contact measurement in such studies not only limits mobility but connecting equipment via tethers could also make the subject conscious of the environment which in turn may affect the results of studies where the effects of stimuli are expected to produce subtle changes in physiological parameters. Due to above reasons we wanted to test the feasibility of using non-contact measurement of HR and BR in our experimental setting as these measurements are used in a wide range of similar types of studies.

The goal of this aim was to test the performance of non-contact measurement in a research environment during studies including stimuli causing comparatively low magnitude change in autonomic response than physical activities like stimuli.

Towards the goal, a system using RGB camera, image and signal processing approach was implemented that worked with varying skin color, in ambient light and in the presence of some movement of the subjects. A recently developed Facemesh method and other widely used methods were used for tracking regions of interests for HR and breathing rate (BR) extraction using videos of the face of the subject.

CHAPTER 2: BACKGROUND

2.1 Role of breathing in effects of music

There has been considerable interest in the cardiovascular, breathing pattern, and neurophysiological effects of listening to songs, including the brain areas involved, which appear to be similar to those involved in arousal [11], [14]. Responses to songs appear to have a "moving" effect on body and mind,[15]–[17] which suggests individual reactions to songs that are dependent on individual preferences, mood, or emotion. The study[3] by Bernardi et al. showed consistent cardiovascular and breathing responses to songs with different styles (raga/techno/classical) in whom arousal was related to the tempo which was confirmed by the same group in the study [18]. Bernardi et al. has also studied the effect of listening to different rhythms of songs in these studies [18]–[20]. In publication [21] we have shown the effect of listening to fast and slow rhythm songs on HR, BR and baroreflex sensitivity. Our group has studied the interaction between songs and brain in these studies[22]–[24]. The study by Bernardi et al.[3] also suggests that listening to songs helps in prolonging the exercise time by elevating the tolerance of pain by distracting from pain. Bringman et al. [25] have shown the application of relaxing songs before the commencement of surgery as a calming down agent, Koelsch et al. [12] have shown the effect of songs on the cardiovascular system. Trappe [26], [27] has shown that songs has an effect on cardiovascular health and hence songs has gained application in intensive care.

Due to known effect of songs on autonomic responses, in many hospitals as well as rehabilitation places music therapy is being used. However, there is no standardized therapy based on the different properties of the songs. The reason could be that the pathway of the effect of listening to songs is unknown. However, studies showing the effect of properties of songs (tempo, pitch and harmony) on cardiovascular and neurological health have helped to narrow down the areas to consider as possible pathways for how the effects come about[17], [18], [28].

Cardiovascular and neurological health is also affected by change in breathing pattern. Bernardi et al. [20] have shown that yoga which is a form of controlling breathing, has an effect on cardiovascular rhythm. The same group has also published a review of studies that have shown that change in breathing pattern is a powerful modulator of HRV

and baroreflex sensitivity [29]. Manipulation of breathing patterns may provide beneficial effects not only on ventilatory efficiency but also of cardiovascular and breathing control in physiologic and pathologic conditions such as chronic heart failure[29]. The same study has suggested the possibility of application of breathing pattern modification in the modulation of cardiovascular rhythm and opens a new area of future research in the better management of patients with cardiovascular autonomic dysfunction.

The study by Bernardi et al. [3] showed consistent cardiovascular and respiratory responses to songs with different styles (raga/techno/classical) in most subjects, in whom arousal was related to tempo and was associated with faster breathing. The studies by Bernardi et al. have suggested that respiration is a powerful modulator of HRV, and baroreflex sensitivity (BRS). These studies suggest that respiration could be an intermediate link between listening to songs and modulation of cardiovascular rhythm. However, whether this is the case has been not directly tested till now. There have been many studies related to studying effects of songs on cardiovascular system. Those studies include the task such as playing songs, singing, listening to songs or any tone and listening to songs before or after any activity. These studies were designed mainly to study the effect of songs from many directions. However, no study has explored the role and the relation between listening to songs and changes in breathing pattern in producing cardio rhythmic effect.

One of the reasons for lack of studies could be, the complex structure of songs or multiple properties of songs such as pitch, harmonics, tempo and bass causing different sensations and effects. Another reason could be finding the relation between listening to songs and changes in breathing pattern makes the study even more complex. However, the benefit of such study can’t be ignored which is studying the relation between songs and change in breathing pattern in affecting cardiovascular health can open the opportunity to better manage the use of these adjuvant therapies in health of patients with cardiovascular disorders with a simplified treatment. To achieve this long-term goal, studies that are designed to address a subset of a complex problem i.e., to find the relation between listening to songs and change in breathing pattern in producing automatically mediated cardiovascular rhythmic changes are necessary.

The above stated reasons provided the motivation behind the design of the study to investigate the effect of listening to songs and the role of changes in breathing pattern by designing and using a visual feedback based program to control breathing.

As described before studies have shown that listening to songs change autonomic responses, listening to songs also change breathing pattern which also changes autonomic responses which suggests that listening to songs could be triggering the changes in breathing pattern which in turn changes the autonomic responses. One possible way to achieve the goal of investigating whether this later is a mechanism would be to make the breathing pattern during listening to songs and not listening to songs as similar as possible followed by studying the changes in autonomic responses. However, the act of control of breathing itself can have an effect on autonomic response [1]. For this reason, we proposed each song trial consisting of three sub-trials. Among the three sub-trials, the first one was to listen to songs while we record the breathing pattern signal followed by not listening to song while controlling the breathing to the previously recorded breathing pattern followed by listening to songs while controlling the breathing pattern. To the best of our knowledge such investigation where the implementation of control of breathing was used while subjects listened to songs of fast and slow rhythm has never been conducted before. The details of the study design are discussed in section 3.2.

In order to get a more broader and insight into the effects of listening to songs on automatically mediated changes in cardiovascular rhythms and in breathing pattern, changes in electrical signals from the brain are also important to study which may permit analysis of the multifaceted effects. Many studies have shown the effect of listening to songs on EEG signals [16], [23], [28]. In previous studies, conducted in our laboratory we have explored the effects of slow song, fast song and favorite song of the subject on different frequency bands of EEG and observed an overall increase in coherencies among EEGs [22]–[24]. We also investigated the effects of known and unknown songs, and different bands of songs such as soprano, mezzo-soprano and high-frequency bands on different bands of EEGs through use of coherence between EEGs [30]. There are many studies which have suggested effects on brain signals due to tasks such as viewing positive and negative emotion images, listening to songs, singing, solving mathematical problem and other tasks to study the neurological engagement and cognition [8], [9], [31]–[33].

However, to best of our knowledge, no study utilized control of breathing task to investigate the effect of listening to songs and of control of breathing on EEG signals. Therefore, in this study, we have explored the effect of control of breathing on EEG bands and the interaction of respiratory changes and those in heart rate with EEG. The details of the analysis and methods can be found in section 3.3.

2.2 Non-contact measurement

During the last 15-20 years there has been substantial research interest in the field of development and implementation of non-contact measurement for HR and BR. Due to the physical limitation of contact measurement, non-contact measurement has attracted many researchers. Researchers have attempted to understand and improve non-contact measurement by proposing widely used models, workflows and techniques [34], instruments for video acquisition or by implementing non-contact measurement in various experimental conditions. Where there have been so many advancements in this field, the most relevant studies which inspired the infrastructure or framework development for non-contact measurement are described below.

Harford et. al [35] have conducted a systematic review of the current availability and performance of non-contact measurement in measuring physiological parameters such as HR, BR and other vital signs. The review [35] has considered 161 articles out of more than 30,000 articles published in the field of non-contact measurement of vital signs. The authors of the review have included studies comparing video-based HR, BR and other vitals monitoring methods against one or more validated reference/ground truth device(s). The studies related to the non-contact measurement of vital signs have used a common framework as described by the investigator [34]. The generalized workflow of non-contact measurement of HR and BR consists of but not limited to the steps and methods shown in the framework by the investigator [34]. For different experiment environments based on illumination, in-door/outdoor, skin-color of the subjects, specification of camera and properties of the video and resolution requirement of non-contact measurement may change the choice of the combination of methods to be used to design the workflow [34].

The first step for collection of data was to find a suitable video camera. Some of the studies have used specific types of cameras such as infrared camera, long-range camera [36], [37] and multimodal imaging[38]. Some of the studies have used more than one

camera [39]–[41]. Studies[42], [43] have used multiple cameras from the same subtype (e.g. smartphones or webcams) to show utilization of software/algorithm across different platforms [43]–[47]. The use of specific types of cameras such as IR camera and five color cameras like complex and delicate cameras increases the cost of the system than a normal camera. Implementation of five colors and similar camera increases the complexity of image analysis. As our goal was to explore the utility of a simpler image analysis based non-contact measurement system, we used RGB digital camera.

Several studies have used a frame rate of 30 frames per second (fps) or less [48]–[50]. Lower frame rates were used in a larger proportion of BR and SpO2 measurement studies rather than those measuring HR or blood pressure (BP) [50]–[52]. The highest frame rates were used for studies monitoring BP (140 fps) by Sugita et al. [52] and 420 fps by Jeong and Finkelstein [51]. However, there are published studies that have shown acceptable results for estimation for non-contact HR with frame rates of 30 fps [53]–[56]. As our study included extraction of HR and BR using a simpler framework satisfying the frame rate requirements of both HR and BR, the videos were collected at 30 fps.

The most common reference device used by studies depended on the physiological parameter of interest. The most used reference devices were ECG (electrocardiograph) and peripheral PPG (photo-plethysmograph). Where PPG monitoring has the advantage of being able to estimate both HR and BR simultaneously, accuracy might be lower than the HR estimated from ECG and BR estimated from respiratory measurement using commercially available chest strap monitors. For example, Al-Naji et al. [57] have used respiratory belt transducers and Capdevila et al. [58] and Cheatham et al. [59] have used polar belt monitors. Studies using chest strap monitor and non-contact measurement of BR

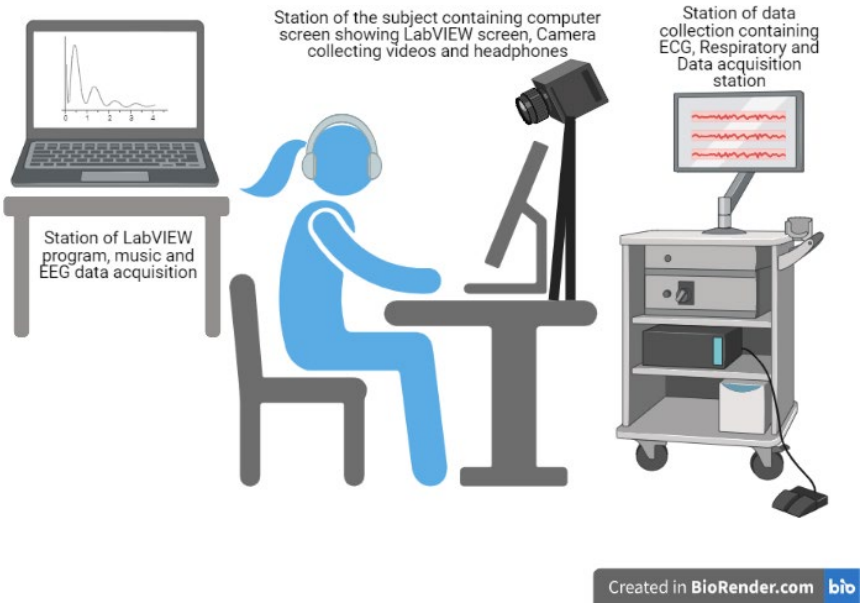

Figure 2-1: Figure showing the experimental set-up (created in Biorender.com)

have shown a good correlation between contact and non-contact measured BR. For our study we used ECG for contact HR and respitrace device with respiratory belts (chest and abdominal) to calculate BR to be used as references for non-contact HR and BR.

While working with images for extraction of vital signs, the distance of measurement can also be a factor affecting the feasibility of the analysis. Studies have focused on near monitoring with the skin-to-camera distance between 0.5 and 2.5 m [55], [56]. Studies have shown satisfactory extraction of HR and BR from distances i.e., between 1 and 2.5 m for

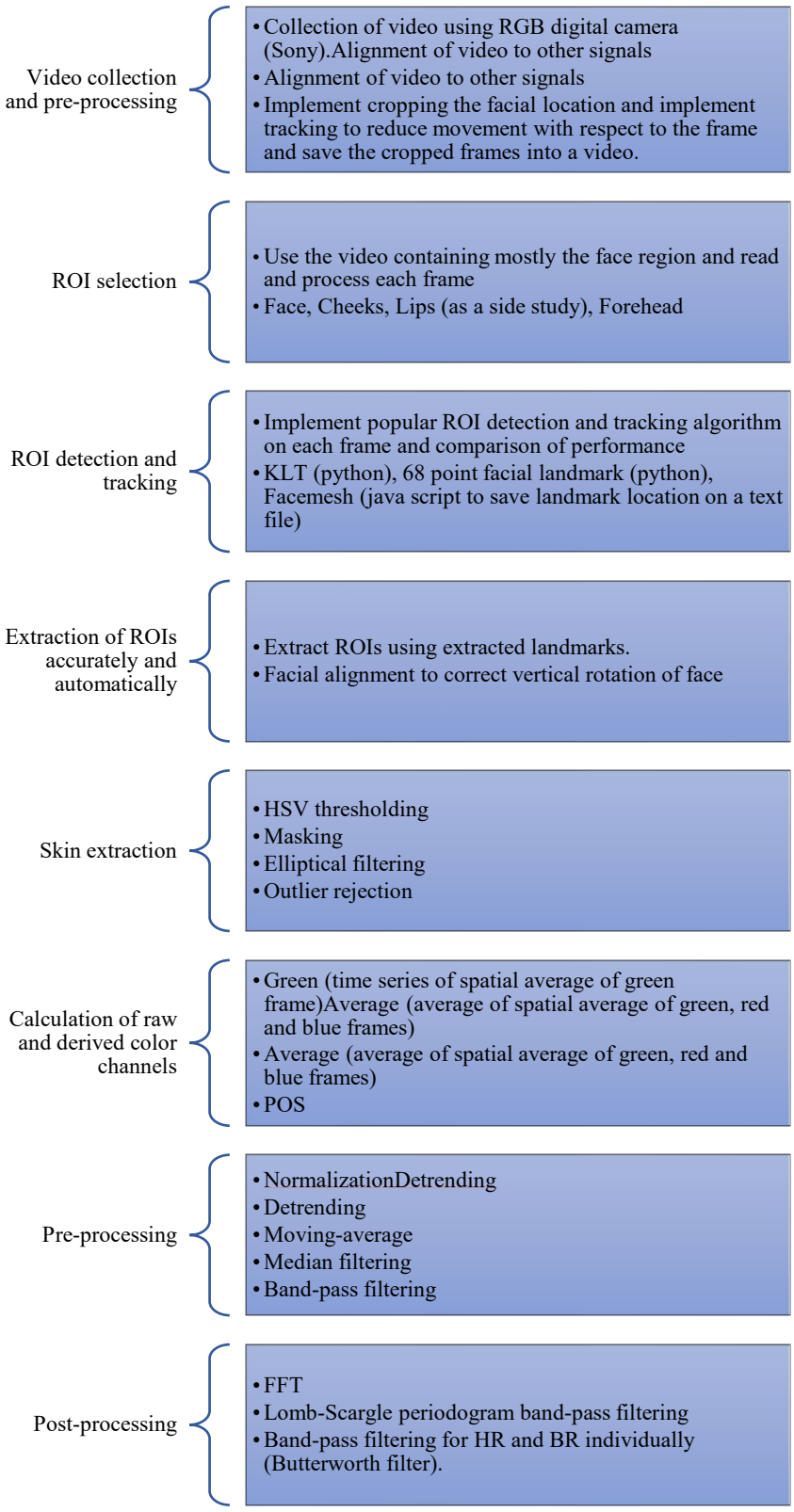

Figure 2-2: Schema listing the methods and techniques explored and implemented for extraction of HR and BR from the video of the faces of the subjects

non-contact measurement algorithms from camera distance above 2.5 m, with the longest distance monitoring being 50 m away from subjects [55], [59]–[64]. In our study the purpose was to study the feasibility of non-contact measurement in an environment where studies such as those exploring effects of music would be conducted. Hence the video camera was situated between 0.75 to 1.5 m from the subject, depending on the subject's sitting location from the video camera and in a manner that would be enough to capture the face of the subject without restricting the natural motion by the subject during trials. As our study included a task that uses a computer monitor, ECG, respiratory and EEG measurements, as shown in Figure 2-1 the video camera was attached on top of the monitor for better organizability in using the space.

As mentioned in a review [66], the two source signals which are widely used for extracting HR and BR from the video of the subjects are photoplethysmography and ballistocardiography. Ballistocardiography is a method for measuring the heart rate by estimating the motion generated by the pumping of blood from the heart at each cardiac cycle. It is one of many methods that rely on the mechanical motion of the cardiovascular systems, such as apex cardiography, kinetocardiograph, phonocardiograph, and seismocardiography [66]. The physiological concept behind this method is that involuntary head movement is caused by blood flow from the heart to the head. At each cardiac cycle, when the heart beats, the left ventricle contracts and ejects blood at a high pressure to the aortic arch. This flow of blood at each cycle passes through the carotid arteries on either side of the neck, generating a force on the head. Therefore, by Newton's 3rd law of force, this force created by the blood flow on the head matches the force of the head acting on the blood flow causing reactionary cyclical head movement. This head movement is too small to be noticed by the naked eye. However, the work presented by Balakrishnan et al. [67], by using video amplification, showed that the head moves periodically to the motion of the heart rate although with a smaller amplitude. Hence this method is highly influenced by the subject's involuntary movements. The ballistocardiography-based approach is advantageous in terms of being least affected by variation in external illumination when the subjects have minimal movement (for example in sleeping position). However, this method is highly dependent on motion due to cyclic blood flow to estimate source signal and highly influenced by natural motion of the subject which is a major drawback of this

method. The most used ballistocardiography extraction methods involve the subject to lay on a plane bed or sitting on a chair with minimal voluntary and involuntary movement [68]. Our goal was to extract HR and BR from the video of the faces of the subjects in normal research conditions. Therefore, our experimental condition would include comparatively more motion due to the expected voluntary and involuntary motion of the subject during the trials. That is why we did not consider ballistocardiography-based method in our analysis.

The concept behind plethysmography relies upon the absorption of light by blood cells. As the movement of blood in blood vessels follows a rhythmic motion, the light absorption depends on the amount of blood flowing through the blood vessels[34]. In photo-plethysmograph varying amounts of light reflected is caught on the photodetector, which produces the signal called photo-plethysmograph (PPG), which contains information about HR and BR. It is thought that incident light gets absorbed by blood cells in blood vessels and also gets reflected through different layers of the skin producing the signal [66]. However, some investigators suggest that the pulsating PPG signal is produced due to the reflection of scattered light from cell layers and blood capillaries [69]. Even though for our purpose, the photoplethysmography source signal is better than ballistocardiography, it is important to note that PPG extraction from video is influenced by external illumination variation and skin color-like factors. That's why it was necessary to build an analysis workflow least affected by the factors affecting the performance of photoplethysmography such as skin color and external illumination variation.

In many studies the light conditions were controlled by adding incident light or using different wavelength cameras such as near infra-red (NIR) [50], [70]–[72]. As our goal was to study the feasibility of non-contact measurement of HR and BR in an environment such as that where studies which investigate effects of music are conducted the light conditions were not changed from the ambient light in the laboratory. Hence in our study RGB camera under ambient lighting was used.

Concept behind the PPG relies on light reflection by blood cells. Different location on face may absorb and reflect light differently. Hence, it was important to explore face locations to find the best possible location for calculation of HR and BR. Different regions of skin including face, neck, upper limb and thorax have been used for clinical monitoring.

Most studies focused on information from skin of the face and neck. HR monitoring was achievable using distance PPG from the face and neck, limbs, and chest. BR studies using visible spectrum cameras used oscillatory chest wall movement [63], [73]–[84]. The BR studies using infrared spectrum cameras also utilized temperature variation in the nasal area[38], [61], [76], [83]–[97]. Poh et al. [55], initially proposed modification on the selection of ROI from a selection of full-face to an ROI of 60% of the width of the full face and full height. Lewandowska et al. [98], and Scalise et al. [99], proposed to select the ROI on the forehead region of the face (i.e. 40% width and 30% height of the full face). Aarts et al. [100], in a pilot study, to monitor the heart rate of infants, used an ROI on the cheek region of the infant's face. Mestha et al. [101] and Lam et al. [102], [103] conducted studies in which the authors used facial landmark fitting algorithm [104] to extract the ROI. The later author used random patches from the landmarks in the facial region. Yong-Poh et al. [55], used an ROI below the eye line with a fixed percentage of height and width, that cover the skin region within the nose and cheeks. McDuff et al. [105], proposed an ROI selection similar to [106] where the eye region was excluded using facial landmarks. Feng et al. [107], proposed a trapezoidal ROI with 50% and 40% width, and 58% height, that covers facial skin region within the low forehead, cheeks, and upper lips. The ROI selection by Poh et al. was modified to exclude non-facial regions that would affect the strength of the PPG signal [55]. The selection of ROI within the facial parts of the cheek, lips and chin, were based on physiological information of the human anatomy based on microvascular tissue bed [34]. These skin regions shown in the article comprise a higher proportion of capillaries that would generate greater signal strength due to the higher absorption of light compared to others in regions of the face [34]. However, researchers have selected the forehead region that consists of a lesser proportion of capillaries underneath the skin. This is because the forehead is less prone to muscle movements compared to other areas of the face [34]. Muscle movements within the face would constitute to weaken the PPG signal strength by adding noise in the form of motion artifacts. As stated in the literature, the eye region was excluded from the ROI since the eye does not consist pulsatile component related to blood volume change and also, blinking of the eye would result in motion artifacts that would weaken the PPG signal [34]. Extracting PPG signal from multiple ROI has been shown to improve the overall signal strength using comparative [92], [108] and

stochastic approaches [103]. As these studies have shown that the good skin source could be face, cheeks and forehead [104]–[106], we considered these locations in our study. The information mentioned above also suggests that in addition to cheeks for measurement of non-contact HR and BR measurement, one could use lips as well. Because, the facial artery, which is a branch of the external carotid artery, perfuses the lips, supporting the use of lips for this purpose. Further, the innervation of the glabrous skin (thin and smooth skin) of the lips is different than that for other regions of the face, because of which there may be some advantages in making these measurements from the lips as well. Apart from this fact many blood capillaries also lie underneath the skin of lips which suggests that it could be a physiologically viable region for extraction of HR and BR. Hence to investigate the viability of lips in finding non-contact HR and BR we conducted a comparison between lips and cheeks during the pilot study [109].

Different studies have shown that non-contact measurement is feasible for different lengths of trials. In our study, as the goal was to test the feasibility of non-contact measurement in a study environment which includes listening to music, therefore the time of recording was kept the same as contact measurement duration which was 3 minutes for each trial (except one subject for 2 minutes).

Several authors stated that the ease of vital signs detection from skin using visible spectrum cameras can vary depending on the skin color (Haan and Jeanne [110], Wang et al. [111]). As our goal was to build and test non-contact measurement model feasible for human studies, it was important to come up with experiment conditions and data analysis techniques fit for a range of different skin color. Individuals who participated in our study had skin tones that ranged from light to dark brown. The study from collecting data to extracting HR and BR was optimized for the skin colors mentioned before.

As described before, the tethered devices could make the subjects conscious of their environment. Hence using non-contact measurement could prove to be advantageous. In studies that use stimuli such as listening to songs, the expected changes in HR and BR are minimal than that observed during physical stimuli such as exercise. Therefore, a non-contact measurement approach has the potential to be valuable in these studies as awareness of tethered devices may potentially obscure some of the subtle effects of such stimuli. In this study we assessed the feasibility of non-contact measurement of HR and

BR by comparing the non-contact measurement against contact measurement during different trials.

As described before, the concept behind plethysmography relies upon the absorption of light by blood cells. As the movement of blood in blood vessels follows a rhythmic motion, the light absorption depends on the amount of blood flowing through the blood vessels. In a photo-plethysmograph, varying amounts of light reflected is caught on the photodetector, which produces PPG, which contains information about HR and BR. It is described before that incident light gets absorbed by blood cells in blood vessels and also gets reflected through different layers of the skin (stratum corneum, epidermis, and dermis) producing the signal [66]. There are studies regarding non-contact measurement in different test cases involving stimuli such as exercise and stress [56], [112]–[120]. Different type of stimulus causes the different magnitude of changes in HR and BR. For example, high-intensity exercises can elevate the HR to 140-160 BPM which is approximately double of resting HR for subjects of age 18-35. Similarly, BR also increases by approximately 9-12 bpm than resting BR for subjects of age 18-35. Even though studies have shown that activities like listening to songs influences HR and BR the magnitude of the change is not as high as that during the high intensity activities. The challenges in detecting HR and BR, especially in setting of modest to small expected changes could be different skin color, minute changes in HR and BR, and ambient lighting conditions. Skin color is an important factor to focus on as the difficulty in extracting the information based on variation in blood flow volume is influenced by skin color. This means that the detection of change in skin color would be easier for lighter skin tone and more difficult in case of darker skin tone.

The above stated reasons were the factors that motivated the design of a workflow starting from choosing facial location and tracking to HR and BR calculation by addressing the following three challenges.

1. Reduce motion artifact to get a reliable source signal containing blood flow information.
2. Minimize effect due to external illumination variation and various skin color affecting various HR and BR extraction methods.

The built workflow which would address aforementioned challenges is explained in detail in section 5.1.

It was recognized that the tasks causing minute changes in HR and BR could make it difficult to implement non-contact measurement. However, testing the non-contact measurement system during such tasks was necessary for advancement of the non-contact measurement.

There are studies which have been designed to test the feasibility of non-contact measurement in a clinical environment, subjects of different ages, animal subjects and during tasks causing relatively larger changes in HR and BR [94], [97], [121]–[123]. However, very few studies have been conducted to test the feasibility of non-contact measurement in a research setting designed for a study focusing on responses while listening to songs and controlling the breathing pattern. Control of breathing is designed in a way that if a subject does a good job of following the recorded breathing pattern, the BR of controlled breathing trial would be same as the recorded breathing pattern that was followed.

PPG signals extracted from facial features are affected by motion artifacts caused by rigid and non-rigid movement of the face and body. Motion artifacts resulting from the rigid movement are due to the change of head orientation or by a change in posture of the body. Motion artifacts caused by the non-rigid movement are due to movements of the face, often caused by expressing facial emotions such as: smiling, yawning and talking. Rigid and non-rigid movement of the face and body creates a change in the illumination on the skin, which results in fluctuation of color intensity values in the region of interest (ROI). Therefore, these movements, generate motion artifacts in PPG signal. This artifact causes the signal to drift from the baseline and attenuate the information present in the signal. The majority of the research has focused on contributing to eliminating the effect caused by motion artifacts. Researchers have treated the issue of motion artifact removal as a blind source separation problem. Initially, Poh et al. [55], [106], applied independent component analysis to separate the source signal from the raw signals which were contaminated by motion artifacts. Lewandowska et al. [98], also treated the motion artifacts removal as a blind source separation problem and applied principal component analysis (PCA) to extract the PPG signal. Following this direction, many investigators have

proposed methods using independent component analysis (ICA) [56], [124]–[128], PCA [99], fast ICA [40], [100] and robust ICA [129]. Each of the methods mentioned above used either ICA or PCA to extract the source signal from the raw signals. Monkaresi et al. [130] proposed to improve the motion artifact removal method involving ICA and machine learning approach to extract the HR. Here the idea was to automate the component selection processes by selecting the best corresponding heart rate. Li et al. [92], proposed a two-step approach to nullify the effect caused by the motion artifacts. The authors employed the KLT (Kanade-Lucas-Tomasi) tracking algorithm to track through the ROI within consecutive frames to minimize the loss of ROI, which causes loss of samples in the signal. Further, the motion artifacts were eliminated by separating the PPG signal into segments and eliminating the segments with the highest standard deviation/fluctuation. Lam et al. [103], proposed an approach using facial landmarks. Seventeen facial landmarks that were less prone to non-rigid motion variance were selected. The authors used 41 × 41 pixel patches on each side of the face and extracted PPG signal and decomposed it using ICA. The ICA component was selected using a majority voting scheme to eliminate the motion artifacts and to estimate an accurate heart rate [103]. Feng et al. [107], proposed an adaptive green and red differentiation operation to remove motion artifacts of the PPG signal. The adaptive green and red differentiation operated based on raw traces that were extracted from the ROI. The difference between the green and the red signals was extracted because the green signal contains information related to the variation in blood volume in the capillaries. Whereas, the red signal contains information related to muscle movements in the face [34], [131]. Wang et al. [111] proposed a motion robust PPG estimation module, by compensating the rigid and non-rigid movement of the ROI. In general, investigators have proposed to overcome the motion artifact problem caused by motion variance as a blind source separation (BSS) problem solving or an adaptive filtering/pruning approach. BSS based motion artifact compensation approach raise the issue of component selection and autonomous heart rate estimation, whereas, the filtering/pruning approaches raise the issue of over compensation/under compensation. The recent direction of motion artifact compensation has evolved in the direction of adaptive matrix computation approach and BSS approach [55], [127], [132]. Most of the studies which have attempted developing ways to mitigate motion artifact, have conducted the studies focusing on working of the

algorithm or the non-contact measurement. However, these types of motion artifact correction methods can't be standardized across different types of application or experimental condition as is. Rather the methods would need modification in research design to fit the non-contact measurement to the actual human study. Our goal was to test the non-contact measurement of HR and BR in research environment where video camera would only be an addition. We implemented a process that included cropping the facial location and tracking of the cropped region to reduce account for movement with respect to the rest of the frame and saving the cropped frames into a video to be used in next step. This step would also reduce the influence of background which was occupying more than 50% of the frame in most of the frames. This method makes sure that the facial location is fully within the frame. Details about this process can be found in section 5.1.

To select the ROI automatically it was necessary to find the best technique to detect and track the ROI. For ROI detection, Paul Viola and Michael Jones [133] developed algorithm known as Viola Jones algorithm can be considered to be the base for multiple object detection algorithms that are in use today. This algorithm is based on Haar-like feature selection, AdaBoost training and cascade classification. The process of tracking the ROI over different frames of video, is referred to as image registration or object tracking. For object tracking, Kanade, Lucas and Tomasi [134], [135] have designed an algorithm which is widely used for tracking detected ROI or objects [134]–[136]. As discussed before, for the task of ROI detection and tracking, KLT is most widely used among other techniques. We initially implemented the KLT tracking in MATLAB which was found to be time-consuming and not as accurate for our proposed approach. The reason being that in our study the intent was to design a robust and scalable workflow that would be less dependent on the type of image, background of the subject, skin-color and illumination. Hence, we explored other possible techniques for tracking. Through review of approaches reported in the literature it was determined that facial landmark models could also be used in development of non-contact measurement. The locations of the fiducial facial landmark points around facial components and facial contour help to capture the rigid and non-rigid facial deformations due to head movements and facial expressions [137]. These fiducial landmarks are hence important for various facial analysis tasks. The facial landmark detection algorithms can be classified into three major categories: holistic methods,

Constrained Local Model (CLM) methods, and regression-based methods [137]–[139]. They differ in the ways to utilize facial appearance and shape information. The holistic methods explicitly build models to represent the global facial appearance and shape information. The CLMs explicitly leverage the global shape model but build the local appearance models. The regression-based methods implicitly capture facial shape and appearance information. Regression-based methods include direct regression, cascaded regression and deep learning-based methods.

The background of the widely used models were studied in detail. The Annotated Facial Landmark in the Wild (AFLW) database contains about 25K images [140]. The annotations include up to 21 landmarks based on their visibility. The Labeled face parts in the wild (LFPW) database contains 1,432 facial images [141]. 29 landmark annotations are provided by the original database. Re-annotations of 68 facial landmarks for 1,132 training images and 300 testing images are provided by Sagonas et al. [142]. The Helen database contains 2,330 high-resolution images with dense 194 facial landmark annotations. Re-annotations of 68 landmarks are also provided by [142]. The annotated Faces in the Wild (AFW) database contains about 205 images with relatively larger pose variations than the other "in-the-wild" databases. 6 facial landmark annotations are provided by the database, and re-annotations of 68 landmarks are provided by [142]. The ibug dataset from 300 faces in the Wild (300-W) database [142]–[144] is the most challenging database so far with significant variations. It only contains 114 faces of 135 images with annotations of 68 landmarks [142]. Using deep learning on various image datasets, 2D facial landmark model was developed by A. Bulat et al., C Zafairious et al. and A. Zadeh et al. which is called 68-point facial landmark model which is shown to be performing acceptably in many studies including non-contact measurement of HR and BR [55], [103], [145]–[147]. Hence, while finding the best method for ROI detection 68-points facial landmark model was identified as a promising method to consider based on the algorithm and previously reported evidence of feasibility. However, 2D model performs badly during vertical motion and sometimes during horizontal motion [148], [149]. The horizontal motion could be corrected by implementing alignment of the face based on the connecting point between two eyes after detection of centroids of the eyes which was implemented in our study for 2D facial landmarks. The vertical motion can't be corrected by alignment. In some cases, alignment

may also fail to correct the horizontal motion due to fitting the detected points over a broader range of pixels. In this case resizing of the image and two-step ROI selection and tracking were found to address the motion artifact. As the facial landmark detects 68-points instead of the corner points of the detected ROI as in Viola and Jones with KLT, the facial landmark detection could be used with or without geometric tracking such as Kalman filtering and KLT tracking [133]. In case of facial landmarks, the landmarks are detected on each image [142], [150]. The detection of a series of images as in the case of video can also be implemented in a similar fashion.

As described before in case of 2D facial landmarks detection, the difficulty in handling the motion around horizontal axis could be handled through implementation of 3D facial landmark model in tracking the ROI and thus in detecting HR and BR. A comprehensive review of studies related to the developed 2D and 3D facial landmark models is available in [148]. As noted by several studies, building 3D facial landmark model from 2D image dataset is an ill-posed problem [148], [149]. Hence implementing 3D models could be tricky. However, the potential utility of 3D facial landmark model in the non-contact measurement of HR and BR may surpass the difficulty which motivated the implementation of 3D facial landmark model and to compare the performance with 2D facial landmark and widely used viola-jones ROI detection and KLT tracking in our study.

Several studies have attempted the development of 3D facial landmark model from 2D image datasets [151]–[153]. Recently a deep learning 3D facial landmark model named "Facemesh facial landmark" was developed by google research (Yury Kartinnik et.al) [154] mainly for the purpose of augmented reality applications i.e., building applications such as image and video filters on Instagram, Snapchat, and Facebook messenger. Even though the developed model contains a detection of 468 points which could make the method memory intensive, the scalability and customizability of this model make the model unique and applicable for our purpose. The Facemesh model is trained on 30,000 images and evaluated on a set of 1,700 images which suggests that it was trained on enough cases by the google research team [154]. In our study, due to the presence of a smaller number of samples in our case and to leverage the model which is trained on a much bigger dataset, we did not focus on training a new model. Rather we focused on implementing the developed opensource Facemesh model as is in our workflow. This model was trained on

resized images of 256x256 pixels. In the future work this model can be improved by training it for custom size images for better ROI detection for images of different sizes. In our study we compared the performance between (Viola-Jones and KLT tracking), 68-point which is referred in this document as “68-points” and the “Facemesh” model.

The next step in workflow was cleaning the image followed by extracting raw photoplethysmographic signal from the video. For cleaning of the frames of the video and extracting skin region, we used HSV (hue, saturation and value) thresholding as studies have suggested use of HSV thresholding in face detection process is responsible for reducing the effect due to external illumination [155]–[157]. For extracting raw photoplethysmographic signal it was necessary to choose the best signal and the color frame for easier and accurate calculation of HR and BR. Unakafov et al. have shown a comparison between POS, chrominance based method and raw color signal differences in the studies [34], [131] and have shown that POS performs better than chrominance based method which is the parent signal from which POS was derived. Other studies have shown that raw green signal performs acceptably well [55], [56], [60]. Our selection of signals was influenced by these previous studies. To find the best signal in our case we conducted a selection of among raw green signal, POS and average of the green, blue and red signal extracted from selected ROIs which were face, forehead, left cheek, right cheek and an average of left and right cheek to find the best performing signal. Results of this analysis have been reported in [109]. For signal processing of the signals extracted from the images various studies have used different approaches to extract HR and BR which mostly involve implementation of moving average filter, band pass filter and adaptive filter as described by Unakafov et al. [34].

The final step of the process was to validate non-contact HR and BR against contact HR and BR. Few studies have used only correlation between contact and non-contact measurement while other studies have used correlation followed by Bland and Altmann technique [34], [55], [56], [60], [66]. Where correlation analysis shows the linear match between contact and non-contact measurement, Bland and Altmann's (otherwise known as Bland-Altmann) plot shows the agreement between average of the two measurements and difference between measures and the information on outlier measurements. In our study we used this method to compare the contact and non-contact measurement of HR and BR.

Part of the results from these studies were reported in a conference proceedings publication [109].

The aforementioned non-contact measurement workflow was designed to investigate the feasibility of the non-contact measurement during the research study environment which is described next.

CHAPTER 3: ROLE OF RESPIRATION IN EFFECTS OF MUSIC

3.1 Development of the approach

Research shows that the changes in breathing pattern change HR and HRV [1]. Music is known to have palliative effect [158]. Bernardi et al. [19] have shown that listening to music changes autonomic parameters such as BR, HR, and HRV. In their study [19] they also suggested that the cardiovascular parameters may be changed due to the change in breathing pattern which changes due to the rhythm and speed of the song, however they did not test this potential link. Kroupi et al. [7] have shown that there is a unidirectional relation between frontal EEG and respiration when exposed to some audiovisual stimuli. The main goal of this study was to determine whether the changes in autonomic and EEG responses that are observed while listening to songs are a direct effect of listening to songs or if they are (partially) due to the changes in breathing pattern which occurs when listening to songs. The rationale behind EEG signal analysis with different sub-trials is described in CHAPTER 1. Towards this goal, a visual-feedback based program to control breathing patterns was developed so that subjects could voluntarily control their breathing to match a pattern that was recorded while they were listening to songs. The details of the development of visual-feedback program are described later. Initially, the thought behind the study design was to record the breathing pattern when the subject listened to a song which would be followed by controlling the breathing pattern to that of the recorded one while not listening to songs. However, since the act of voluntary control of breathing itself may affect autonomic responses such as HRV[1], the initial study design was modified by adding one more sub-trial to the initial song sub-trials. During the added sub-trial, the subjects would be listening to the same song while controlling the breathing pattern that was recorded previously when they listened to the same song. Below the study design is described in more detail.

3.2 Study Design

The proposed study's objective was to find whether changes in breathing pattern that occur while listening to songs are responsible for the changes in the physiological parameters (HR and HRV), along with any changes in EEGs or if changes in these are independently caused by listening to songs. It is possible that the changes are caused by

both, in that case the expectation was that the study would provide information about the relative contribution of each pathway. Each trial consisted of three sub-trials. In sub-trial 1 the subject listened to a song during which their breathing patterns (recorded using respitrace bands around the chest and abdomen) were recorded using a commercial data acquisition device. Simultaneously, these two signals were also recorded using a custom program through a USB analog to digital converter (National Instruments). The sum of the two patterns (chest and abdominal) was used as the target breathing. In sub-trial 2 the subject was asked to control the breathing pattern to their own breathing pattern/signal that was recorded when the subject was listening to the song. During this sub-trial, the subjects were not listening to any song. In sub-trial 3 the subject was asked to control their breathing pattern to the breathing pattern recorded during sub-trial 1, while the subject was listening to the same song as in sub-trial 1. To better describe the process, from point forward, the signal recorded when the subject listens to the song while spontaneously breathing would be referred to as the 'target signal,' and the real-time collected and displayed signal during the voluntary control of breathing task would be referred to as the 'controlled signal'. The trial during which target signal was recorded would be referred to as 'spontaneous' and the trial during which the controlled signal would be recorded would be called 'control of breathing'. Figure 3-1 visually represents the sequences of trials and sub-trials followed during the experiment. A custom program was designed which displayed the target signal in one color (white) as scrolling from right to left and in a different color (red) the control signal (which is the breathing pattern of the subject displayed in real-time) scrolling from left to right both on the same screen. As examples screenshots of what was visible to the subject during spontaneous breathing and control of breathing are shown in Figure 3-2 and Figure 3-3 respectively. The subjects were asked to breathe in such a manner that the controlled signal would overlay the target signal. This way if the subject controlled the breathing well, then the breathing pattern during listening to songs and not listening to songs would be nearly the same. Sub-trial 3 would allow investigating the effect of control of breathing on cardiac regulation while listening to songs. The songs were played in random order for different subjects and control of breathing sub-trials of song trials were also randomized for subjects. To make the task further easier for the subjects to follow, before start of control of breathing trials, the subjects were asked to control their breathing

pattern according to the 1-2 minutes of recorded spontaneous breathing pattern as a practice run. This way they were able to follow the task before the actual recording of control of breathing pattern. The control of breathing program development is described in detail in section 3.4.1. During the trials, ECG (Biopac), and breathing pattern (Ambulatory Monitoring; chest and abdominal) were recorded using a commercial data acquisition device (WINDAQ) and EEG was recorded using OpenBCI. During the study two songs were used based on the rhythm in beats per minute. Song1 was fast rhythm song and Song2 was slow rhythm song. The order of the songs was randomized for all the subjects.

3.3 Statistical Analysis and Data Analysis

If the observed responses remained approximately similar when compared between spontaneous breathing (listening to songs) and control of breathing (no song), then it would indicate that change of breathing pattern entrains HR, HRV and changes in EEG. If the responses are significantly different between spontaneous breathing and control of breathing, then that would suggest change of breathing pattern is a separate effect of listening to songs and not the sole driver of the changes in HR, HRV, and in EEG parameters.

3.3.1 Calculation of auto-spectrum of RRI (HRV), sum of breathing pattern, BR and HR

RRI were calculated from ECG from which HRV was computed using Welch's auto

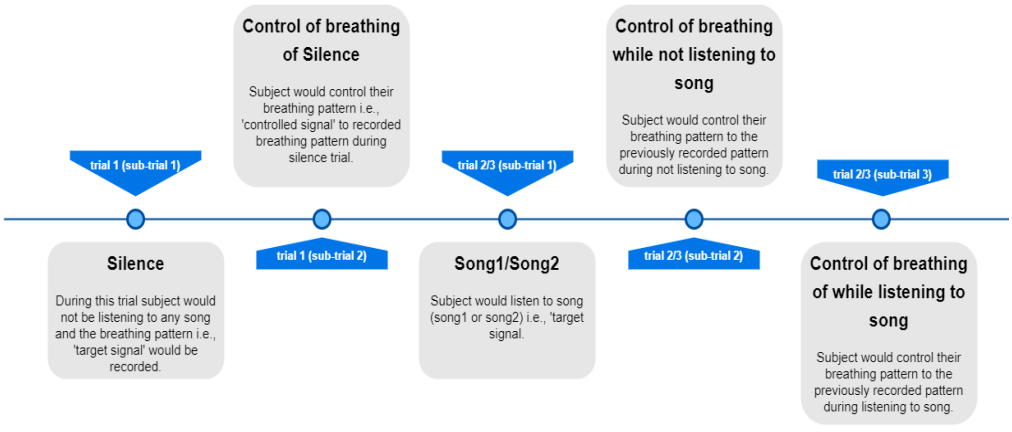

Figure 3-1: Visual representation of trial sequence showing silence trial followed by song trials where song trials were randomized

spectrum. Breathing rate was calculated from auto-spectrum of sum of breathing pattern (sum of chest and abdominal breathing pattern). All the above parameters were calculated

from contact measurement devices. Details about signal processing algorithm used to calculate HR and BR is described in section 5.1.3.1.

3.3.2 Calculation of HF, LF power, and HF/LF power ratio

In order to study the sympathovagal balance, from the RRI spectra, high-frequency (HF) power, low-frequency (LF) power, and HF/LF power ratio were calculated. HF power was calculated by integrating the RRI auto-spectrum in the frequency range of 0.15 to 0.4 Hz and LF power was calculated in the frequency range of 0.03 to 0.15 Hz [159]. The HF/LF power was found by calculating the ratio of HF and LF power [159]. The HF/LF

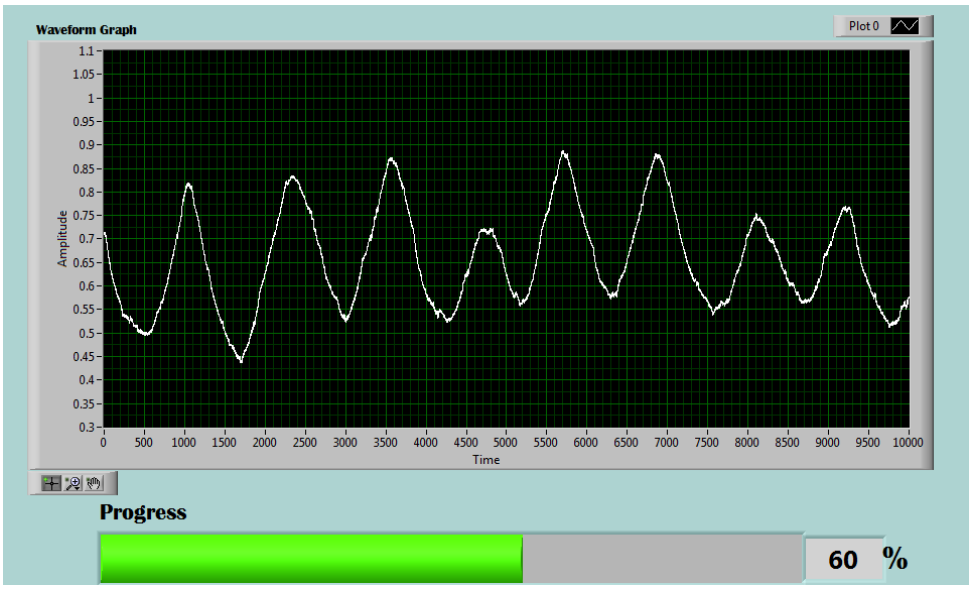

Figure 3-2: Front panel of the program during spontaneous breathing trial while recording target signal (as visible on the screen in front of the subject).

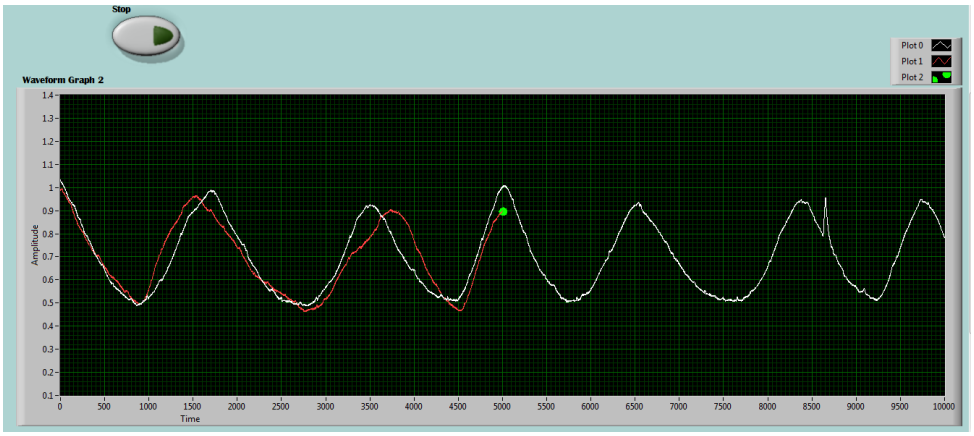

Figure 3-3: Front panel of the control of breathing program during control of breathing trial (as visible on the computer screen in front of the subject).

power ratio reflects the sympathovagal balance only when the respiratory oscillations remain in the HF band[2].

3.3.3 Coherence analysis

To find the interaction between different signals, coherence (mean squared coherence) was calculated. Coherence values range between 0-1 and shows the degree of similarity between two signals, where 0 suggests largely dissimilar signals and 1 suggesting very similar or nearly identical signals. In this study, the coherencies between a pair of signals selected from RRI, the sum of breathing patterns and frequency bands/features extracted from EEG recorded from locations F3, F4, P3, P4, T3, T4, O1 and O2 were calculated. The combinations were among aforementioned signals which were collected during different silence and song trials (song1 and song2) as shown in Figure 3-4.

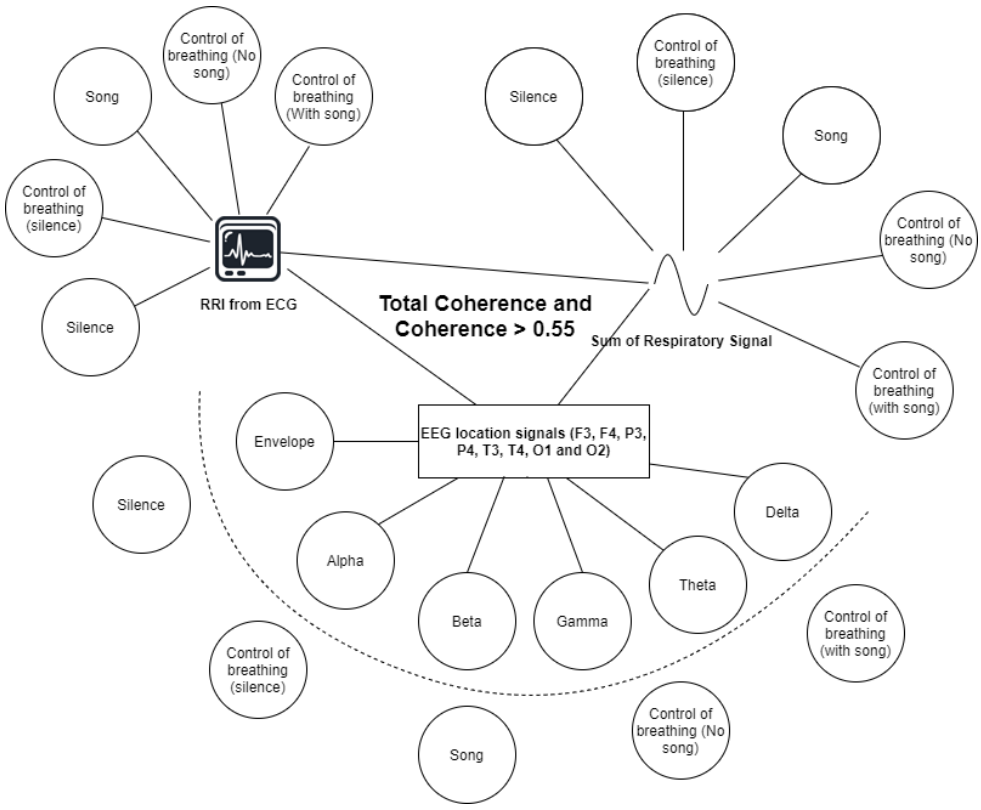

Figure 3-4: Schematic of coherence analysis showing signals and frequency bands calculated from the raw signals collected during different trials considered in multiple combinations to calculate total coherence and effective coherence (coherence above 0.55)

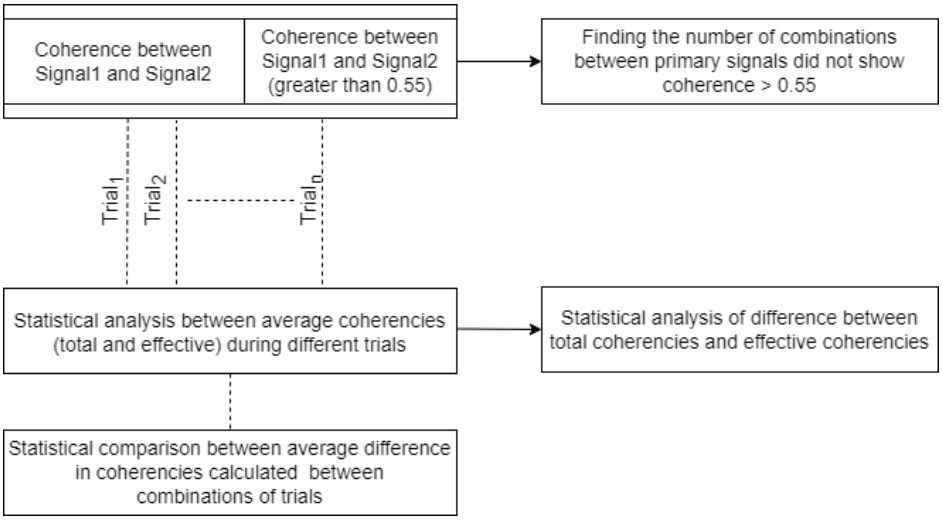

Figure 3-5: The steps of analysis using coherence and statistics to find relationship between signals during different trials.

The framework designed for coherence analysis is illustrated as a schematic in Figure 3-5. The figure shows the steps involved during computation of coherencies and statistical analysis followed in our study. The first step was to calculate coherence between two signals from sum of breathing patterns, RRI and EEG frequency band during each trial. Along with finding total coherence, the effective coherence, which was defined as coherence above 0.55 was calculated. The reason for using the threshold was that we were also interested in the interaction with the degree of similarity more than 50%. This step was followed by statistical analysis between the difference between average of total coherence and average of effective coherence among trials, to find if any trial showed significant difference between total bandwidth of coherence and effective bandwidth against another trial.

We also conducted statistical analysis of differences between average of coherence (total and effective individually) between combination of trials. For example, the average coherence between sum of breathing patterns during listening to song1 and RRI during listening to song1 while controlling breathing pattern against average coherence between sum of breathing patterns during song1 and RRI during control of breathing while not listening to song1. This step was followed by statistical analysis between relationships derived using coherence during combinations of trials. For example, the statistical analysis

between the average difference in coherence between two sets of trial combination with another two sets of trial combination.

While calculating the coherence above 0.55, some combinations showed non-existence of coherence above 0.55 which suggested that those combinations have less than 55% interaction, i.e., suggestive of poor interaction. For the coherence between RRI or sum of breathing patterns with EEG bands, the total number of non-existing coherence combinations showing coherence less than 0.55 were determined. This helped in understanding the strength of the relationship of EEG bands with sum of breathing patterns and RRI.

3.4 Control of breathing

Control of breathing program was designed such that the subjects could control their breathing pattern to the recorded breathing pattern. The development was done in LabVIEW environment and the breathing pattern acquisition was conducted using a USB analog to digital converter (NI USB 6001). Examples of the program's front panels are shown in Figure 3-2 and Figure 3-3, where Figure 3-2 shows an example of front panel visible to the subject while recording target signal and Figure 3-3 shows the front panel visible to the subject while trying to control their breathing pattern to the already recorded target signal.

In the control of breathing program, the already recorded target signal was shown in white while the current, i.e., real-time, signal was shown in red which traversed from left to the middle of the window. The subjects were asked to overlay the red signal on the white signal. To aid in this purpose, the end of the red signal was indicated by a green dot as shown in Figure 3-3.

3.4.1 Development of the program

The process of development of the control of breathing program included ideation, execution, CI (Control interface) and UX (User-experience) planning, designing and troubleshooting. The above steps helped in deciding the series of actions in backend and front-end to achieve the goal of the study i.e., subjects being able to control the breathing pattern effectively and as effortlessly as possible. As described before, to make following control of breathing task easier for the subjects i.e., to be able to overlay the current breathing pattern on the recorded one, a green dot was added at the end of the current

signal. It was felt that, not knowing the duration, i.e., how much time remaining, in real-time could make some subjects feel conscious about time remaining during trial. Hence, as shown in Figure 3-2 on the front panel a bar showed the percentage of completion of trial, in terms of duration was added. As the study involves controlling the breathing trial while listening to songs, hence it was necessary to follow similar timeline to play the song while controlling the breathing pattern i.e., the song should be played when the control of breathing task starts i.e., when the recorded target signal reaches the middle of the screen rather than the initial waiting time when the recorded target signal is travelling from the right to the middle of the screen. Towards this goal, a modified audio file was created for control of breathing task while listening to songs. In the aforementioned audio file, silence, of the duration ame as the duration taken for the recorded signal to play from right to the middle, was introduced to match the total duration of control of breathing sub-trial. As shown in Figure 3-6, the developed program contained option to browse audio file, prename the file in which the target signal and/or control of breathing signal would be written into as well as reading the file containing target signal. As the program involves the real-time display of signal along with data acquisition which means this program would include two different rates (sampling rate for incoming data and display rate on the screen). Hence it was necessary to synchronize the two rates. The approach used to address this problem is described in section 3.4.2.

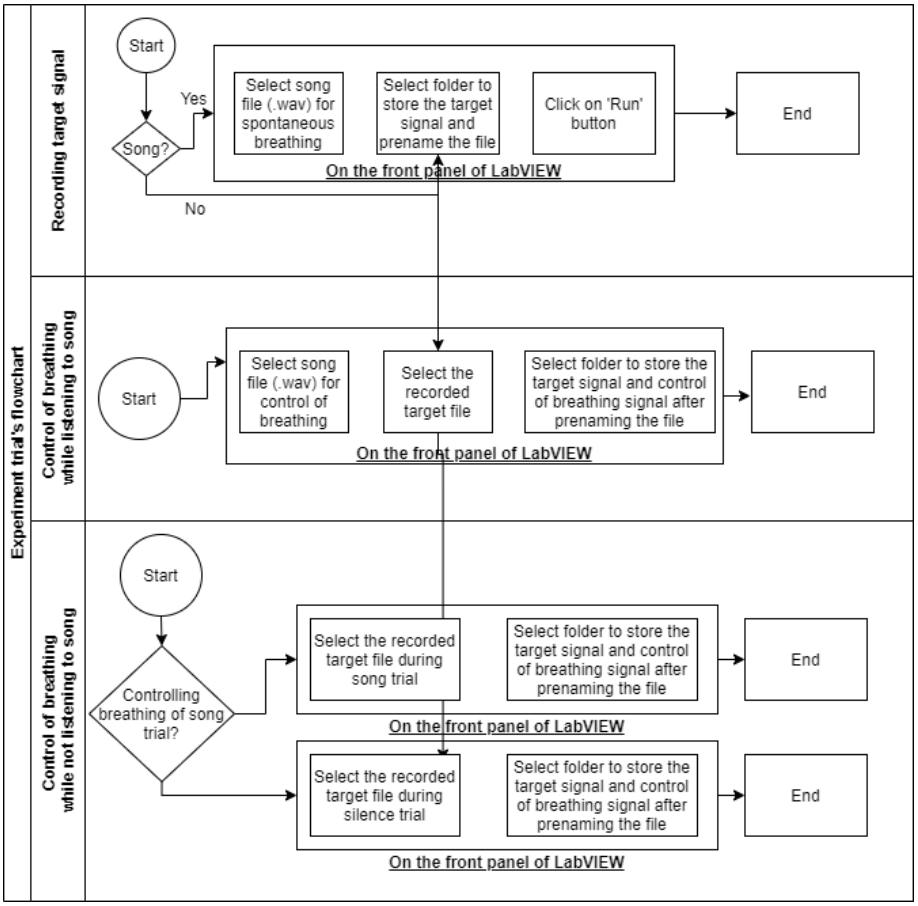

Figure 3-6: Flow diagram showing the flowchart of actions taken on LabVIEW program during different sub-trials showing actual trials (excluding practice trials which occurred before the control of breathing trials)

3.4.2 Testing and synchronization

To test the synchronization between the visual feedback and the collected data the following factors were considered. (a) Change in frequency and/or amplitude between target and the displayed signal. (b) Synchronization between breathing pattern recorded by the commercial data acquisition system and the feedback based control program. And (c) Synchronization between the start of control of breathing to that of the song for easier alignment between collected signals.

3.4.2.1 Change in frequency and/or amplitude between target and controlled signal

This test was necessary to check if the frequency remains same throughout the trials and there was no offset between target and controlled signal.

- Once the control of breathing program was run after the target signal was collected, the video screen was recorded over 2-3, 30 seconds intervals throughout the control of breathing trial. The aforementioned process was conducted with a square wave being the input to the USB DAQ (NI USB 6001) and the commercial data acquisition system (DAS). Different frequencies of the square wave was input to the program using a function generator. The videos were collected using a phone camera at 120 fps. This process was followed by extracting frames from the collected videos.
- The synchronization during the beginning of the trial was tested as follows. The delay between the target signal and the controlled signal was set to 30 seconds. This meant that 30 seconds was the time taken by the target signal (white) to reach the middle of the screen which showed the end point of the control signal (in red with green dot at the end). The extracted frames were used to calculate the number of frames between two events which are, target signal started entering the screen and target signal reaching the middle of the screen. If the number of frames divided by 120 fps was 30 seconds, it was concluded that the target signal and control signal are recorded and displayed at the same sampling rate.
- To test the synchronization at any other time duration of the trial, the time needed for completion of one period of square wave each from target and controlled signal was calculated. If the time duration in terms of number of frames was same, that showed that the program was not changing display rate and hence frequency over time during the control of breathing trial.

3.4.2.2 Synchronization between breathing pattern collected using commercial DAS and USB DAQ

This testing was conducted using target signal and controlled signal recorded using USB DAQ and commercial DAS individually, which means the recorded signal on USB DAQ was compared to that of the commercial DAS signal collected during the same trial. Similarly, the controlled signal recorded during control of breathing to that of the signal recorded on commercial DAS during the same trial. Figure 3-6 shows the algorithm or flow diagram showing steps taken on LabVIEW to acquire, display and compute during the study.

Figure 3-6 shows that, to conduct the test the following method was used. The breathing patterns collected simultaneously using the two data acquisition systems (USB DAQ and commercial DAS) were aligned to each other using method of cross-correlation. A correlation coefficient was calculated between two signals to quantify the synchronization. It was understood that there might be an offset and/or scaling difference between the two measurements. Hence the offset was manually corrected and the visual as well as quantitative comparison was carried out on the normalized signals collected using the two systems.

To further check for alignment RMSE value was calculated between the two normalized signals and low RMSE suggested good alignment.

3.4.2.3 Synchronize the start of control of breathing to that of the song for easier alignment between collected signals

As described in the study design and as shown in Figure 3-1, during one of the sub-trials the subjects were asked to control their breathing while listening to songs. In the control of breathing program, there was a delay for the displayed recorded signal (white) to traverse from right to the middle of the screen for the subjects to start controlling their

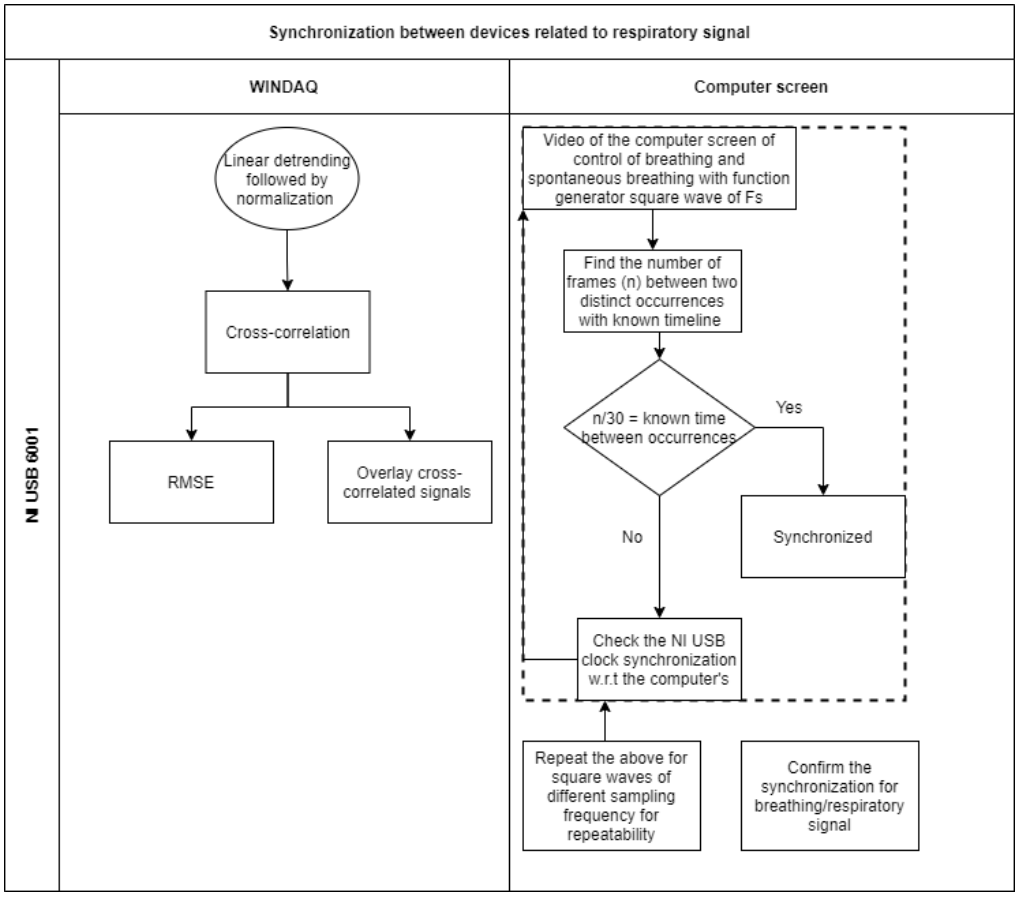

Figure 3-7: Flow diagram showing synchronization test between instruments used to acquire (commercial DAS, USB DAQ), display (computer screen) and compute (LabVIEW on Computer using USB DAQ)

current breathing pattern (red) to be overlaid on the recorded signal. For this reason, it was necessary for the song to start at same time as that of the start of control of breathing. As it is illustrated in the flow diagram of Figure 3-6, the aforementioned was achieved by playing the song using trigger through the program at the instant when current and recorded signals meet in the middle and when the subjects would start controlling their breathing pattern to match the target signal. The song also stopped playing when the control of

breathing trial ended. The song trials were of 3 minutes duration (2 minutes for only one subject).

3.4.3 Performance measurement

IRB approval for the study was obtained. After approval, recruitment of subjects was started. All subjects provided written consent. Data were collected during 8 studies conducted from 7 subjects (4 male, 3 female) who participated in the study, out of which one did not perform well in matching the breathing pattern. All subjects were comfortable in matching their breathing pattern using control of breathing program. Some subjects described the control of breathing task to be fun. The performance, i.e., match between the signals was calculated in time domain.

To obtain a quantitative measurement of how well the subjects were able to reproduce their spontaneous breathing pattern during controlled breathing, performance parameters were computed for each subject for each trial in comparison to other trials during which the subject was controlling or spontaneously breathing to the same breathing pattern. The performance quantifying parameters were computed as follows. For each subject, the root means square error (RMSE) between target and controlled breathing pattern was computed. RMSE was normalized by each subject's average signal value during the same trial to minimize the influence of different breathing patterns and tidal volumes. The mentioned RMSE was called NRMSE (normalized RMSE). NRMSE was calculated using the equation 1. The NRMSE was calculated for all the subjects during all the trials. The NRMSE or the error among the subjects was approximately between 0-15% which suggested that the subjects performed well in terms of matching their breathing pattern during control of breathing sub-trials.

$$\boldsymbol{NRMSE} = \frac{\sqrt[2]{\{\frac{1}{N}\sum[target\,(n\Delta t) - control(n\Delta t)]^2\}}}{\frac{1}{N}\sum target(n\Delta t)} \quad \ldots\ldots\ldots\ldots\ldots\ldots\ldots\ldots 1$$

The average and standard deviation of NRMSE and R values between combinations are shown in Table 3-2. NRMSE between mentioned trials was calculated in time domain.

Table 3-1: Trial code to corresponding sub-trial

Sub-trial	*Sub-trial code*
Control trial's **C**ontrol (silence)	CC
Control trial's **C**ontrol of **B**reathing	CCB
Song trial's **C**ontrol (listening to song1)	SC1
Listening to **S**ong1 while **C**ontrolling **B**reathing	SCB1
Not listening to **S**ong1 while **C**ontrolling **B**reathing	NSCB1
Song trial's **C**ontrol (listening to song2)	SC2
Listening to **S**ong2 while **C**ontrolling **B**reathing	SCB2
Not listening to **S**ong2 while **C**ontrolling **B**reathing	NSCB2

The trial combinations follow the format of "**sub-trial1**-**sub-trial2**" where sub-trial1 and sub-trial2 suggest two different sub-trials during which the subject breathed spontaneously or using control of breathing program following breathing pattern recorded during spontaneous breathing. The sub-trial codes used in the subject-combination in Table 3-2 are same as shown in Table 3-1. For simplicity these sub-trial codes would be used here onwards instead of the whole sub-trial description.

In time-domain the R-value was above 86% which suggested overall good performance in matching the breathing pattern during spontaneous breathing (target signal) and control of breathing (controlled signal). The NRMSE value was found to be 0.3 as

Table 3-2: Performance indicators (NRMSE and R) for all the subjects during each trial

Combination	***NRMSE (t)***	***R (t)***
CC-CCB	.13 +/- .22	.92 +/- .07
SC1-NSCB1	.13 +/- .1	.86 +/- .26
SC1-SCB1	.11 +/- .07	.83 +/- .33
SC2-NSCB2	.19 +/- .15	.91 +/- .13
SC2-SCB2	.3 +/- .33	.88 +/- .21

maximum average in time-domain which suggested reasonably low difference between two sub-trials.

Following the verification of control of breathing, the physiological parameters such as BR, HR, respiratory autospectrum (also referred as BRV), RRI autospectrum (which is also referred to as HRV in some studies) and features from EEG signals were calculated.

CHAPTER 4: RESULTS

In this chapter the results of the pilot study conducted to determine the role of control of breathing pattern and listening to songs on cardiorespiratory and neural interaction are discussed.

4.1 Effects on breathing pattern and ECG signal

For studying the autonomic responses, HR, BR, HF power, LF power and HF/LF ratio difference were calculated between sub-trial combinations as showed in the "Combinations" column of Table 4-1. Table 4-1 shows the combination of the aforementioned parameters which include CC or CCB which are the silence sub-trial and control of breathing sub-trial while controlling the breathing pattern to the silence sub-trial respectively. Table 4-2 shows the parameters for only song sub-trials without any silence sub-trials.

Table 4-1: Difference between average HF/LF ratio, average HF power, average HR, average LF power and average BR between combinations of trials

Combinations	*Avg-HF-LF ratio difference*	*Avg-HF-difference*	*Avg-HR-difference*	*Avg-LF-difference*	*Avg-BR-difference*
CC-CCB	-0.14	8.09	-3.71	5.43	0
CC-SC1	0.14	9.63	-1.86	-33.93	-0.71
CC-SCB1	0.02	17.62	-3.86	17.6	-0.71
CC-NSCB1	0.16	15.14	-5.14	-25.87	-0.71
CC-SC2	0.04	19.72	-1.71	9.26	-1.14
CC-SCB2	-0.26	14.75	-3.71	18.94	-1.14
CC-NSCB2	-0.08	24.51	-4.57	32.91	-1.14
CCB-SC1	0.28	1.54	1.86	-39.36	-0.71
CCB-SCB1	0.16	9.53	-0.14	12.17	-0.71
CCB-NSCB1	0.3	7.05	-1.43	-31.3	-0.71
CCB-SC2	0.18	11.63	2	3.83	-1.14
CCB-SCB2	-0.12	6.66	0	13.51	-1.14
CCB-NSCB2	0.06	16.42	-0.86	27.48	-1.14

In Table 4-1 the Combinations including same song trial are colored similar. None of the comparison showed significant difference in parameters including song sub-trial. As the differences are between the average of the parameters calculated for all the subjects during sub-trials (left-right) of the combination, the negative values would suggest that the parameter for right sub-trial was higher than the left one and vice-versa. The HR was found not following any consistent pattern and was independent of control of breathing sub-trial of the silence sub-trial.

Table 4-2: Table showing the trends derived from Table 4-1

Combinations	*Trend in Avg HF/LF difference*	*Trend in Avg HF power difference*	*Trend in Avg HR Difference*	Trend in Avg LF power	Trend in Avg BR difference
CC-Song1	NSCB1>SC1>SCB1	SCB1>NSCB1>SC1	SC1>SCB1>NSCB1	SCB1>NSCB1>SC1	All equal
CCB-Song1	NSCB1>SC1>SCB1	SCB1>NSCB1>SC1	SC1>SCB1>NSCB1	SCB1>NSCB1>SC1	All equal
CC-Song2	SC2>NSCB2>SCB2	NSCB2>SC2>SCB2	SC2>SCB2>NSCB2	NSCB2>SCB2>SC2	All equal
CCB-Song2	SC2>NSCB2>SCB2	NSCB2>SC2>SCB2	SC2>SCB2>NSCB2	NSCB2>SCB2>SC2	All equal

Table 4-2 shows the clear however not significant trends found out from the variation in parameters shown in Table 4-1. In Table 4-2, the difference of average parameters in combinations of CC - song1-subtrials and CCB - song2-subtrials are color coded where blue shows there was a trend in combinations including song1 sub-trials and green including song2 sub-trials shows that there was a trend in the order as given in the cell. None of the comparisons in this table were significant. However, the repeatability in the trends suggests the possible directions of results. As it can be seen the trends were repeated for each song irrespective of the fact that the combination includes spontaneous or control of breathing of silence trial which suggests that even though control of breathing induces effect, the repeatability is noteworthy. Another interesting finding was that the trends varied only due to listening to the songs in all parameters except HR and BR which suggested that the sympathovagal balance was affected by listening to different songs

Table 4-3: HR, BR, HF power, LF power and HF/LF ratio difference between combinations of trials containing breathing during silence and breathing during song trials

Combinations	*Avg-HF-LF ratio difference*	*Avg-HF-difference*	*Avg-HR-difference*	*Avg-LF-difference*	*Avg-BR-difference*
SC1-SCB1	-0.12	8	-2	51.53	0
SC1-NSCB1	0.02	5.51	-3.29	8.05	0
SCB1-NSCB1	0.14	-2.48	-1.29	-43.48	0
SC2-SCB2	-0.3	-4.98	-2	9.68	0
SC2-NSCB2	-0.12	4.79	-2.86	23.65	0
SCB2-NSCB2	0.19	9.76	-0.86	13.97	0
SC1-SC2	-0.1	10.1	0.14	43.19	-0.43
SCB1-SCB2	-0.28	-2.88	0.14	1.33	-0.43
NSCB1-NSCB2	-0.23	9.37	0.57	58.78	-0.43
SC1-SCB2	-0.4	5.12	-1.86	52.86	-0.43
SC1-NSCB2	-0.22	14.88	-2.71	66.83	-0.43
SCB1-SC2	0.02	2.1	2.14	-8.34	-0.43
SCB1-NSCB2	-0.09	6.89	-0.71	15.3	-0.43
NSCB1-SC2	-0.12	4.58	3.43	35.14	-0.43
NSCB1-SCB2	-0.42	-0.39	1.43	44.81	-0.43

irrespective of the act of control of breathing and when there was no change in BR.

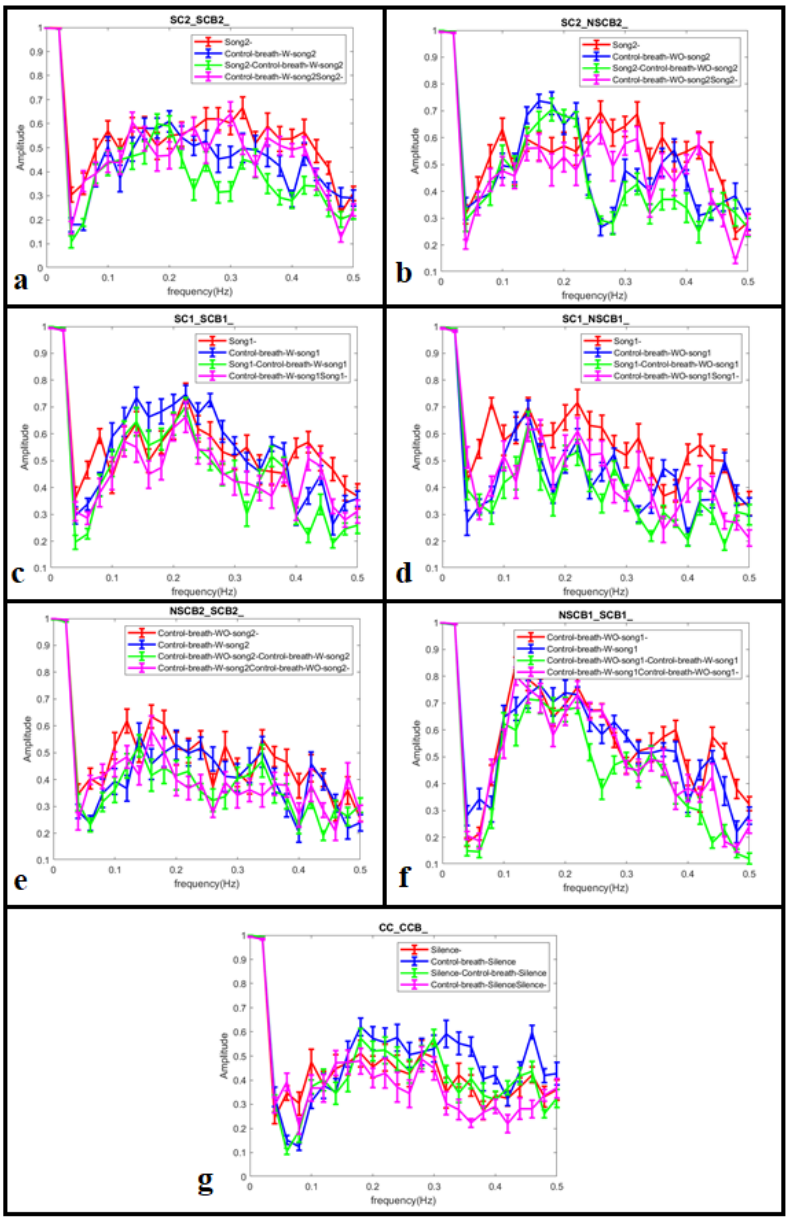

Figure 4-1: Coherencies (with standard error) between combinations as written in titles of the plots, (a) SC2-SCB2 (Song2-Song2 while controlling breathing and listening to song) , (b) SC2-NSCB2 (Song2-Song2 while controlling breathing without listening to song), (c) SC1-SCB1 (Song1-Song1 while controlling breathing and listening to song), (d) SC1-NSCB1 (Song1-Song1 while controlling breathing without listening to song), (e) NSCB2-SCB2 (Song2 while controlling breathing without listening to song-Song2 while controlling breathing and listening to song), (f) NSCB1-SCB1 (Song1 while controlling breathing without listening to song-Song1 while controlling breathing and listening to song), (g) CC-CCB (Control/Silence's control-Control/silence's control of breathing), where the red shows the coherence between the RRI and breathing pattern of the left sub-trial of the combination, blue shows the coherence of the signal collected during right side sub-trial of the combination, green shows the coherence between RRI of the left and breathing pattern of the right sub-trial and pink shows the coherence between RRI of the right and breathing pattern of the left sub-trial of the combination.

However, to statistically confirm the finding further investigation with more subjects would be necessary.

To study the cardiorespiratory interaction between sub-trials of silence (CC, CCB), song1 (SC1, SCB1 and NSCB1) and song2 (SC2, SCB2 and NSCB2), coherencies between envelopes of RRI and breathing pattern were calculated between different combinations. Figure 4-1 shows the coherencies calculated between sub-trials, the specific subtrial combination is given as the title of each plot. Each plot contains four coherencies for four combinations of the sub-trials. In Figure 4-1, the red and blue plot show the coherence between the RRI and breathing pattern recorded during same sub-trial (shown on the legends). Green plot shows the coherence between RRI and breathing pattern of the sub-trials mentioned on left and right side respectively on the legends and pink shows the coherence between RRI and breathing pattern of the subtrials mentioned on the right and left side of the legends.

Coherence shows the interaction or similarity between two signals and ranges between 0-1, where 0 is no interaction and 1 being nearly identical signals. Figure 4-1, shows that the degree of similarity between RRI and breathing pattern were higher during listening to songs than during control of breathing with or without listening to songs as can be seen from Figure 4-1 (a), (b) and (d) except Figure 4-1 (c). This suggests that the interaction between RRI and breathing pattern during song1, song2 was higher in comparison to interaction during control of breathing while not listening to songs for both the songs. In case of song2, the interaction during song2 was higher than interaction during control of breathing while listening to the same song. However, for song1 this was not the case. In case of control of breathing while listening to song1, 2 out of 7 experiments did not show the pattern. These results suggest that the interaction between RRI and breathing pattern during listening to songs without control of breathing remained higher than other combinations which included control of breathing. This suggested that between RRI and breathing pattern the interaction with the original song's breathing pattern showed higher interaction with RRI suggesting that the change in breathing pattern may be a secondary effect. Song1 was the fast rhythm song and song2 was the slower rhythm song. From our finding the interaction during slow rhythm song was more distinct than fast rhythm song.

The reasons for this difference were not explored in this study and could be the focus of future exploration.

The cross-interaction was also studied visually followed by quantitatively which suggested the following. While the red (RRI with breathing pattern while listening to songs) and pink (RRI of control of breathing with breathing pattern during listening to songs) plots followed each other closely, blue (RRI with breathing patterns during control of breathing) and green (RRI of song with breathing pattern of control of breathing) plot also followed each other closely. These findings suggest the possibility of a common factor being the cause behind such influence on coherencies. Where the common factor between red and pink plot was breathing pattern collected during listening to songs, the common factor between blue and green was breathing pattern collected during control of breathing irrespective of listening to songs while controlling the breathing. This phenomenon indicates that the breathing pattern plays some role in such commonality feature in coherencies.

However, while comparing the magnitude difference between the plots following each other visually the red and pink plots are closer to each other in case of interaction between song and control of breathing while listening to songs than that of the interaction between song and control of breathing while not listening to songs. This phenomenon was visible for song2. In case of song1, for 5 out of 7 subjects the above phenomenon existed. This suggests that even though the act of control of breathing may induce changes in cardiovascular rhythms, addition of the trial of control of breathing while listening to songs would help us distinguish the effect of song over control of breathing if there is any. Control of breathing while listening to songs followed the red plot more closely than control of breathing while not listening to songs. This suggests that even though control of breathing may have an effect on cardiovascular rhythms, listening to songs surpassed the effect due to control of breathing. These findings suggest that the study design contains the ability to investigate the effects of listening to songs against control of breathing.

The overall findings suggested that listening to songs along with change in breathing pattern changes the cardiovascular rhythm and that even though the act of control of breathing may affect cardiovascular rhythms, the effect of listening to songs may surpass the effect of control of breathing irrespective of the rhythm of song.

Even though the sample size was small, as an exploratory step in a pilot study, to verify the above inferences, t-tests between the coherencies were conducted. In the t-test the significant values suggest that the averages of two samples considered are significantly different. Our goal was to find the combinations which were non-significantly similar to each other which is just another way of investigating interaction. Hence, in the t-test the significant combinations were ignored from consideration.

Where Table 4-4 shows the p-value and differences in average of total coherencies between two combinations separated by ":", Table 4-5 shows the p-value and difference in average of coherence values in the range 0.06-0.42 Hz. The reason behind choosing this range was as follows. In Figure 4-1, the plots were observed to follow each other closely in the region of 0.06-0.42 Hz. Hence this region was used to find outlier as well as hidden interactions. The color coding on Table 4-4 and Table 4-5 combinations was kept same as that of the plots in Figure 4-1 for clarity.

In both Table 4-4 and Table 4-5, the combinations which showed closer interactions are shown with a "*" beside the combination. Results in Table 4-4 are consistent with the aforementioned finding that the interaction due to listening to songs was higher than other combinations as was observed from the positive difference in average. In Table 4-5, the average difference between coherence of song1 (between RRI and breathing pattern) and control of breathing while listening to song1 was negative while in Table 4-4 the difference was positive even though these differences were very small. The reason behind such change could be the presence of outliers. 5 out of 7 showed positive differences while other 2 did not. The 2 subjects showed opposite effect of the other 5 mainly in the range 0.06-0.42 Hz which may have resulted in such difference in pattern. These were small changes, therefore the interpretation of these is speculative.

While comparing this phenomenon to the silence, the comparison between silence and control of breathing to the pattern recorded during silence, was negative i.e., the interaction between control of breathing RRI and breathing pattern was higher than silence which suggests the presence of effect of control of breathing during silence which is consistent with the previous reports [1]. However, listening to songs showed significantly higher coherence than any other combination involving breathing patterns collected during listening to songs. This finding indicated that even though control of breathing act could

instill changes in cardiac rhythms and cardiorespiratory interaction, the interaction during listening to songs would surpass the interaction (due to control of breathing with or without listening to songs) in magnitude. This finding suggests that the study design helps quantify the effect of listening to songs in comparison to control of breathing.

Blue (Control of breathing with or without listening to songs) and green (RRI of song and breathing pattern while controlling breathing with or without listening to songs) plot pairs for song1 and song2 as shown in Figure 4-1, showed the effect of controlling breathing patterns. For song1 i.e., the fast rhythm song, the interaction between RRI and breathing pattern due to control of breathing while listening to song1 was not significantly different from control of breathing while not listening to song1. However, the aforementioned relation was not observed in case of song2 or slow rhythm song as the coherences were significantly different in Table 4-4 and Table 4-5.

Table 4-4: Paired coherences between two sets of total coherencies (between 0-0.5Hz)

Combination of coherence comparison	*p-value*	*Average difference*
Silence:Control-breath-Silence	0.043	-0.045
Silence:Control-breath-Silence-Silence*	0.641	0.007
Silence:Silence-Control-breath-Silence	0.000	0.045
Control-breath-Silence:Control-breath-SilenceSilence-	0.001	0.052
Control-breath-Silence:Silence-Control-breath-Silence	0.002	0.091
Control-breath-SilenceSilence:Silence-Control-breath-Silence*	0.069	0.038
Song1:Control-breath-WO-song1	0.000	0.109
Song1:Control-breath-WO-song1-Song1	0.000	0.166
Song1:Song1--Control-breath-WO-song1	0.000	0.110
Control-breath-WO-song1:Control-breath-WO-song1Song1-	0.003	0.056
Control-breath-WO-song1:Song1-Control-breath-WO-song1*	0.987	0.000
Control-breath-WO-song1Song1:Song1-Control-breath-WO-song1	0.004	-0.056
Song1:Control-breath-W-song1*	0.939	0.002
Song1:Control-breath-W-song1-Song1-	0.001	0.088
Song1:Song1--Control-breath-W-song1	0.000	0.076
Control-breath-W-song1:Control-breath-W-song1Song1-	0.000	0.086
Control-breath-W-song1:Song1-Control-breath-W-song1	0.000	0.074
Control-breath-W-song1Song1:Song1-Control-breath-W-song1*	0.523	-0.012
Song2:Control-breath-WO-song2*	0.053	0.063
Song2:Control-breath-WO-song2-Song2-	0.003	0.100
Song2:Song2--Control-breath-WO-song2	0.000	0.071
Control-breath-WO-song2:Control-breath-WO-song2Song2-	0.002	0.037
Control-breath-WO-song2:Song2-Control-breath-WO-song2*	0.799	0.008
Control-breath-WO-song2Song2:Song2-Control-breath-WO-song2*	0.320	-0.029
Song2:Control-breath-W-song2	0.000	0.074
Song2:Control-breath-W-song2-Song2	0.000	0.136
Song2:Song2-Control-breath-W-song2	0.000	0.059
Control-breath-W-song2:Control-breath-W-song2Song2	0.000	0.061
Control-breath-W-song2:Song2-Control-breath-W-song2*	0.426	-0.015
Control-breath-W-song2Song2:Song2-Control-breath-W-song2	0.003	-0.077
Control-breath-WO-song1:Control-breath-W-song1*	0.209	0.022
Control-breath-WO-song1:Control-breath-W-song1-Control-breath-WO-song1-	0.000	0.116
Control-breath-WO-song1:Control-breath-WO-song1--Control-breath-W-song1	0.002	0.061
Control-breath-W-song1:Control-breath-W-song1Control-breath-WO-song1-	0.000	0.094
Control-breath-W-song1:Control-breath-WO-song1-Control-breath-W-song1	0.025	0.039
Control-breath-W-song1Control-breath-WO-song1:Control-breath-WO-song1-Control-breath-W-song1	0.007	-0.055
Control-breath-WO-song2:Control-breath-W-song2	0.004	0.055
Control-breath-WO-song2:Control-breath-W-song2-Control-breath-WO-song2-	0.000	0.093
Control-breath-WO-song2:Control-breath-WO-song2--Control-breath-W-song2	0.000	0.075
Control-breath-W-song2:Control-breath-W-song2Control-breath-WO-song2-	0.012	0.038
Control-breath-W-song2:Control-breath-WO-song2-Control-breath-W-song2*	0.354	0.020
Control-breath-W-song2Control-breath-WO-song2:Control-breath-WO-song2-Control-breath-W-song2*	0.281	-0.018

Table 4-5: Coherence comparison between coherencies calculated between 0.06-0.42 Hz as this region showed higher synchronization between signals

Combination of coherence comparison	*p-value*	*Average difference*
Silence:Control-breath-Silence*	0.20	-
Silence:Control-breath-Silence-Silence*	0.59	0.0
Silence:Silence-Control-breath-Silence	0.00	0.0
Control-breath-Silence:Control-breath-SilenceSilence-	0.01	0.0
Control-breath-Silence:Silence-Control-breath-Silence	0.01	0.0
Control-breath-SilenceSilence:Silence-Control-breath-Silence*	0.11	0.0
Song1:Control-breath-WO-song1	0.00	0.1
Song1:Control-breath-WO-song1-Song1	0.00	0.1
Song1:Song1--Control-breath-WO-song1	0.00	0.1
Control-breath-WO-song1:Control-breath-WO-song1Song1-	0.00	0.0
Control-breath-WO-song1:Song1-Control-breath-WO-song1*	0.78	-
Control-breath-WO-song1Song1:Song1-Control-breath-WO-song1	0.00	-
Song1:Control-breath-W-song1*	0.52	-
Song1:Control-breath-W-song1-Song1-	0.01	0.0
Song1:Song1--Control-breath-W-song1	0.00	0.0
Control-breath-W-song1:Control-breath-W-song1Song1-	0.00	0.0
Control-breath-W-song1:Song1-Control-breath-W-song1	0.00	0.1
Control-breath-W-song1Song1:Song1-Control-breath-W-song1*	0.69	0.0
Song2:Control-breath-WO-song2*	0.05	0.0
Song2:Control-breath-WO-song2-Song2-	0.00	0.1
Song2:Song2--Control-breath-WO-song2	0.00	0.0
Control-breath-WO-song2:Control-breath-WO-song2Song2-	0.00	0.0
Control-breath-WO-song2:Song2-Control-breath-WO-song2*	0.77	-
Control-breath-WO-song2Song2:Song2-Control-breath-WO-song2*	0.14	-
Song2:Control-breath-W-song2	0.00	0.0
Song2:Control-breath-W-song2-Song2	0.00	0.1
Song2:Song2-Control-breath-W-song2	0.00	0.0
Control-breath-W-song2:Control-breath-W-song2Song2	0.00	0.0
Control-breath-W-song2:Song2-Control-breath-W-song2*	0.13	-
Control-breath-W-song2Song2:Song2-Control-breath-W-song2	0.00	-
Control-breath-WO-song1:Control-breath-W-song1*	0.53	0.0
Control-breath-WO-song1:Control-breath-W-song1-Control-breath-	0.00	0.0
Control-breath-WO-song1:Control-breath-WO-song1--Control-breath-	0.00	0.0
Control-breath-W-song1:Control-breath-W-song1Control-breath-WO-	0.00	0.0
Control-breath-W-song1:Control-breath-WO-song1-Control-breath-	0.15	0.0
Control-breath-W-song1Control-breath-WO-song1:Control-breath-	0.02	-
Control-breath-WO-song2:Control-breath-W-song2	0.01	0.0
Control-breath-WO-song2:Control-breath-W-song2-Control-breath-	0.00	0.1
Control-breath-WO-song2:Control-breath-WO-song2--Control-breath-	0.00	0.0
Control-breath-W-song2:Control-breath-W-song2Control-breath-WO-	0.00	0.0
Control-breath-W-song2:Control-breath-WO-song2-Control-breath-	0.31	0.0
Control-breath-W-song2Control-breath-WO-song2:Control-breath-	0.29	-

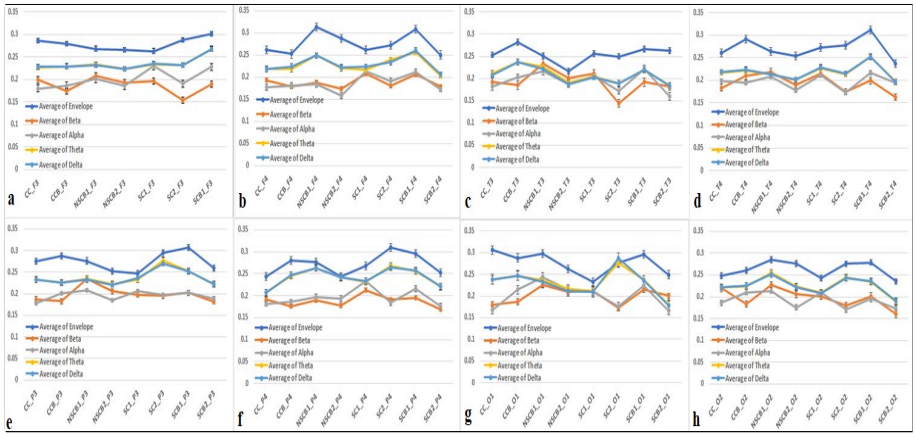

Figure 4-2: Coherence between breathing pattern and EEG-frequency bands

The difference between coherence pairs including listening to songs while spontaneously breathing and listening to songs while controlling the breathing pattern was found to be less different than that of the comparison between listening to songs and controlling breathing while not listening to songs.

Our finding from the aforementioned results was that the change in breathing pattern as well as listening to songs could be the reason behind changing the autonomic responses. To study any possible effect of listening to songs and change of breathing in electrical activity of the brain, we studied the interaction between autonomic responses and cardiorespiratory effects and EEGs. To study the interaction between RRI and EEG as well as breathing pattern and EEG, the coherence between RRI, breathing pattern individually with various EEG features was calculated. The EEG features included envelope, and frequency bands which included alpha (8-12 Hz), beta (13-30 Hz), gamma (above 30 Hz), delta (0-4 Hz) and theta (4-8 Hz) to study the effect in different frequency bandwidths. The results of coherence between breathing pattern and EEG bands are shown in Figure 4-2. Figure 4-3 shows the coherence of more than 0.55 between breathing pattern and EEG bands. Figure 4-4 shows the total coherence between RRI and EEG bands. The coherence (>0.55) between RRI and EEG bands is shown in the Figure 4-5.

4.2 Relation between Cardiorespiratory and neural effect

Figure 4-2 shows the average coherence calculated between breathing pattern and EEG band calculated for 8 different locations F3, F4, T3, T4, P3, P4, O1, and O2. These are shown in Figure 4-2 (a), (b), (c), (d), (e), (f), (g) and (h) respectively. For all the locations EEG-envelope was found to show highest coherence than other bands. Delta and theta were found to be synchronous to each other in terms of the coherence between

breathing pattern and EEG bands. Alpha and beta bands were found to follow each other

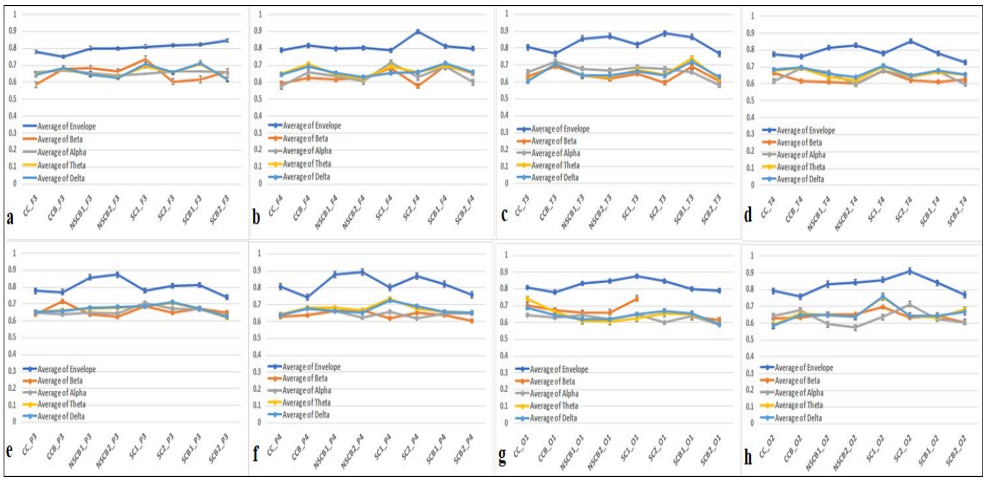

Figure 4-3: Coherence (above 0.55) between breathing pattern and EEG frequency bands

closely in most of the cases. The pattern of change between sub-trials was found to be similar for most sub-trials in case of envelope of EEG in case of P3-P4, T3-T4, O1-O2. However, for F3-F4 none of the EEG bands showed a similar pattern of change. Hence, it was decided to find coherence above 0.55 to consider only the effective bandwidth (defined using 0.55 threshold) rather than total bandwidth (0-0.5 Hz). The threshold of 0.55 was selected to identify the interactions which were more than 50%. Although somewhat arbitrary, as the study used stimuli (songs) which were expected to cause small magnitude of effects in physiological parameters, a threshold of 55% or 0.55 was selected. The average coherence values that exceeded this threshold with standard error are shown in Figure 4-3 (a-h denoting same locations as in Figure 4-2). Unlike Figure 4-2, Figure 4-3 shows that alpha, beta, delta and theta did not show distinct magnitude difference. Coherence between breathing pattern and envelope of EEG was observed to be higher than the coherence between breathing pattern and other EEG bands. A previous study by Horton et al. has shown that the envelopes of EEGs are better indicators of attention than alpha, beta and other bands [160]. With the exception of SC1 (listening to song1 while spontaneously breathing) and for F3 and F4 EEG locations, for all other trials and EEG-locations, the envelope showed higher coherence for song trials than that of silence (CC and CCB). From P3 and P4 it was observed that for control of breathing trial without listening to songs showed higher average coherence than other trials. This shows that control of breathing effect was observed in signals acquired from surface of the peripheral

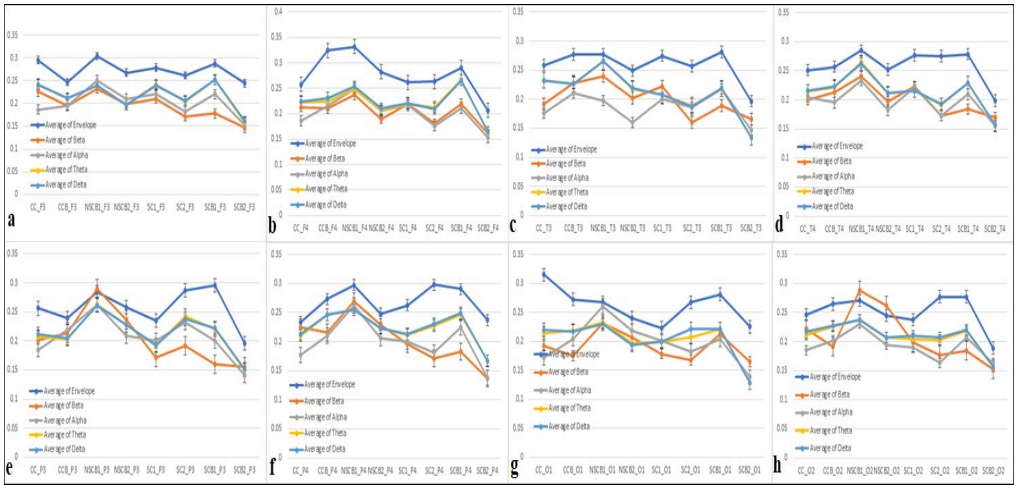

Figure 4-4: Coherence between RRI and EEG frequency bands

brain. However, in case of O1 and O2, all trials (SC, NSCB and SCB) showed higher average coherence than silence. This suggested that during song trials the coherence between EEG and breathing pattern was higher than silence irrespective of act of control of breathing.

In this study, one of our main goals was to study the cardiorespiratory effect of listening to songs. Studying the interaction between breathing pattern with EEG as well as studying interaction between RRI with EEG individually followed by investigating these interactions has the potential to bring more insights related to how cardiorespiratory interaction changes during listening to songs of fast and slow rhythms with respect to neurological effect. Figure 4-4 (total coherence) and Figure 4-5 (coherence above 0.55)

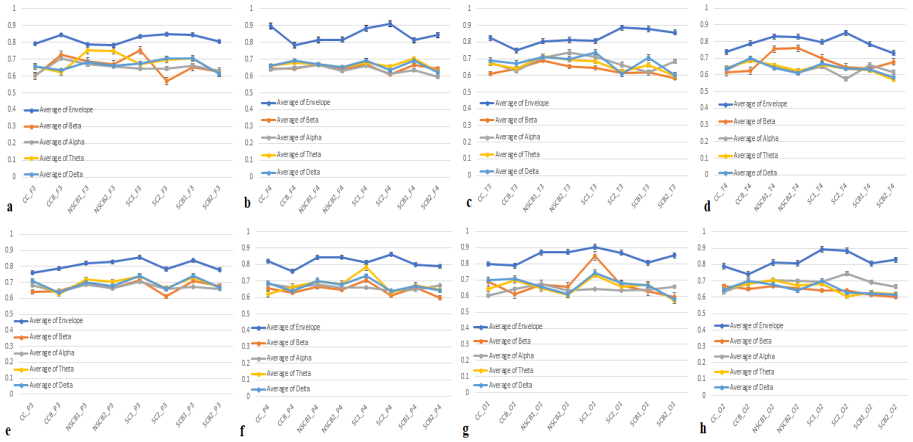

Figure 4-5: Coherence (above 0.55) between RRI and EEG frequency bands

show average coherence between RRI and EEG bands extracted from 8 different EEG locations. Like the coherence between breathing pattern and EEG, in case of coherence between RRI and EEG the envelope of EEG showed higher coherence in comparison to other EEG bands. The coherence between EEG bands and RRI other than envelopes showed closer values as shown in the figures (Figure 4-4). Hence to study the interaction coherence above 0.55 were calculated whose results are shown in Figure 4-5. 0.55 value was arbitrarily chosen to consider coherences with above 50% similarity. Figure 4-5 showed the average of coherence above 0.55 with standard error for different sub-trials on the x-axis and magnitude of average of coherence in the y-axis. Similar to the findings before, the envelope of EEG showed higher effective coherence (>0.55) with RRI than other EEG bands. From figure, it was observed that, O1 and O2 showed highest coherence magnitude between RRI and envelope of EEG than other locations. Alpha wave in case of O1 showed comparatively higher magnitude than other locations. In case of O2, envelope of EEG as well as alpha wave showed higher effective coherence than other bands. O1 and O2 are known to be the locations showing alpha-activity if any[161], [162]. Meditation and relaxing activities are known to induce alpha waves[163]–[165]. The aforementioned finding suggested that the reduction of stress induces alpha waves, and such activity was observed during listening to songs. During listening to song1 and song2 while spontaneously breathing the effective coherence (>0.55) was found to be more than other song trials as well as silence trials (CC and CCB). This finding suggested that the cardio-neurological interaction was more during listening to songs than any other trials. This suggested effect of listening to songs was inducing more interaction between RRI and EEG than that during control of breathing.

While comparing the effective coherence between breathing pattern and EEG bands with that of RRI and EEG bands it was observed that for O1 and O2 the coherence due to RRI was higher than that of breathing pattern. One interesting phenomenon was observed which was, during NSCB1 and NSCB2 i.e., controlling the breathing pattern to the pattern recorded during listening to songs without listening to songs, showed similar coherence between RRI and EEG band (>0.55) during SCB1 and SCB2 i.e., the control of breathing trial while listening to songs showed difference in magnitude. This finding showed that control of breathing may result in similar interaction irrespective of the pattern being

different. But listening to songs surpasses the similarity of the effects of control of breathing and results in different effects. As shown in the above figures, the EEG bands other than envelope-EEG, showed comparatively lower magnitude change. Different EEG bands are thought to be responsible for different functions such as alpha is triggered when a person is relaxed or focusing while relaxed, beta is activated with attentional activation, gamma is responsible as an indication of higher cognitive processes and theta is associated with emotional valence[163], [166]–[169]. Listening to songs is known to soothe the listener and for some listeners listening to songs triggers emotions and is known to trigger cognitive processes[17], [25].

CHAPTER 5: NON-CONTACT MEASUREMENT

During human studies where measurements such as ECG and, breathing pattern with wired connections are utilized and, the responses in physiological parameters is expected to be of small magnitude, there is potential that avoiding the wired connections that the subjects might feel conscious of may improve the result of the studies.

Towards the goal of exploring the use of non-contact measurement of HR and BR, the following were proposed.

- Development of workflow to extract Heart rate (HR) and breathing rate (BR) from videos of the faces of the subjects.
- Comparison of performance of different methods used for extraction of ROI and/or landmarks followed by BR and HR data comparison against gold standard, i.e., contact measurement.

To achieve the proposed, the following objective was defined. Design of a non-contact measurement system using a digital RGB camera and implement the system in control of breathing experiment for the purpose of comparison between contact and noncontact measurement.

The following sub-sections contain the description of the design of the non-contact measurement of BR and HR which includes ROI detection and tracking until BR and HR extraction and validation against contact measurements.

5.1 Design of a non-contact measurement system

The field of non-contact measurement has caught the interest of many researchers who have developed various techniques to approach the problem of non-contact measurement of heart rate (HR), respiratory rate/breathing rate (BR). Most of this research use similar framework to build the algorithm to extract non-contact HR and BR from video of the face of human subjects and/or animal subjects [70], [81], [94], [106], [108], [120], [170], [171].

Most of the articles have used the skin region of the face or skin of different regions of the face such as cheek or forehead to extract HR and BR as these regions are considered to contain most information regarding blood flow [172]–[174]. For this reason, it was

necessary to extract the selected regions such as cheeks and forehead accurately which was why in our case two widely used ROI detection and tracking methods were used. Table 5-1: contains the comparison between ROI detection and tracking using KLT, 68 facial points method and 3D Facemesh model (recently developed)[55], [120], [134], [135], [154]. Further, a detailed comparison of 3D with KLT and 68 facial points method is provided based on results of our study. The reason behind choosing these KLT and 68-points methods was that these are the most widely used tracking methods. The comparison in Table 5-1: between methods is based on publications and experience during the present study while working with all three methods.

Table 5-1:Comparison between KLT, 68-points and Facemesh ROI detection and tracking

KLT	68-points	Facemesh
• Tracks the ROI rectangle and tracks it through geometric tracking over frames. • Chances of false positive i.e., the chances of tracking other features in a frame as ROI is higher than others. • Skin-color and external light sensitive. • Not fit for pictures with dimension more than 500x500. • Could not be used in BR and HR extraction as in some trials the method was not detecting for more than half of the trial duration.	• The only information gets transferred from frame to frame is the face ROI on which the 68 landmark points are detected. • Chances of false positives are much less as this technique uses ROI and the landmarks detection. • This model is found to be less sensitive to skin-color and external lighting than KLT. • Fit for pictures having dimension up to 1920x1000. Cropping the picture increases the performance. • With large movement of face some landmarks may be detected with high errors. For this reason, rotating the face using the straight-line connecting center of the landmarks two eyes helps in managing rotation around vertical axis. • Takes longer than Facemesh (approx. 30 minutes more).	• Facemesh depends on the detection model for detection of 468 landmarks on the face with the 3D tensors information. The only information gets transferred between frames is the ROI which contains the face. • Chances of false positives are much lower than other two methods. • Model was found to be least sensitive to external light and skin-color. • Rotation of face was not necessary in this case. • It is found to perform well under high movement conditions as well. • Running the model using Tensorflow in backend proved to make the landmark detection faster by 53% than running on CPU and it was faster than 68-points.

5.1.1 Finding the most accurate ROI detection method among widely used methods

5.1.1.1 3D Vs 2D

As it is given in Table 5-1, the 68-points method does a good job at tracking the ROI. However, to do so, it needs alignment or rotation of the face if the movement is in 2D. However, face alignment would not help the purpose of extraction of cheek correctly while there is self-occlusion due to 'yaw' movement or movement across the y-axis as described in [175]. As suggested by google research (Kartynnik et.al), landmark annotation in 2D is confounded by inconsistency in the landmark positions across different poses and self-occlusions [154]. Such inconsistency in landmark position occurs when high movement is there, or the subject is not facing the camera. Such inconsistency can be avoided by using 3D meshes by selecting a dense set of 3D points [149].

Our initial estimation about Facemesh model suggested that as the use of the 68-points system ([x, y]) requires considerable time and processor memory , Facemesh which is a 468 points system ([x, y, depth]) would make the processing even lengthier and can only be achieved on computers with high processing power such as systems with external graphics processing unit (GPU). However, we observed that this was not the case. This model could run even on a mobile phone if implemented on HTML and .js environments[154]. The reason being the model originally was trained on tfjs (tensorflow.js) which is a library of machine learning in java script which gives options to run the code with 'WASM' (backend) environment which makes the processing approximately 10 times faster than if the processing would be done on CPU [154].

The research and development team of Google has implemented and named this model as 'Facemesh' model [154]. As given in the article [154], the purpose of this model is to build applications that would involve AR (augmented reality) which is already being implemented by Instagram which is called Instagram filters, by Facebook messenger and iPhones. However, this method is not widely used to extract HR and BR. The reason could be that this model is very recent and the compatibility to MATLAB like 68-points is not available. Hence only open-source environment users would be able to use such model.

5.1.1.2 Implementing detection and tracking ROI through frames of videos

5.1.1.2.1 KLT

For the implementation of KLT to extract the facial ROI, the Haar-like features cascade model was used with OpenCV2 library and tracking was implemented using 'dlib tracker' which uses geometric tracking[135], [176], [177]. KLT detects the rectangle containing the face and the output contains the coordinates of the four corners of the detected rectangle. The centroid of the four coordinates was later compared against the centroids calculated using Facemesh and 68-points method.

5.1.1.2.2 Facemesh

The 468 facial landmark detection trained model was implemented [178]. Facemesh facial landmark detection model is an algorithm that detects facial points using which silhouette of the face, eyebrows, eyes, nose, lips (inner and outer), and other regions can be detected. For face recognition and landmark detection, Tensorflow and OpenCV2 libraries were used. All the libraries used are open-source. The video processing was conducted in Java environment and the frame by frame detected facial landmarks along with annotation were saved for the following. Later the saved facial landmark locations and annotation were used on python environment for rendering the coordinates of landmark locations and the video processing. Java environment was used because of its faster processing than python.

An article at the referenced URL shows the image containing the facial landmarks detection model of Facemesh [179]. To assess the performance of the method in detecting and tracking facial ROI the centroid of the face silhouette was calculated using 36 silhouette coordinates. The annotated locations include a single coordinate for each cheek which was used to compare against the centroid calculated using 68-points method.

5.1.1.2.3 68-Points

Studies [180]–[183] have implemented the 68 point a facial landmark detection trained model using 68 points to calculate HR and/or BR. 68-points facial landmark detection model is an algorithm that detects facial points using which eyebrows, eyes, nose, lips, and jawline can be detected [183]–[186]. Even though in the beginning phase of development, a workflow was designed on MATLAB using the image processing toolbox. The processing time was higher by approximately 10 times more than python or Java.

Python environment is open source and has more options in terms of building new libraries as well as using existing libraries which are based on current advancements. Therefore, for subsequent development python environment was used. For face recognition and landmark detection, the imutils library, OpenCV2 libraries were used [187]. Imutils library is the library designed by Adrian Rosebrock, which contains functions related to image processing [188]. All the libraries used are open-source, and all of the video processing was done in the python environment. The 68-points landmarks detection model has been used in some studies and has performed well in facial feature detection before calculating HR and BR [189], [190].

The libraries mentioned above were used and modified according to the requirements of this study. To compare the performance of facial landmarks/facial ROI/total ROI the jaw points (0-16) were used to calculate the centroid in case of 68-points.

After the facial landmarks detection, the rectangle for the left, as well as right cheek portions, was defined using points of left-eyebrow (17-20), right eyebrow (23-26) nose (28-33) and some points of mouth (48 for left cheek and 54 for right cheek). To compare the performance of 68-points in detecting and tracking cheeks, the aforementioned set of points were used for the calculation of the centroid.

5.1.2 Comparison in performance while tracking the ROI

In order to find the best method of ROI detection and tracking in case of the collected videos, the comparison of performance was necessary. To execute the comparisons a series of steps were taken for different methods which are shown in Figure 5-1. As shown in Figure 5-1 to obtain a fair comparison among methods, instead of the raw video, the pre-processed video was used.

For video pre-processing, the video quality was kept unchanged. Pre-processing involved the selection of ROI (around the face) on the first frame of the video and the selected region was tracked through frames. The whole process was automated other than selecting the ROI on the first frame. This process reduced spontaneous motion by focusing

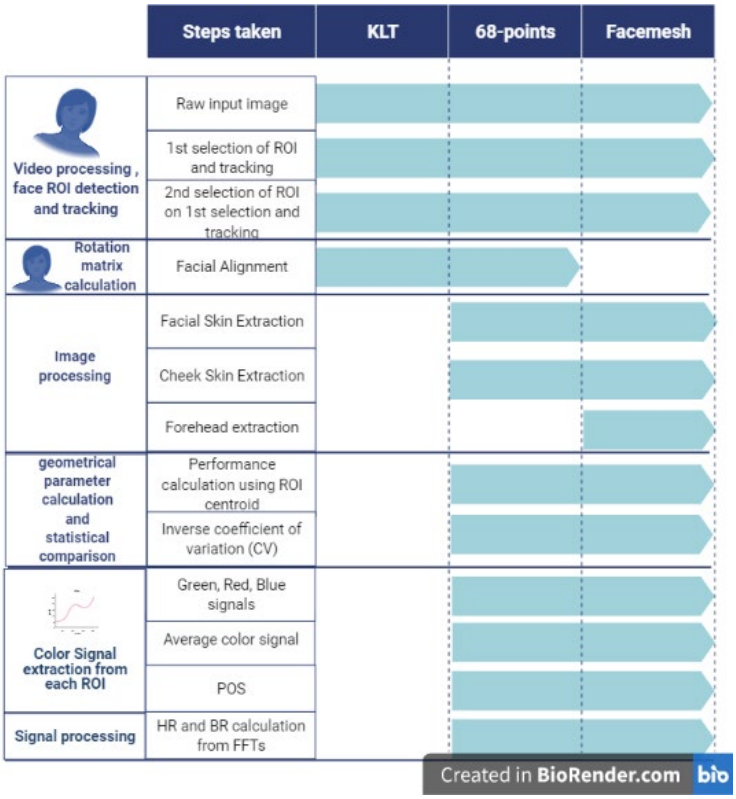

Figure 5-1: The series of steps taken from input of raw images till HR and BR calculation using KLT, 68-points and Facemesh

only on the face. This video was further used for ROI detection and tracking using KLT, 68-points and Facemesh methods.

5.1.2.1 Performance estimation using Total-ROI centroid variation

Once the relative motion of face was nearly negligible, variation in centroid movement after the video pre-processing showed how each method performed with respect to each other.

Figure 5-2: Detection of rectangle ROI using KLT as shown in blue color

As shown in Figure 5-2, KLT detects the coordinates of the rectangle (n=4) which contains the face in the image. This article shows the facial landmarks of 68-points method[191]. In this method, the centroid was calculated from the points (n=17) representing the jaw. Only outermost points (n=36) which represent the silhouette of the face were used to calculate the centroid of the total ROI. Figure 5-3 shows the scatter plot between X and Y coordinates (in pixels) of the centroids calculated per frame of the videos collected over all the trials for all the subjects.

As it was assumed that motion of the face with respect to frames was negligible, the more spread out the scatter plot would indicate poorer performance in tracking of the total ROI. Figure 5-3 shows that Facemesh performed best among the three methods. It was also necessary to analyze the performance of ROI detection and tracking for all subjects (unique n=6). For this purpose, the X and Y pixels were normalized to restrict the variation between 0-1. Figure 5-3 shows that for all the subjects, the detected centroid variation was least scattered for Facemesh while for KLT the variation was most scattered. Consistent conclusions through all the subjects suggested that Facemesh performed good for all the

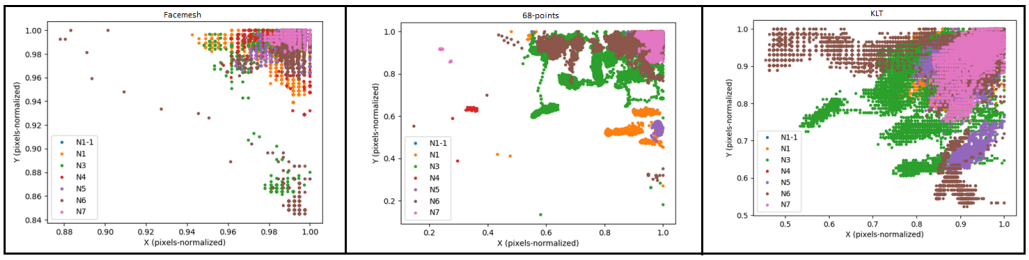

Figure 5-3: Detected centroid variation over each subject for all the trials for facemesh, 68-points and KLT (left to right)

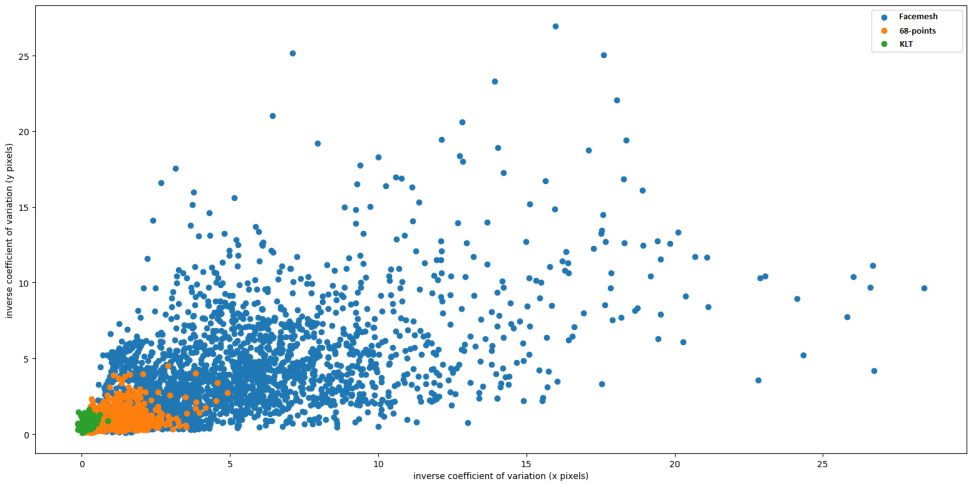

Figure 5-4: Inverse coefficient of variation calculated over each frame for all the trials for all the subjects using Facemesh (blue), 68-points (orange) and KLT (green)

subjects irrespective of different facial features. However, KLT was influenced by different facial features which is consistent with what is reported by other studies [176].

After analyzing the performance through visualization, inverse coefficient of variation was used to analyze the performance of different methods visually as well as quantitatively.

$$CV^{-1} = \frac{\mu}{\sigma} \dots\dots\dots\dots\dots\dots\dots 2$$

The equation 2 was used to find the inverse coefficient of variation. The coefficient of variation is a quantitative measure of the dispersion of data mainly used to measure

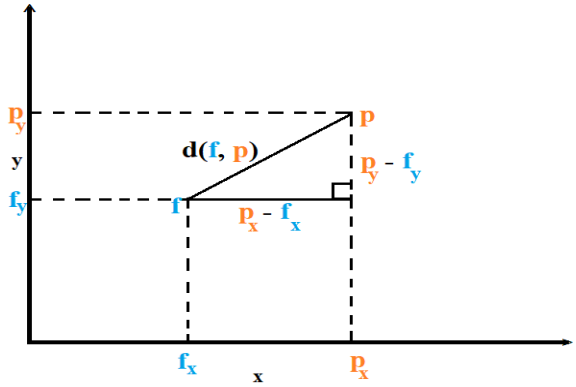

Figure 5-5: Euclidian distance (d(f,p)) calculation where f represents the center of centroid cluster calculated using Facemesh and p represents the centroid of the cluster of the 68-points

variation in the measurement. The lower the coefficient of variation, the better is the performance. The inverse coefficient of variation was calculated to visually present the results. As opposed to the coefficient of variation, in case of inverse coefficient of variation the higher the inverse coefficient of variation, the better would be the performance. Using this inverse coefficient of variation, Figure 5-4 showed that Facemesh performed better than 68-points and KLT.

KLT was more influenced by the different factors such as external illumination and failed to detect any ROI for approximately more than half of the total duration during some of the trials for 2 subjects. In addition, several investigators have shown that 68-points method performs fairly well to detect and track ROI to calculate HR and BR. Hence in further comparison only Facemesh and 68-points were considered, in order to access how Facemesh performed against 68-points for each subject and trial.

To quantify the comparison, Euclidian distance was calculated between clusters of centroids calculated using Facemesh (blue) and 68-points (orange) using below equation 3. In the equation "f" is the center of the cluster of centroids calculated using Facemesh and "p" is the center of the cluster of centroids calculated using 68-points and d(f,p) is the

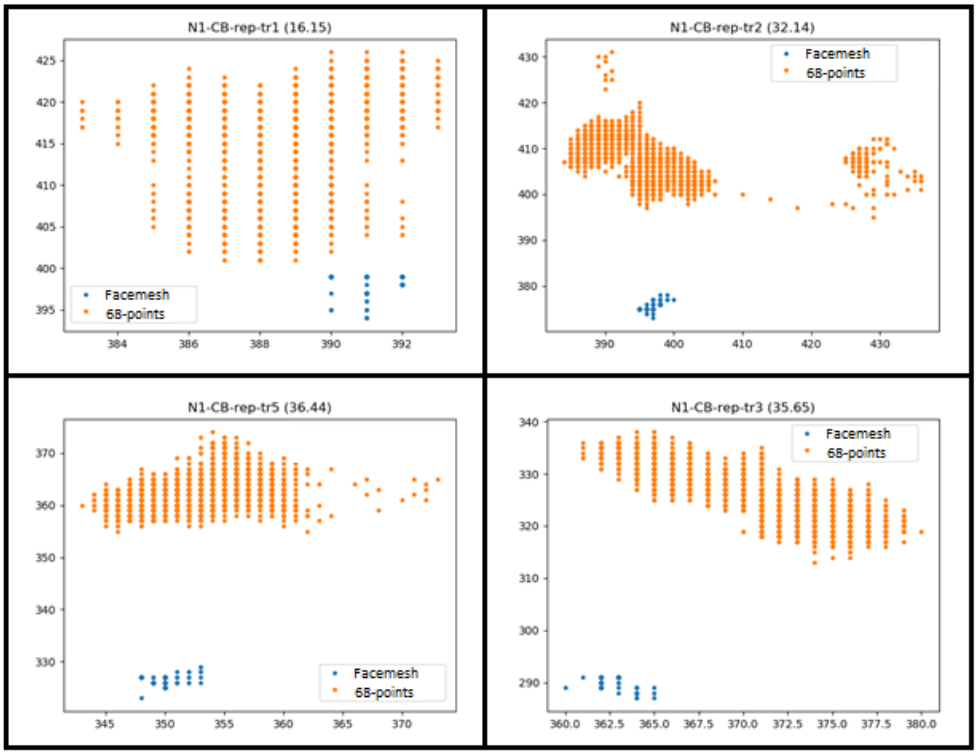

Figure 5-6: An example of comparison of total-ROI between Facemesh (blue) and 68-points (orange)

Euclidian distance. Figure 5-5 represents the below equation visually where the f and p follow the color scheme same as it is shown later in Figure 5-6.

$$d(f,p) = \sqrt{\sum_{i=x,y}(p_i - f_i)^2} \ldots\ldots\ldots\ldots\ldots 3$$

Figure 5-6 shows example scatters plots showing centroid coordinates (X (pixels) and Y(pixels)) calculated over frames during four different trials for a single subject. The heading for each subplot shows the Euclidian distance between the clusters of centroids calculated using Facemesh and 68-points for that trial. The maximum Euclidian distance for all the subjects during all the trials was approximately 45 pixels which is a small value while the distribution of centroids detected was less for Facemesh than 68-points. This suggests the following. The total-ROI detected using Facemesh were spatially as accurate as 68-points which is a widely used method for ROI detection and tracking. Facemesh was found less susceptible to the minimal motion of the faces of the subjects with respect to the video frame than 68-points.

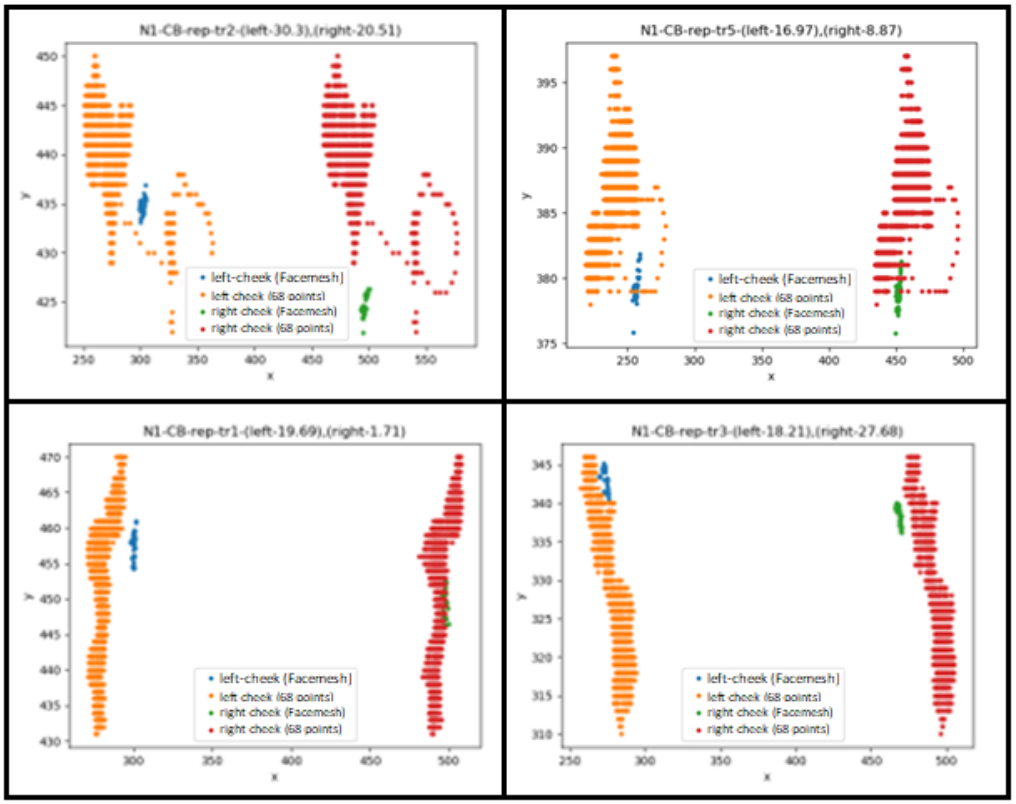

Figure 5-7: Centroid of the left cheek and right cheek detected and tracked using Facemesh and 68-points

5.1.2.2 Performance estimation using cheeks-ROI centroid variation

As discussed before investigators have shown that cheeks and foreheads are the regions that appear to be the most viable regions to contain information regarding blood flow that can be used for extraction of HR and BR. The article shows the 68 points cover the region between eyebrows and chin[191]. Hence forehead couldn't be directly extracted from the 68-points method. That's why 68-points approach was used only for extraction of face and cheeks. From Facemesh face, cheeks and forehead were extracted in the frame for all the frames of the collected videos. In this section, the comparison of performance in extracting cheeks using Facemesh and 68-points approach is discussed. For visual and quantitative comparison, the centroid of left-cheek and right cheek were calculated over frames of the videos of all the subjects for every trial. Figure 5-7 shows an example of the centroids of the cheeks tracked through frames using Facemesh and 68-points. In the captions for each plot the Euclidian distance is included which shows the Euclidian distance between right and left cheeks tracked across frames. The Euclidian distance calculated for all the videos for all the subjects and trials showed a maximum Euclidian distance of approximately 30 pixels which suggests that the spatial difference between the cheeks detected was very minimal while the distribution of centroids of the cheeks was lesser for Facemesh than 68-points. This suggests the following two findings. First, cheeks detected using Facemesh were spatially as accurate as 68-points which is a widely used method in detecting and tracking ROI to find HR and BR. Second, Facemesh is more susceptible to the minimal motion of the faces of the subjects with respect to the video frame and 68-points.

5.1.3 Comparison between non-contact and contact HR and BR

Data were collected during a study which was approved by the Institutional Review Board at the University of Kentucky (IRB), and all subjects provided written consent before the start of the experiment. The details about the study during which the data for non-contact and contact measurement were recorded are given in section 3.2. Subjects (3 female and 3 male, age 18-30) sat in a comfortable chair. A single lead of ECG was recorded for calculation of HR, i.e., referred to as contact HR. Respitrace signals (abdominal and chest breathing pattern) were used for calculation of breathing rate, i.e., referred to as contact BR. Video of the face was collected using SONY digital camera

RX100, videos were collected at 30 frames per second (fps). ECG and breathing pattern were digitized at 1000 Samples/second using a commercial data acquisition system. Video, ECG and breathing pattern were recorded simultaneously for about 2-3 minutes in each trial.

5.1.3.1 Signal processing of contact measurements

ECG signal was used to calculate R peaks followed by computation of RRI. HR in beats per minute (BPM) was computed from the RRI.

For BR, the abdominal and thoracic breathing patterns were added together to create one breathing pattern. The auto spectrum of the breathing pattern was calculated using Welch's method with 100 secs window length, Hanning window and 50% overlap. From the auto spectrum, BR was found out by computing the corresponding frequency of the highest peak in the frequency region 0.1-0.4 Hz [192]. The frequency in Hz was multiplied by a factor of 60 to calculate BR in breaths per minute (bpm).

5.1.3.2 Video processing

The algorithm used for the calculation of non-contact HR and BR is as depicted in the flowchart shown in Figure 5-8 and described below.

- Individual frames were extracted from the video as shown in the flowchart.
- As described before 68-points and Facemesh were used to implement detection and tracking of ROI such as face, left cheek and right cheek using both methods and forehead using Facemesh.
- As in the face only skin region contains the blood flow-related information, it is necessary to filter out noise from the face such as beard, eyebrows, glass frames, eyes and light-reflected regions. For this reason, HSV (hue, saturation, value) thresholding followed by extracting skin mask by a series of erosion and dilation was carried out using an elliptical kernel. The aforementioned skin mask was used on the image to extract the skin region only.
- As described before, green channel is known to contain most information about the blood flow. Researchers have found out that plane orthogonal skin (POS) performed fairly well in comparison to using the raw green and average of green, blue, and red channels.

- As shown in Figure 5-8, the left cheek and, right cheek were extracted from the red, green, and blue frame which was followed by calculation of the spatial average of the frames.

$$POS(t)=X1(t)+\frac{\sigma 1(t,L)}{\sigma 2(t,L)}X2(t)\ldots\ldots\ 4$$

$$X1(t)=G(t)-B(t)\ldots\ldots\ldots\ldots\ldots\ 5$$

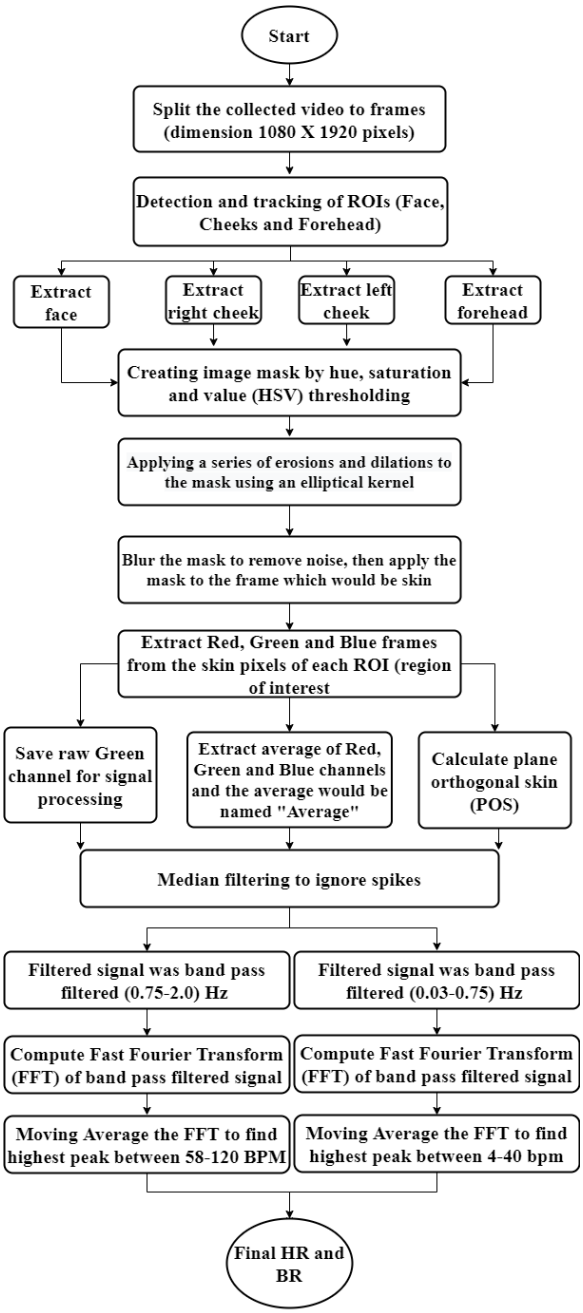

Figure 5-8: Flowchart showing image and signal processing workflow to find HR and BR

$$X2(t)=G(t)+B(t)-2R(t) \quad \ldots\ldots\ldots\ldots 6$$

Where, G(t) = Green channel,

B(t) = Blue channel,

R(t) = Red channel

σ_1 and σ_2 are the running standard deviation of *X1* and *X2,* while the length of L was 1.6s [34].

- In a previous study, it was shown that plane orthogonal skin (POS) showed an acceptable correlation with the contact measurement[34]. The authors discussed that POS cancels out the noise due to speckle contrast and variation in the illumination of the incident light. As in our case the experiment was done in ambient light condition, plane orthogonal skin (POS) was calculated using the equation above which was reported by Unakafov et. al [34].

5.1.3.3 Signal processing of non-contact channels

As shown in Figure 5-1 and flowchart Figure 5-8, raw green, average , and POS signals were median filtered to remove unwanted spikes which were occasionally observed in signals extracted from the lip region. The median filtered signal was bandpass filtered to get HR and BR. For HR, the signal was bandpass filtered in the range 0.75-2.0 Hz, followed by calculation of fast Fourier transform (FFT). As the end step for HR calculation, the FFT of the signal was filtered using a moving average filter, and the highest peak detected in the range of 58-120 BPM was used to calculate the HR.

For BR calculation, the signal was bandpass filtered in the range 0.03-0.75 Hz, followed by calculation of FFT of the filtered signal. As the end step for calculation of BR, the FFT was filtered using a moving average filter, and the maximum peak was calculated in the range 4-40 bpm. All signal processing was done using open-source python programming.

For overall comparison between contact and non-contact measurement correlation method followed by the Bland and Altmann method was used. Scatterplots showing the correlation coefficient were used to check the linear relation between the two measurements. A higher correlation between contact and non-contact measurement would suggest linear relation between non-contact and

contact measurements. Bland and Altmann method was used to evaluate the agreement between two measurements. Bland and Altman plot is a graphical method to plot the difference scores of two measurements against the mean of the measurements for each trial [193], [194].

For the comparison at a granular level, the scatterplot with the correlation between measurements was evaluated in two ways, per subject and per trial. The plots per subject for all the trials showed the linear relationship (if any) between the measurements calculated over trials. The plots per trial for all subjects showed the linear relationship (if any) between the measurements calculated during the same trial for all the subjects. This comparison was done to investigate whether the measurement match was consistent for all the subjects for the same trial.

While the granular level comparison was helpful in quantifying the performance for each trial and each subject, statistical analysis was not conducted due to limited sample size i.e., 6 subjects who participated in 7 studies with 8 trials in each study (one study was repeated). These comparisons are discussed in the following sections.

5.1.3.4 Comparison between non-contact and contact BR

In this section the performance of BR measurement using non-contact and contact methods are discussed in detail.

5.1.3.4.1 Facemesh

As described before, Facemesh showed the best performance among all three methods used to extract ROI. BR was calculated by following the aforementioned video and signal processing workflow which was followed by validation against contact measurement. Figure 5-9, Figure 5-10, Figure 5-11 and Figure 5-12 show the Bland and Altman plot (left) and scatterplot showing correlation coefficient and regression fit along with univariate distribution (right) for the contact BR and non-contact BR extracted from face, forehead, left-cheek and right-cheek respectively. Figure 5-9 shows that the sample points lied well within the 95% confidence interval and the difference between contact and non-contact BR extracted from face was maximum of 3 bpm while most of the points lied between 0-1 bpm. The scatterplot showing regression fit shows that the correlation was approximately 94%. Figure 5-10 shows that while the sample points lied within the 95%

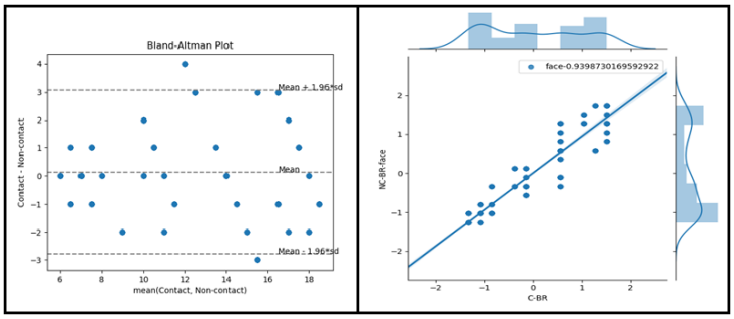

Figure 5-9: Bland-Altmann plot (left) and correlation plot (right) with probability distribution of contact and non-contact (face) BR using Facemesh

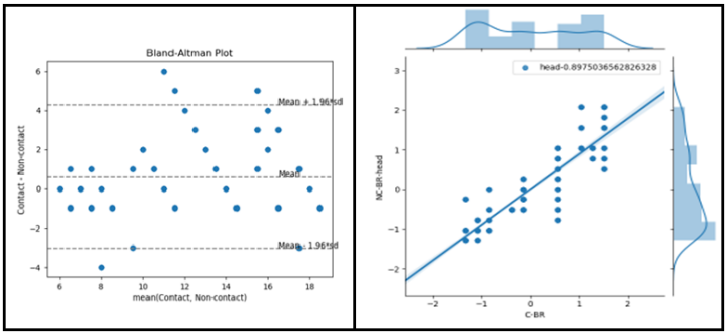

Figure 5-10: Bland-Altmann plot (left) and correlation plot (right) with probability distribution of contact and non-contact (forehead) BR using Facemesh

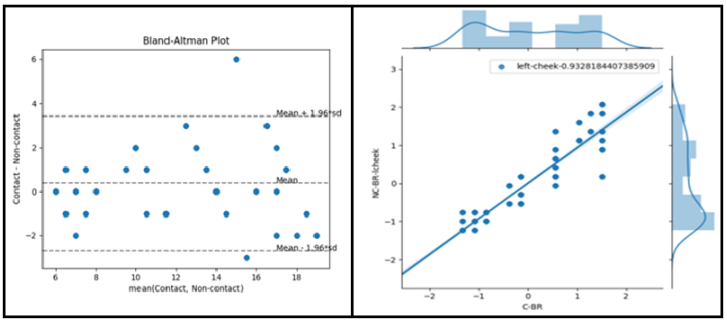

Figure 5-11: Bland-Altmann plot (left) and correlation plot (right) with probability distribution of contact and non-contact (left-cheek) BR using Facemesh

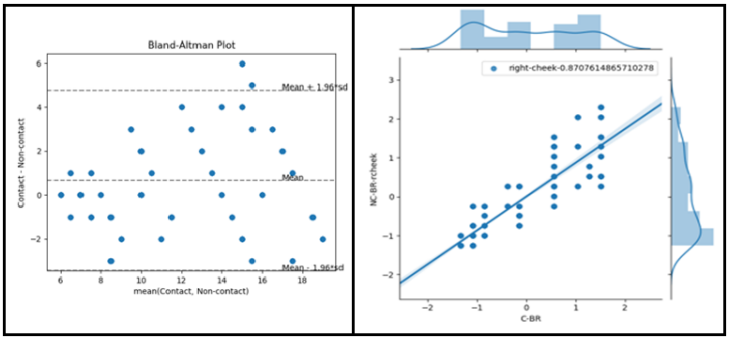

Figure 5-12: Bland-Altmann plot (left) and correlation plot (right) with probability distribution of contact and non-contact (right-cheek) BR using Facemesh

confidence interval there were more outliers in comparison to Figure 5-9 (left) suggesting

the forehead's better performance than that of the entire face. The difference between contact and non-contact BR extracted from forehead was a maximum of 4 bpm. The scatterplot showing regression fit shows that the correlation coefficient was approximately 90%. The difference between contact and non-contact BR extracted from the left-cheek was approximately 3 bpm. The scatterplot showing regression fit shows that the correlation coefficient was approximately 0.93. The difference between contact and non-contact BR extracted from right-cheek was approximately 4 bpm. The scatterplot showing regression fit shows that the correlation coefficient was approximately 87%.

The non-contact BR calculated from face performed best among all the locations extracted from the face using Facemesh. After face, left-cheek performed better than right-cheek and forehead in calculation of BR.

5.1.3.4.2 68-points

Next to Facemesh, 68-points showed acceptable performance in extracting ROI. In this section, the performance of 68-points in calculating BR in comparison to contact BR is discussed in detail. Figure 5-13, Figure 5-14, and Figure 5-15 show the Bland-Altman plot (left) and scatterplot showing correlation coefficient and regression fit along with univariate distribution (right) for the contact BR and non-contact BR extracted from face, left-cheek and right-cheek respectively. 68-points facial landmark system did not allow direct extraction of forehead. Therefore face, left-cheek and right-cheek were the regions

considered for non-contact BR extraction. Figure 5-13 shows that the difference between contact and non-contact BR extracted from face was approximately 3 bpm. The scatterplot

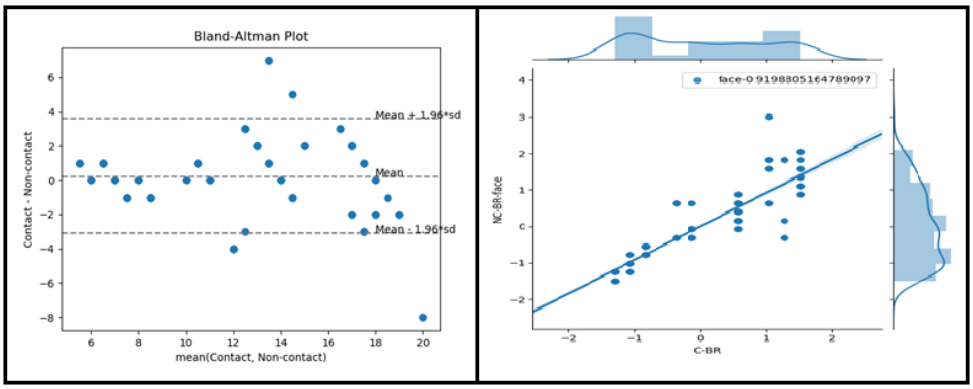

Figure 5-13: Bland-Altmann plot (left) and correlation plot (right) with probability distribution of contact and non-contact (face) BR using 68-points

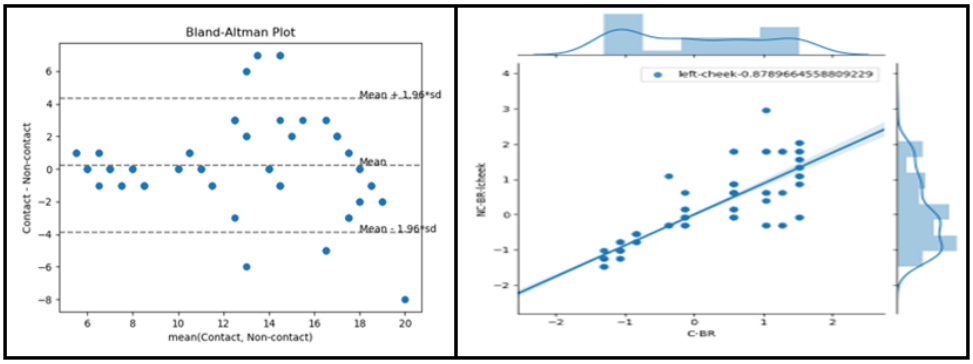

Figure 5-14: Bland-Altmann plot (left) and correlation plot (right) with probability distribution of contact and non-contact (left-cheek) BR using 68-points

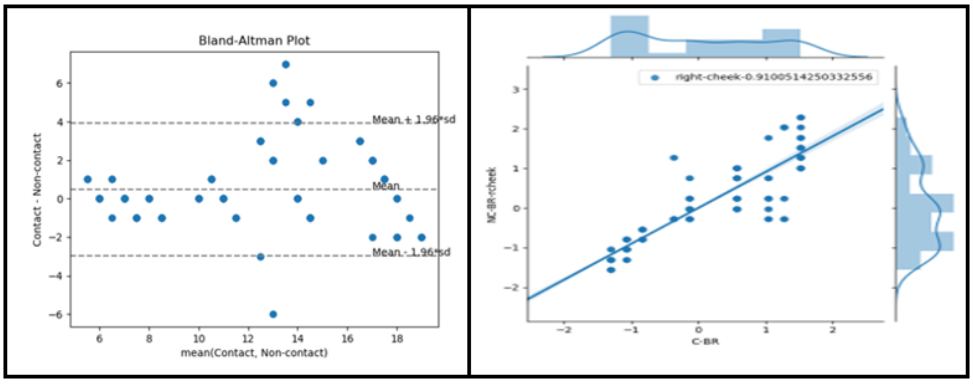

Figure 5-15: Bland-Altmann plot (left) and correlation plot (right) with probability distribution of contact and non-contact (right-cheek) BR using 68-points

with regression fit shows the correlation to be approximately 92%. Figure 5-14 shows that the difference between contact and non-contact BR extracted from the left-cheek was approximately 4 bpm and the regression fit shows a correlation of approximately 88%.

Figure 5-15 shows that the BRs extracted from right-cheek show a difference of

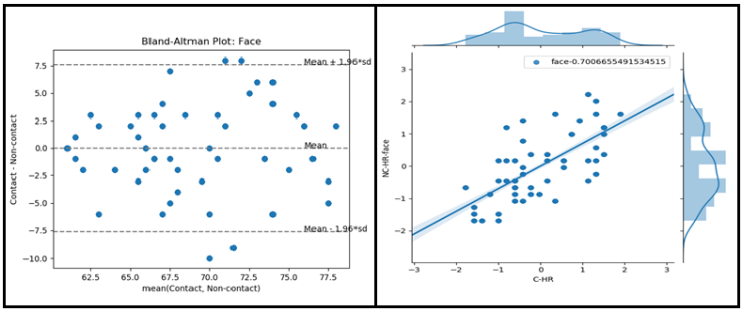

Figure 5-16: Bland-Altmann plot (left) and correlation plot (right) with probability distribution of contact and non-contact (face) HR using Facemesh

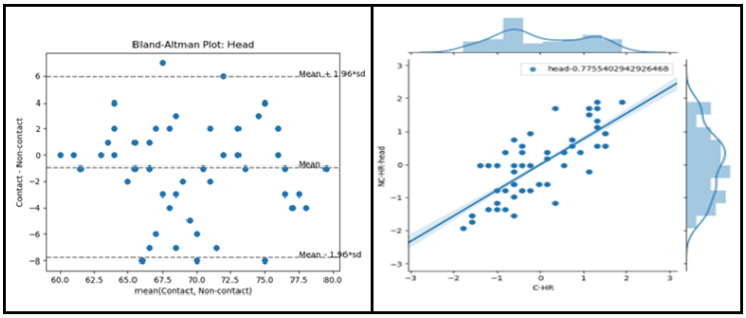

Figure 5-17: Bland-Altmann plot (left) and correlation plot (right) with probability distribution of contact and non-contact (forehead) HR using Facemesh

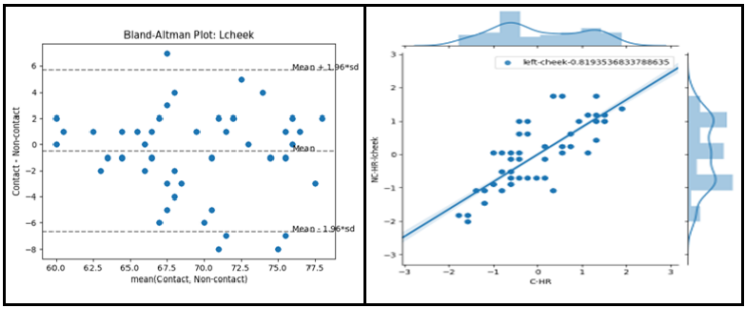

Figure 5-18: Bland-Altmann plot (left) and correlation plot (right) with probability distribution of contact and non-contact (left-cheek) HR using Facemesh

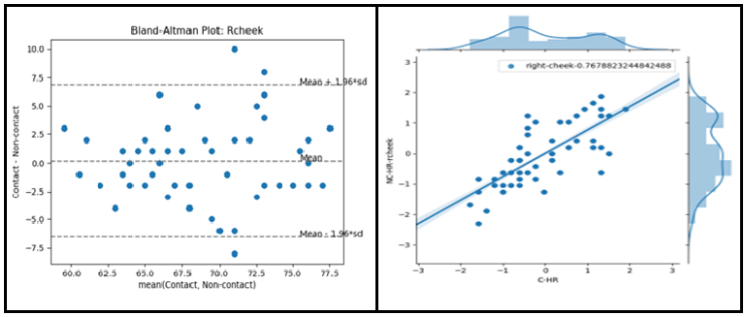

Figure 5-19: Bland-Altmann plot (left) and correlation plot (right) with probability distribution of contact and non-contact (right-cheek) HR using Facemesh

approximately 4 bpm and the correlation was approximately 91%. In case of Facemesh as well as 68-points, face performed best among all the locations.

5.1.3.5 Comparison between non-contact and contact HR

In this section the performance of HR measurement using non-contact and contact methods are discussed in detail.

5.1.3.5.1 Facemesh

HR was calculated by following the aforementioned video and signal processing workflow. Figure 5-16, Figure 5-17, Figure 5-18, and Figure 5-19 show the Bland and Altman plot (left) and regression fit (right) showing correlation coefficient along with univariate distribution for the contact HR and non-contact HR extracted from face, forehead, left-cheek and right-cheek respectively. Figure 5-16 shows that all the sample points but 4 lied well within the 95% confidence interval and the difference between contact and non-contact HR extracted from face was approximately 7 beats per minute (BPM). The scatterplot showing regression fit shows that the correlation coefficient was approximately 70% which suggests moderate match between contact and non-contact HR calculated from face. Figure 5-17 shows that all the sample points lied within the 95% confidence interval and the differences between contact and non-contact HR extracted from forehead was approximately 6 BPM. The regression fit showed approximately 78% correlation which was better than that for the face. Figure 5-18 shows that the difference between contact and non-contact HR extracted from the left-cheek was approximately 6 BPM i.e., same as that of forehead. The scatterplot showing regression fit shows correlation of approximately 82% which is better than the forehead. Figure 5-19 shows the difference between contact and non-contact HR extracted from right-cheek was approximately 7 BPM. The scatterplot showing regression fit shows that the correlation coefficient was approximately 77%. This suggested that in HR calculation using Facemesh, left-cheek performed better than other locations. Face and right-cheek showed similar match between contact and non-contact HR.

5.1.3.5.2 68-points

In this section, the performance of 68-points in calculating non-contact HR in comparison to contact HR is discussed in detail. Figure 5-20, Figure 5-21 and Figure 5-22 show the Bland and Altman plot (left) and scatterplot showing correlation coefficient and regression fit along with univariate distribution (right) for the contact HR and non-contact HR extracted from face, left-cheek and right-cheek respectively. Face, left-cheek and right-cheek extracted from video of the faces of the subjects using 68-points were the regions

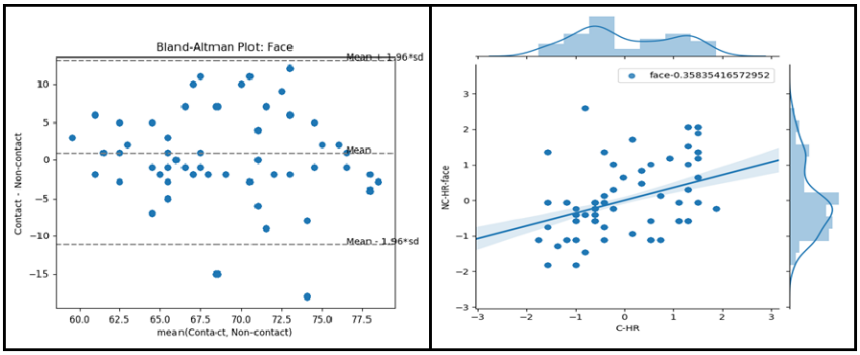

Figure 5-20: Bland-Altmann plot (left) and correlation plot (right) with probability distribution of contact and non-contact (face) HR using 68-points

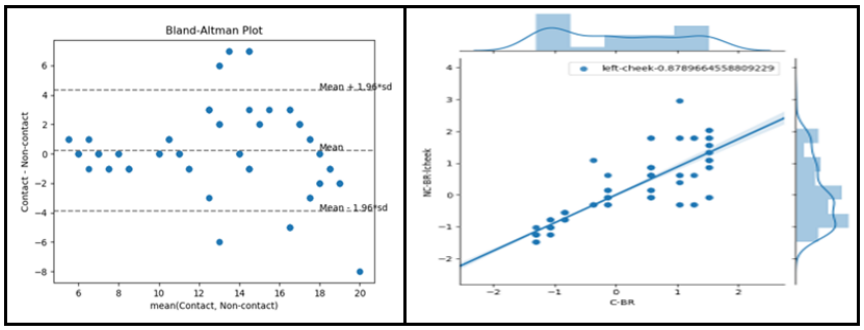

Figure 5-21: Bland-Altmann plot (left) and correlation plot (right) with probability distribution of contact and non-contact (left-cheek) HR using 68-points

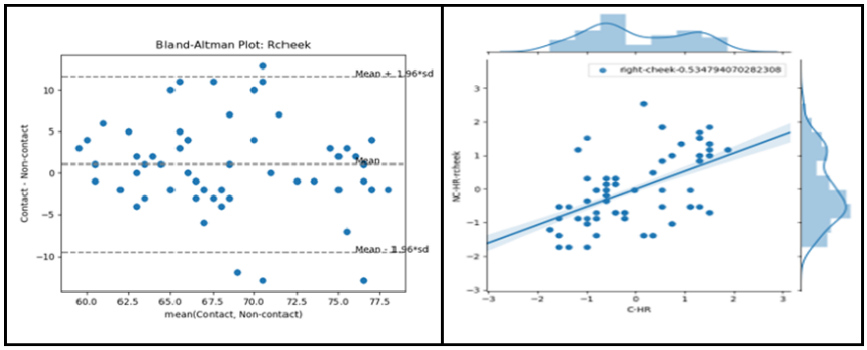

Figure 5-22: Bland-Altmann plot (left) and correlation plot (right) with probability distribution of contact and non-contact (right-cheek) HR using 68-points

considered for non-contact HR extraction. The difference between contact and non-contact HR extracted from face was approximately 10 BPM. The regression fit shows that the correlation coefficient was approximately 36%. Figure 5-21 shows that the difference between contact and non-contact HR extracted from left-cheek was approximately 10 BPM and the correlation between contact and non-contact HR extracted from the left-cheek was approximately 54%. Figure 5-22 shows the difference between contact and non-contact HR extracted from right-cheek was approximately 10 BPM and the correlation between contact HR and non-contact HR extracted from right-cheek showed a correlation of approximately 53%. As was also the case with Facemesh, using 68-points method showed that left-cheek performed better than other locations for calculation of HR. The above discussed results suggest that 68-points did not perform as well as Facemesh. Overall, the method used to calculate non-contact HR did not perform as accurately as that of BR.

A review by Hassan et al. [66] states that the performance (Bland-Altman plots) of HR, for the studies mentioned in the review, that the best performing HR showed a difference ranging between -5 to +15 BPM and according to the studies mentioned before the difference range was between -40 to +45 BPM. In our case the performance was found to be better than the aforementioned studies which suggested that the proposed workflow provided improved accuracy. However, in the context of subtle changes as those expected in our study, further refinement of the algorithm including recruitment of more subjects may be necessary.

High accuracy in calculation of BR than that of HR suggests the extraction of higher frequency component (0.75-2.0 Hz) was more influenced by external illumination variation, than that of lower frequency component. It suggests that the low-frequency component was less influenced by external factors such as illumination. This might explain no difference between contact BR and non-contact BR during most trials.

CHAPTER 6: CONCLUSION

In the first aim of the study, the goal was to determine whether the changes in autonomic and EEG responses that are observed while listening to songs are a direct effect of listening to songs or if they are (or partially) due to the changes in breathing pattern which occurs when listening to songs. Towards this goal, a visual-feedback based program was developed and tested in order for subjects to be able to voluntarily control their breathing to reproduce the breathing pattern recorded during listening to songs.

This was a pilot study and hence the results of this study are considered to be preliminary in nature. Therefore, although we did find interesting trends, further investigation with larger pool of subjects would be necessary before conclusions regarding the effects can be drawn. The cardiorespiratory trends were observed for each song irrespective of whether spontaneous or control of breathing was used which indicates that even though control of breathing may have an effect, which suggested that the effects produced by listening to different songs were present irrespective of the act of control of breathing and no change in breathing pattern.

The interaction between RRI and breathing signal while listening to songs showed higher interaction with RRI than of the control of breathing sub-trials of the song suggesting the effects due to change in breathing pattern may be secondary.

From coherencies, it was also found out that, the breathing pattern plays some role in commonality between coherencies of RRI and breathing pattern of song sub-trials. Therefore, results of our analysis suggested that listening to the song as well as change in breathing patterns had an effect on autonomic responses, but it is possible that the effect of listening to songs may surpass the effect due to control of breathing.

The visual feedback-based control of breathing program, although developed for the specific study described here, has the potential to be useful in other applications as well. Subjects found that controlling their breathing using the developed software was easy. Therefore, the developed program could be used in studies and applications where modification of breathing patterns is likely to be useful.

Below is a summary of key points for aim 1.

- A visual-feedback based program was developed and tested in order for subjects to be able to voluntarily control their breathing to reproduce the breathing pattern recorded during listening to songs.
- This was a pilot study and hence the results of this study are considered to be preliminary in nature.
- The cardiorespiratory trends suggested that even though control of breathing may have an effect, the effects produced by listening to songs surpassed the act of control of breathing.
- Coherence results also suggested that, listening to the song as well as change in breathing patterns had an effect on autonomic responses, but it is possible that the effect of listening to songs may surpass the effect due to control of breathing.
- The visual feedback-based control of breathing program, although developed for the specific study, has the potential to be useful in other applications as well. Subjects found that controlling their breathing using the developed software was easy. Therefore, the developed program could be used in other studies and applications where modification of breathing patterns is likely to be useful.

In the second aim of this study the goal was to develop the non-contact measurement system using RGB camera and to test it in a study condition where the physiological parameters were expected to change minimally (listening to songs) to determine if the non-contact measurement is feasible in measuring HR and BR with adequate resolution. We tested the non-contact measurement without changing the study design and subject recruitment i.e., used the non-contact measurement with subjects of different skin color, variable distance of the subject from the camera (less than 2 meters) and ambient light conditions. Towards this goal, a data analysis framework was designed incorporating new and widely used methods for different stages of analysis. Results showed that non-contact BR extraction performed better than non-contact HR when compared with contact measurements. The Facemesh method performed better than 68-points in ROI detection which improved the performance of BR and HR extraction. Because the BR performance was more accurate than HR, this suggested that the proposed framework was able to extract low-frequency range parameters better than high-frequency range parameters. At this point, our study suggests that the non-contact measurement system could be useful for BR

extraction in case of the studies where relatively less changes in these are expected, however, for HR extraction more refinement including different approaches for extraction of information from the ROI would be necessary. Although the designed framework performed better than widely used methods, we recognize that there is still a lot of room for improvement to achieve better performance of the measurements.

Below is a summary of the key findings from the study for aim 2.

- Non-contact BR extraction performed better than non-contact HR when compared with contact measurements.
- The Facemesh method performed better than 68-points in ROI detection which improved the performance of BR and HR extraction.
- The BR performance was more accurate than HR, which suggested that the proposed framework was able to extract low-frequency range parameters better than high-frequency range parameters.
- Our results suggest that the non-contact measurement system, with some refinement, could be useful for BR extraction in case of the studies where relatively less changes in these are expected, however, for HR extraction significant refinement including different approaches for extraction of information from the ROI would be necessary.

CHAPTER 7: FUTURE DIRECTIONS

The first aim of the study investigated effects of two songs (fast and slow tempo) on brain signals, RR intervals obtained from ECG and breathing pattern while subjects breathed spontaneously vs when they voluntarily controlled their breathing. This study was a pilot study. Results showed some trends which need to be explored further by recruiting more subjects in order to test for statistically significant effects. While investigation of effects using moving window has the potential to reveal trends over time, the small magnitude of effects indicates that much longer duration or studies would be needed. Two types of songs were used, song1 was fast rhythm song and song2 was slow rhythm song. The trends were not similar for both the songs for all of the physiological parameters. Hence it would be helpful to further study the effects of the rhythm of song on these physiological parameters. Further, longer duration trials could be helpful in investigating any possible trends as well as for more averaging.

Along with finding cardiorespiratory interaction, we also explored the interaction between RR intervals, and breathing pattern with EEG. Our approach involved investigation of interaction between frequency bands of EEG (recorded from F3, F4, T3, T4, P3, P4, O1 and O2) and other signals using coherence. Time-frequency analysis could add more insights about this interaction in terms of frequency variation with time.

Conducting similar study with songs of different genre which has been suggested to affect autonomic response may be helpful in studying the role of respiration in producing the autonomic responses. Using different breathing patterns may help for stress release but through pathways that may be complementary but somewhat different than those that produce the effects of listening to songs. The developed software could also be used if breathing to certain patterns is desired, for example if effects of different inspiratory/expiratory intervals are to be studied during metronomic breathing. Therefore, the developed biofeedback software has the capability to be useful in a variety of studies or applications where voluntary control of breathing to produce different breathing patterns would be beneficial.

The objective of the second aim was to develop a framework and workflow for the extraction of HR and BR that could be used in studies where non-contact measurements may be advantageous. There has been a lot of interest in the area of non-contact

measurement using cameras and similarly, there has been a lot of advancement in terms of algorithm development and optimization. In this study some of the widely used methods, for source location on face and, the extracted source signal was used to find non-contact HR and BR. Using other approaches was felt to be helpful to compare their performance against the proposed approach using Facemesh. The proposed algorithm was designed to work with different skin colors in ambient lighting to find the possibility of using non-contact measurement in an environment similar to where the described study was conducted.

While use of Facemesh (explained in CHAPTER 5) showed improvement in terms of estimation of HR and BR over the currently widely used methods, refinement of the approach would be needed to get the precision that would be needed to detect subtle changes as would be expected in the types of study that was conducted. While Facemesh helps with tracking of ROI, exploration of other spectroscopic methods to extract better information from the ROI are likely to be helpful.

As the results show, the algorithm performed better in extracting BR than HR i.e., the workflow worked better for lower frequency range than for higher range. One possible reason could be the variation in illumination and/ or skin color variation. To verify whether these factors affected the performance in different frequency ranges and to further improve the workflow, the same workflow can be tested in different environments in terms of illumination and with a wider range of subject skin tones. Another approach would be to control the illumination or making the illumination more even on the skin. Although in our present approach we wanted to explore the feasibility of making non-contact measurements without changing ambient lighting conditions, it may be worth to try illumination changes in future studies with a focus on improving the accuracy of the HR and BR estimation.

In this study the non-contact measurement was used without any skin-prep before the start of the study. The designed image processing workflow for extraction of skin from the frames was successful in extracting skin with the exception of skin-portion affected by reflection of light on the skin. The skin portion that included light reflection due to the oily texture of the skin was not detected as skin by the image processing algorithm which might have affected the performance of the different locations on the face. Skin-prep before the experiment could be helpful in taking out any possible oil residue from the face. One other

option would be to consider other locations than that of the face such as neck which contains fewer oil glands than the face.

Facemesh landmarks include 468 points which represent different locations of the face such as eyes, eyebrows, cheeks, inner lips, outer lips, nose, silhouette of the face, and forehead. The possibility of extracting the aforementioned locations with a greater number of points, has the advantage of extracting larger or smaller area for cheek extraction, extraction of adaptive sized patches rather than fixed area from the skin region from the frame. The same workflow could be used to explore whether different patches or combination of patches of the skin to lead to improved measurement of HR and BR.

The base machine learning (ML) architecture behind Facemesh is MobilenetV2 which is a light model which makes it easier for landmark detection on WASM environment. Recently there has been more advancement in the ML model architecture for the purpose such as face and object detection and tracking. Training the Facemesh with newer alternative architecture which is even faster than MobilenetV2 could be helpful in building real-time, easy implement and scalable applications for the extraction of HR and BR. Although this may not necessarily improve accuracy, but it would improve speed.

The thought behind using this workflow approach was that the need for higher computational power would be less than other approaches and that it would be comparatively easier to implement it in real-time in the future.

APPENDIX: GLOSSARY

Names and Abbreviations	Description
HR	Heart rate
BR	Breathing rate
HRV	Heart rate variability
BRV	Breathing rate variability
ECG	Electrocardiograph
EEG	Electroencephalograph
IR	Infra-red
RGB	Red, Green, Blue
RRI	RR interval
ROI	Region of interest
KLT	Kanade-Lucas-Tomasi
AR	Augmented reality
68-points	68-points landmarks system
POS	plane orthogonal skin
LF	Low-frequency
HF	High-frequency
HF/LF ratio	HF to LF power ratio
FFT	Fast frequency transform
HSV	Hue, Saturation, Value
PPG	Photoplethysmograph
Commercial DAS	Commercial data acquisition system
USB DAQ	NI USB 6001
fps	Frames per second
BPM	Beats per minute
bpm	Breaths per minute
RMSE	Root mean squared error
NRMSE	Normalized root mean squared error
CC	**C**ontrol trial's **C**ontrol (silence)
CCB	**C**ontrol trial's **C**ontrol of **B**reathing

SC1	**S**ong trial's **C**ontrol (listening to song1)
SCB1	Listening to **S**ong1 while **C**ontrolling **B**reathing
NSCB1	**N**ot listening to **S**ong1 while **C**ontrolling **B**reathing
SC2	**S**ong trial's **C**ontrol (listening to song2)
SCB2	Listening to **S**ong2 while **C**ontrolling **B**reathing
NSCB2	**N**ot listening to **S**ong2 while **C**ontrolling **B**reathing
WO-song1	While not listening to song1
W-song1	While listening to song1
WO-song2	While not listening to song2
W-song2	While listening to song2
CPU	Computer processing unit
GPU	Graphics processing unit
CV	Coefficient of variation

REFERENCES

[1] A. Patwardhan, S. Vallurupalli, J. Evans, E. Bruce, and C. Knapp, "Override of spontaneous respiratory pattern generator reduces cardiovascular parasympathetic influence," *Journal of Applied Physiology*, vol. 79, no. 3, pp. 1048–1054, 1995.

[2] L. Bernardi *et al.*, "Effects of controlled breathing, mental activity and mental stress with or without verbalization on heart rate variability," *Journal of the American College of Cardiology*, vol. 35, no. 6, pp. 1462–1469, 2000.

[3] L. Bernardi, C. Porta, and P. Sleight, "Cardiovascular, cerebrovascular, and respiratory changes induced by different types of music in musicians and non-musicians: the importance of silence," *Heart*, vol. 92, no. 4. pp. 445–52, 2006. doi: hrt.2005.064600 [pii] 10.1136/hrt.2005.064600.

[4] G. Wannamethee, A. G. Shaper, and P. W. Macfarlane, "Heart rate, physical activity, and mortality from cancer and other noncardiovascular diseases," *American journal of epidemiology*, vol. 137, no. 7, pp. 735–748, 1993.

[5] L. Bernardi, F. Valle, M. Coco, A. Calciati, and P. Sleight, "Physical activity influences heart rate variability and very-low-frequency components in Holter electrocardiograms," *Cardiovascular research*, vol. 32, no. 2, pp. 234–237, 1996.

[6] A. Emaus *et al.*, "Does a variation in self-reported physical activity reflect variation in objectively measured physical activity, resting heart rate, and physical fitness? Results from the Tromsø study," *Scandinavian journal of public health*, vol. 38, no. 5_suppl, pp. 105–118, 2010.

[7] E. Kroupi, J.-M. Vesin, and T. Ebrahimi, "Driver-response relationships between frontal EEG and Respiration during affective audiovisual stimuli," in *2013 35th Annual International Conference of the IEEE Engineering in Medicine and Biology Society (EMBC)*, 2013, pp. 2911–2914.

[8] J. Bhattacharya, H. Petsche, and E. Pereda, "Interdependencies in the spontaneous EEG while listening to music," *International Journal of Psychophysiology*, vol. 42, no. 3, pp. 287–301, Nov. 2001, doi: 10.1016/S0167-8760(01)00153-2.

[9] S. Ogata, "Human Eeg Responses to Classical Music and Simulated White Noise: Effects of a Musical Loudness Component on Consciousness," *Percept Mot Skills*, vol. 80, no. 3, pp. 779–790, Jun. 1995, doi: 10.2466/pms.1995.80.3.779.

[10] A. Dey, S. K. Palit, D. K. Bhattacharya, D. N. Tibarewala, and D. Das, "STUDY OF THE EFFECT OF MUSIC ON CENTRAL NERVOUS SYSTEM THROUGH LONG TERM ANALYSIS OF EEG SIGNAL IN TIME DOMAIN," *International Journal of Engineering Sciences*, vol. 5, no. 1, p. 9.

[11] S. Koelsch and W. A. Siebel, "Towards a neural basis of music perception," *Trends in cognitive sciences*, vol. 9, no. 12, pp. 578–584, 2005.

[12] S. Koelsch and L. Jäncke, "Music and the heart," *Eur Heart J*, vol. 36, no. 44, pp. 3043–3049, Nov. 2015, doi: 10.1093/eurheartj/ehv430.

[13] I. Grishchenko, A. Ablavatski, Y. Kartynnik, K. Raveendran, and M. Grundmann, "Attention Mesh: High-fidelity Face Mesh Prediction in Real-time," *arXiv preprint arXiv:2006.10962*, 2020.

[14] E. Altenmüller, K. Schürmann, V. K. Lim, and D. Parlitz, “Hits to the left, flops to the right: different emotions during listening to music are reflected in cortical lateralisation patterns,” *Neuropsychologia*, vol. 40, no. 13, pp. 2242–2256, 2002.
[15] O. Grewe, F. Nagel, R. Kopiez, and E. Altenmüller, “How does music arouse ‘chills’? Investigating strong emotions, combining psychological, physiological, and psychoacoustical methods,” *Annals of the New York Academy of Sciences*, vol. 1060, no. 1, pp. 446–449, 2005.
[16] J. Panksepp and G. Bernatzky, “Emotional sounds and the brain: the neuro-affective foundations of musical appreciation,” *Behavioural processes*, vol. 60, no. 2, pp. 133–155, 2002.
[17] A. J. Blood and R. J. Zatorre, “Intensely pleasurable responses to music correlate with activity in brain regions implicated in reward and emotion,” *Proceedings of the national academy of sciences*, vol. 98, no. 20, pp. 11818–11823, 2001.
[18] L. Bernardi *et al.*, “Dynamic Interactions Between Musical, Cardiovascular, and Cerebral Rhythms in Humans,” *Circulation*, vol. 119, no. 25, pp. 3171–3180, Jun. 2009, doi: 10.1161/CIRCULATIONAHA.108.806174.
[19] L. Bernardi, C. Porta, and P. Sleight, “Cardiovascular, cerebrovascular, and respiratory changes induced by different types of music in musicians and non-musicians: the importance of silence,” *Heart*, vol. 92, no. 4, pp. 445–452, 2006.
[20] L. Bernardi *et al.*, “Effect of rosary prayer and yoga mantras on autonomic cardiovascular rhythms: comparative study,” *BMJ*, vol. 323, no. 7327, pp. 1446–1449, Dec. 2001, doi: 10.1136/bmj.323.7327.1446.
[21] D. Biswal, M. J. Mollakazemi, S. Thyagarajan, J. Evans, and A. Patwardhan, “Baroreflex Sensitivity During Listening to Music Computed from Time Domain Sequences and Frequency Domain Transfer Function,” in *2018 40th Annual International Conference of the IEEE Engineering in Medicine and Biology Society (EMBC)*, 2018, pp. 2776–2779.
[22] M. J. Mollakazemi, D. Biswal, J. Evans, and A. Patwardhan, “Eigen Decomposition of Cardiac Synchronous EEGs for Investigation of Neural Effects of Tempo and Cognition of Songs,” in *2018 40th Annual International Conference of the IEEE Engineering in Medicine and Biology Society (EMBC)*, 2018, pp. 2402–2405.
[23] M. Mollakazemi, D. Biswal, S. Elayi, S. Thyagarajan, J. Evans, and A. Patwardhan, “Synchronization of Autonomic and Cerebral Rhythms During Listening to Music: Effects of Tempo and Cognition of Songs.,” *Physiological research*, vol. 68, no. 6, 2019.
[24] M. J. Mollakazemi, D. Biswal, and A. Patwardhan, “Target Frequency Band of Cognition and Tempo of Music: Cardiac Synchronous EEG,” in *2018 IEEE International Symposium on Signal Processing and Information Technology (ISSPIT)*, 2018, pp. 696–700.
[25] H. Bringman, K. Giesecke, A. Thörne, and S. Bringman, “Relaxing music as pre-medication before surgery: a randomised controlled trial,” *Acta Anaesthesiologica Scandinavica*, vol. 53, no. 6, pp. 759–764, Jul. 2009, doi: 10.1111/j.1399-6576.2009.01969.x.
[26] H.-J. Trappe, “The effects of music on the cardiovascular system and cardiovascular health,” *Heart*, vol. 96, no. 23, pp. 1868–1871, Dec. 2010, doi: 10.1136/hrt.2010.209858.

[27] H.-J. Trappe, “Role of music in intensive care medicine,” *Int J Crit Illn Inj Sci*, vol. 2, no. 1, p. 27, 2012, doi: 10.4103/2229-5151.94893.
[28] S. Koelsch and J. Mulder, “Electric brain responses to inappropriate harmonies during listening to expressive music,” *Clinical Neurophysiology*, vol. 113, no. 6, pp. 862–869, Jun. 2002, doi: 10.1016/S1388-2457(02)00050-0.
[29] L. Bernardi, C. Porta, A. Gabutti, L. Spicuzza, and P. Sleight, “Modulatory effects of respiration,” *Auton Neurosci*, vol. 90, no. 1–2. pp. 47–56, 2001. doi: S1566-0702(01)00267-3 [pii] 10.1016/S1566-0702(01)00267-3.
[30] D. Biswal, M. J. Mollakazemi, and A. Patwardhan, “Changes in Coherent Activity Between EEG and Various Frequency Components of Music While Listening to Familiar and Unfamiliar Songs,” in *2020 IEEE International Symposium on Smart Electronic Systems (iSES) (Formerly iNiS)*, 2020, pp. 31–34. doi: 10.1109/iSES50453.2020.00018.
[31] L. A. Schmidt and L. J. Trainor, “Frontal brain electrical activity (EEG) distinguishes valence and intensity of musical emotions,” *Cognition and Emotion*, vol. 15, no. 4, pp. 487–500, Jul. 2001, doi: 10.1080/0269993004200187.
[32] S. Weiss and H. M. Mueller, “The contribution of EEG coherence to the investigation of language,” *Brain and Language*, vol. 85, no. 2, pp. 325–343, May 2003, doi: 10.1016/S0093-934X(03)00067-1.
[33] S. Schneider, V. Brümmer, T. Abel, C. D. Askew, and H. K. Strüder, “Changes in brain cortical activity measured by EEG are related to individual exercise preferences,” *Physiology & Behavior*, vol. 98, no. 4, pp. 447–452, Oct. 2009, doi: 10.1016/j.physbeh.2009.07.010.
[34] A. M. Unakafov, “Pulse rate estimation using imaging photoplethysmography: generic framework and comparison of methods on a publicly available dataset,” *Biomedical Physics & Engineering Express*, vol. 4, no. 4, p. 045001, 2018.
[35] M. Harford, J. Catherall, S. Gerry, J. D. Young, and P. Watkinson, “Availability and performance of image-based, non-contact methods of monitoring heart rate, blood pressure, respiratory rate, and oxygen saturation: a systematic review,” *Physiological measurement*, vol. 40, no. 6, p. 06TR01, 2019.
[36] E. B. Blackford, J. R. Estepp, A. M. Piasecki, M. A. Bowers, and S. L. Klosterman, “Long-range non-contact imaging photoplethysmography: cardiac pulse wave sensing at a distance,” in *Optical Diagnostics and Sensing XVI: Toward Point-of-Care Diagnostics*, 2016, vol. 9715, p. 971512.
[37] E. B. Blackford and J. R. Estepp, “Using consumer-grade devices for multi-imager non-contact imaging photoplethysmography,” in *Optical Diagnostics and Sensing XVII: Toward Point-of-Care Diagnostics*, 2017, vol. 10072, p. 100720P.
[38] M. Hu *et al.*, “Dual-mode imaging system for non-contact heart rate estimation during night,” in *2017 IEEE International Conference on Multimedia & Expo Workshops (ICMEW)*, 2017, pp. 97–102.
[39] O. Gupta, D. McDuff, and R. Raskar, “Real-time physiological measurement and visualization using a synchronized multi-camera system,” in *Proceedings of the IEEE Conference on Computer Vision and Pattern Recognition Workshops*, 2016, pp. 46–53.
[40] J. R. Estepp, E. B. Blackford, and C. M. Meier, “Recovering pulse rate during motion artifact with a multi-imager array for non-contact imaging

photoplethysmography," in *2014 IEEE International Conference on Systems, Man, and Cybernetics (SMC)*, 2014, pp. 1462–1469.

[41] E. B. Blackford and J. R. Estepp, "Using consumer-grade devices for multi-imager non-contact imaging photoplethysmography," San Francisco, California, United States, Feb. 2017, p. 100720P. doi: 10.1117/12.2253409.

[42] K. M. Lee and ACCV, Eds., *Computer vision - ACCV 2012: 11th Asian Conference on Computer Vision, Daejeon, Korea, November 5 - 9, 2012; revised selected papers. Pt. 2: ...* Berlin: Springer, 2013.

[43] S. Xu, L. Sun, and G. K. Rohde, "Robust efficient estimation of heart rate pulse from video," *Biomed. Opt. Express*, vol. 5, no. 4, p. 1124, Apr. 2014, doi: 10.1364/BOE.5.001124.

[44] R. R. Fletcher, D. Chamberlain, N. Paggi, and X. Deng, "Implementation of smart phone video plethysmography and dependence on lighting parameters," in *2015 37th Annual International Conference of the IEEE Engineering in Medicine and Biology Society (EMBC)*, 2015, pp. 3747–3750.

[45] R. Koprowski, "Blood pulsation measurement using cameras operating in visible light: limitations," *Biomedical engineering online*, vol. 15, no. 1, pp. 1–15, 2016.

[46] T. Coppetti *et al.*, "Accuracy of smartphone apps for heart rate measurement," *European journal of preventive cardiology*, vol. 24, no. 12, pp. 1287–1293, 2017.

[47] K.-Z. Lee, P.-C. Hung, and L.-W. Tsai, "Contact-free heart rate measurement using a camera," in *2012 Ninth Conference on Computer and Robot Vision*, 2012, pp. 147–152.

[48] M. Rapczynski, P. Werner, and A. Al-Hamadi, "Effects of video encoding on camera-based heart rate estimation," *IEEE Transactions on Biomedical Engineering*, vol. 66, no. 12, pp. 3360–3370, 2019.

[49] A. Gudi, M. Bittner, R. Lochmans, and J. van Gemert, "Efficient real-time camera based estimation of heart rate and its variability," in *Proceedings of the IEEE/CVF International Conference on Computer Vision Workshops*, 2019, pp. 0–0.

[50] E. Magdalena Nowara, T. K. Marks, H. Mansour, and A. Veeraraghavan, "SparsePPG: Towards driver monitoring using camera-based vital signs estimation in near-infrared," in *Proceedings of the IEEE conference on computer vision and pattern recognition workshops*, 2018, pp. 1272–1281.

[51] I. C. Jeong and J. Finkelstein, "Introducing contactless blood pressure assessment using a high speed video camera," *Journal of medical systems*, vol. 40, no. 4, p. 77, 2016.

[52] N. Sugita, K. Obara, M. Yoshizawa, M. Abe, A. Tanaka, and N. Homma, "Techniques for estimating blood pressure variation using video images," in *2015 37th annual international conference of the IEEE engineering in medicine and biology society (EMBC)*, 2015, pp. 4218–4221.

[53] T. Blöcher, J. Schneider, M. Schinle, and W. Stork, "An online PPGI approach for camera based heart rate monitoring using beat-to-beat detection," in *2017 IEEE Sensors Applications Symposium (SAS)*, 2017, pp. 1–6.

[54] C. Wang, T. Pun, and G. Chanel, "A Comparative Survey of Methods for Remote Heart Rate Detection From Frontal Face Videos," *Front Bioeng Biotechnol*, vol. 6, May 2018, doi: 10.3389/fbioe.2018.00033.

[55] M.-Z. Poh, D. J. McDuff, and R. W. Picard, “Non-contact, automated cardiac pulse measurements using video imaging and blind source separation,” *Opt. Express*, vol. 18, no. 10, p. 10762, May 2010, doi: 10.1364/OE.18.010762.
[56] D. McDuff, S. Gontarek, and R. Picard, “Remote measurement of cognitive stress via heart rate variability,” in *2014 36th Annual International Conference of the IEEE Engineering in Medicine and Biology Society*, 2014, pp. 2957–2960.
[57] A. Al-Naji, K. Gibson, and J. Chahl, “Remote sensing of physiological signs using a machine vision system,” *Journal of medical engineering & technology*, vol. 41, no. 5, pp. 396–405, 2017.
[58] L. Capdevila, L. Capdevila, J. Moreno, J. Movellan, E. Parrado, and J. Ramos-Castro, “HRV based health&sport markers using video from the face,” in *2012 Annual International Conference of the IEEE Engineering in Medicine and Biology Society*, 2012, pp. 5646–5649.
[59] S. W. Cheatham, M. J. Kolber, and M. P. Ernst, “Concurrent validity of resting pulse-rate measurements: a comparison of 2 smartphone applications, the polar H7 belt monitor, and a pulse oximeter with bluetooth,” *Journal of sport rehabilitation*, vol. 24, no. 2, pp. 171–178, 2015.
[60] D. McDuff and E. Blackford, “iphys: An open non-contact imaging-based physiological measurement toolbox,” in *2019 41st Annual International Conference of the IEEE Engineering in Medicine and Biology Society (EMBC)*, 2019, pp. 6521–6524.
[61] M. van Gastel, S. Stuijk, and G. de Haan, “Motion robust remote-PPG in infrared,” *IEEE Transactions on Biomedical Engineering*, vol. 62, no. 5, pp. 1425–1433, 2015.
[62] E. B. Blackford, A. M. Piasecki, and J. R. Estepp, “Measuring pulse rate variability using long-range, non-contact imaging photoplethysmography,” in *2016 38th Annual International Conference of the IEEE Engineering in Medicine and Biology Society (EMBC)*, 2016, pp. 3930–3936.
[63] A. Al-Naji and J. Chahl, “Simultaneous tracking of cardiorespiratory signals for multiple persons using a machine vision system with noise artifact removal,” *IEEE journal of translational engineering in health and medicine*, vol. 5, pp. 1–10, 2017.
[64] A. Al-Naji and J. Chahl, “Remote respiratory monitoring system based on developing motion magnification technique,” *Biomedical Signal Processing and Control*, vol. 29, pp. 1–10, 2016.
[65] M. I. Davila, G. F. Lewis, and S. W. Porges, “The Physiocam: a novel non-contact sensor to Measure heart rate Variability in clinical and Field applications,” *Frontiers in public health*, vol. 5, p. 300, 2017.
[66] M. A. Hassan *et al.*, “Heart rate estimation using facial video: A review,” *Biomedical Signal Processing and Control*, vol. 38, pp. 346–360, 2017.
[67] G. Balakrishnan, F. Durand, and J. Guttag, “Detecting pulse from head motions in video,” in *Proceedings of the IEEE Conference on Computer Vision and Pattern Recognition*, 2013, pp. 3430–3437.
[68] O. T. Inan, “Recent advances in cardiovascular monitoring using ballistocardiography,” in *2012 Annual International Conference of the IEEE Engineering in Medicine and Biology Society*, 2012, pp. 5038–5041.

[69] S. Sanyal and K. K. Nundy, "Algorithms for monitoring heart rate and respiratory rate from the video of a user's face," *IEEE Journal of translational engineering in health and medicine*, vol. 6, pp. 1–11, 2018.
[70] R. Rahman, K. Ukai, and S. Kobashi, "A filter-based method to calculate heart rate from near infrared video," in *2018 Joint 10th International Conference on Soft Computing and Intelligent Systems (SCIS) and 19th International Symposium on Advanced Intelligent Systems (ISIS)*, 2018, pp. 1154–1159.
[71] N. Martinez, M. Bertran, G. Sapiro, and H.-T. Wu, "Non-contact photoplethysmogram and instantaneous heart rate estimation from infrared face video," *arXiv preprint arXiv:1902.05194*, 2019.
[72] C. Barbosa Pereira, H. Dohmeier, J. Kunczik, N. Hochhausen, R. Tolba, and M. Czaplik, "Contactless monitoring of heart and respiratory rate in anesthetized pigs using infrared thermography," *PloS one*, vol. 14, no. 11, p. e0224747, 2019.
[73] K. S. Tan, R. Saatchi, H. Elphick, and D. Burke, "Real-time vision based respiration monitoring system," in *2010 7th International Symposium on Communication Systems, Networks & Digital Signal Processing (CSNDSP 2010)*, 2010, pp. 770–774.
[74] R. Iles, "145 structured light plethysmography, a non invasive, non contact method of recording respiratory function," *Archives of Disease in Childhood*, vol. 97, no. Suppl 2, pp. A41–A41, 2012.
[75] M. Bartula, T. Tigges, and J. Muehlsteff, "Camera-based system for contactless monitoring of respiration," in *2013 35th Annual International Conference of the IEEE Engineering in Medicine and Biology Society (EMBC)*, 2013, pp. 2672–2675.
[76] A. Loblaw, J. Nielsen, M. Okoniewski, and M. A. Lakhani, "Remote respiratory sensing with an infrared camera using the Kinect (TM) infrared projector," in *Proceedings of the International Conference on Image Processing, Computer Vision, and Pattern Recognition (IPCV)*, 2013, p. 1.
[77] F. Benetazzo, A. Freddi, A. Monteriù, and S. Longhi, "Respiratory rate detection algorithm based on RGB-D camera: theoretical background and experimental results," *Healthcare technology letters*, vol. 1, no. 3, pp. 81–86, 2014.
[78] A. Cenci, D. Liciotti, E. Frontoni, A. Mancini, and P. Zingaretti, "Non-contact monitoring of preterm infants using RGB-D camera," in *International Design Engineering Technical Conferences and Computers and Information in Engineering Conference*, 2015, vol. 57199, p. V009T07A003.
[79] R. Janssen, W. Wang, A. Moço, and G. De Haan, "Video-based respiration monitoring with automatic region of interest detection," *Physiological measurement*, vol. 37, no. 1, p. 100, 2015.
[80] Y. Nam, Y. Kong, B. Reyes, N. Reljin, and K. H. Chon, "Monitoring of heart and breathing rates using dual cameras on a smartphone," *PloS one*, vol. 11, no. 3, p. e0151013, 2016.
[81] J. Jorge *et al.*, "Non-contact assessment of peripheral artery haemodynamics using video infrared thermography," *IEEE Transactions on Biomedical Engineering*, 2020.
[82] B. A. Reyes, N. Reljin, Y. Kong, Y. Nam, and K. H. Chon, "Tidal volume and instantaneous respiration rate estimation using a volumetric surrogate signal

acquired via a smartphone camera," *IEEE journal of biomedical and health informatics*, vol. 21, no. 3, pp. 764–777, 2016.

[83] R. Murthy, I. Pavlidis, and P. Tsiamyrtzis, "Touchless monitoring of breathing function," in *The 26th Annual International Conference of the IEEE Engineering in Medicine and Biology Society*, 2004, vol. 1, pp. 1196–1199.

[84] J. Fei, Z. Zhu, and I. Pavlidis, "Imaging respiratory rate in the CO2 absorption band," in *Proceedings of the 27th Annual International Conference of the IEEE Engineering in Medicine and Biology Society,(Shanghai, China)*, 2005, pp. 700–590.

[85] Z. Zhu, J. Fei, and I. Pavlidis, "Tracking human breath in infrared imaging," in *Fifth IEEE Symposium on Bioinformatics and Bioengineering (BIBE'05)*, 2005, pp. 227–231.

[86] J. Fei and I. Pavlidis, "Thermistor at a distance: unobtrusive measurement of breathing," *IEEE transactions on biomedical engineering*, vol. 57, no. 4, pp. 988–998, 2009.

[87] A. K. Abbas, K. Heimann, K. Jergus, T. Orlikowsky, and S. Leonhardt, "Neonatal non-contact respiratory monitoring based on real-time infrared thermography," *Biomedical engineering online*, vol. 10, no. 1, pp. 1–17, 2011.

[88] A. K. Abbas, K. Heiman, T. Orlikowsky, and S. Leonhardt, "Non-contact respiratory monitoring based on real-time IR-thermography," in *World Congress on Medical Physics and Biomedical Engineering, September 7-12, 2009, Munich, Germany*, 2009, pp. 1306–1309.

[89] G. F. Lewis, R. G. Gatto, and S. W. Porges, "A novel method for extracting respiration rate and relative tidal volume from infrared thermography," *Psychophysiology*, vol. 48, no. 7, pp. 877–887, 2011.

[90] L. J. Goldman, "Nasal airflow and thoracoabdominal motion in children using infrared thermographic video processing," *Pediatric pulmonology*, vol. 47, no. 5, pp. 476–486, 2012.

[91] J. H. Klaessens, M. Van Den Born, A. van der Veen, J. Sikkens-van de Kraats, F. A. van den Dungen, and R. M. Verdaasdonk, "Development of a baby friendly non-contact method for measuring vital signs: first results of clinical measurements in an open incubator at a neonatal intensive care unit," in *Advanced biomedical and clinical diagnostic systems XII*, 2014, vol. 8935, p. 89351P.

[92] X. Li, J. Chen, G. Zhao, and M. Pietikainen, "Remote Heart Rate Measurement from Face Videos under Realistic Situations," in *2014 IEEE Conference on Computer Vision and Pattern Recognition*, Columbus, OH, USA, Jun. 2014, pp. 4264–4271. doi: 10.1109/CVPR.2014.543.

[93] S. L. Bennett, R. Goubran, and F. Knoefel, "The detection of breathing behavior using Eulerian-enhanced thermal video," in *2015 37th Annual International Conference of the IEEE Engineering in Medicine and Biology Society (EMBC)*, 2015, pp. 7474–7477.

[94] C. B. Pereira, X. Yu, M. Czaplik, R. Rossaint, V. Blazek, and S. Leonhardt, "Remote monitoring of breathing dynamics using infrared thermography," *Biomedical optics express*, vol. 6, no. 11, pp. 4378–4394, 2015.

[95] H. Jeong, Y. Matsuura, and Y. Ohno, "Measurement of Respiration Rate and Depth Through Difference in Temperature Between Skin Surface and Nostril by Using

Thermal Image.," *Studies in health technology and informatics*, vol. 245, pp. 417–421, 2017.

[96] A. Kwasniewska, J. Ruminski, and J. Wtorek, "The motion influence on respiration rate estimation from low-resolution thermal sequences during attention focusing tasks.," in *Annual International Conference of the IEEE Engineering in Medicine and Biology Society. IEEE Engineering in Medicine and Biology Society. Annual International Conference*, 2017, vol. 2017, pp. 1421–1424.

[97] K. Mutlu, J. E. Rabell, P. M. Del Olmo, and S. Haesler, "IR thermography-based monitoring of respiration phase without image segmentation," *Journal of neuroscience methods*, vol. 301, pp. 1–8, 2018.

[98] M. Lewandowska, J. Rumiński, T. Kocejko, and J. Nowak, "Measuring pulse rate with a webcam—a non-contact method for evaluating cardiac activity," in *2011 federated conference on computer science and information systems (FedCSIS)*, 2011, pp. 405–410.

[99] L. Scalise, N. Bernacchia, I. Ercoli, and P. Marchionni, "Heart rate measurement in neonatal patients using a webcamera," in *2012 IEEE International Symposium on Medical Measurements and Applications Proceedings*, 2012, pp. 1–4.

[100] L. A. Aarts *et al.*, "Non-contact heart rate monitoring utilizing camera photoplethysmography in the neonatal intensive care unit—A pilot study," *Early human development*, vol. 89, no. 12, pp. 943–948, 2013.

[101] L. K. Mestha, S. Kyal, B. Xu, L. E. Lewis, and V. Kumar, "Towards continuous monitoring of pulse rate in neonatal intensive care unit with a webcam," in *2014 36th Annual International Conference of the IEEE Engineering in Medicine and Biology Society*, 2014, pp. 3817–3820.

[102] S. C. K. Lam, K. L. Wong, K. O. Wong, W. Wong, and W. H. Mow, "A smartphone-centric platform for personal health monitoring using wireless wearable biosensors," in *2009 7th International Conference on Information, Communications and Signal Processing (ICICS)*, 2009, pp. 1–7.

[103] A. Lam and Y. Kuno, "Robust Heart Rate Measurement from Video Using Select Random Patches," in *2015 IEEE International Conference on Computer Vision (ICCV)*, Dec. 2015, pp. 3640–3648. doi: 10.1109/ICCV.2015.415.

[104] J. M. Saragih, S. Lucey, and J. F. Cohn, "Deformable model fitting by regularized landmark mean-shift," *International journal of computer vision*, vol. 91, no. 2, pp. 200–215, 2011.

[105] D. McDuff, S. Gontarek, and R. W. Picard, "Improvements in remote cardiopulmonary measurement using a five band digital camera," *IEEE Transactions on Biomedical Engineering*, vol. 61, no. 10, pp. 2593–2601, 2014.

[106] M.-Z. Poh, D. J. McDuff, and R. W. Picard, "Advancements in noncontact, multiparameter physiological measurements using a webcam," *IEEE transactions on biomedical engineering*, vol. 58, no. 1, pp. 7–11, 2010.

[107] L. Feng, L.-M. Po, X. Xu, Y. Li, and R. Ma, "Motion-resistant remote imaging photoplethysmography based on the optical properties of skin," *IEEE Transactions on Circuits and Systems for Video Technology*, vol. 25, no. 5, pp. 879–891, 2014.

[108] M. Kumar, A. Veeraraghavan, and A. Sabharwal, "DistancePPG: Robust non-contact vital signs monitoring using a camera," *Biomed. Opt. Express*, vol. 6, no. 5, p. 1565, May 2015, doi: 10.1364/BOE.6.001565.

[109] D. Biswal, M. J. Mollakazemi, B. Place, and A. Patwardhan, “Heart Rate and Breathing Rate Calculated from Cheeks and Lips Using Green and Derived Colors from Video,” in *2020 IEEE International Symposium on Smart Electronic Systems (iSES)(Formerly iNiS)*, 2020, pp. 23–26.
[110] G. De Haan and V. Jeanne, “Robust pulse rate from chrominance-based rPPG,” *IEEE Transactions on Biomedical Engineering*, vol. 60, no. 10, pp. 2878–2886, 2013.
[111] W. Wang, S. Stuijk, and G. De Haan, “Exploiting spatial redundancy of image sensor for motion robust rPPG,” *IEEE transactions on Biomedical Engineering*, vol. 62, no. 2, pp. 415–425, 2014.
[112] H. Aoki and H. Nakamura, “Non-contact respiration measurement during exercise tolerance test by using kinect sensor,” *Sports*, vol. 6, no. 1, p. 23, 2018.
[113] F. Bevilacqua, P. Backlund, and H. Engstrom, “Proposal for non-contact analysis of multimodal inputs to measure stress level in serious games,” in *2015 7th international conference on games and virtual worlds for serious applications (VS-Games)*, 2015, pp. 1–4.
[114] F. Bousefsaf, C. Maaoui, and A. Pruski, “Remote assessment of the heart rate variability to detect mental stress,” in *2013 7th International Conference on Pervasive Computing Technologies for Healthcare and Workshops*, 2013, pp. 348–351.
[115] F. Bousefsaf, C. Maaoui, and A. Pruski, “Remote assessment of physiological parameters by non-contact technologies to quantify and detect mental stress states,” in *2014 International Conference on Control, Decision and Information Technologies (CoDIT)*, 2014, pp. 719–723.
[116] F. Chen, L. Kong, Y. Zhao, L. Dong, M. Liu, and M. Hui, “Non-contact measurement of mental stress via heart rate variability,” in *Applications of Digital Image Processing XLIII*, 2020, vol. 11510, p. 115101I.
[117] K. Iuchi *et al.*, “Stress levels estimation from facial video based on non-contact measurement of pulse wave,” *Artificial Life and Robotics*, vol. 25, no. 3, pp. 335–342, 2020.
[118] C. Puri, L. Olson, I. Pavlidis, J. Levine, and J. Starren, “StressCam: non-contact measurement of users’ emotional states through thermal imaging,” in *CHI’05 extended abstracts on Human factors in computing systems*, 2005, pp. 1725–1728.
[119] S. Nikolaiev, S. Telenyk, and Y. Tymoshenko, “Non-contact video-based remote photoplethysmography for human stress detection,” *Journal of Automation Mobile Robotics and Intelligent Systems*, vol. 14, 2020.
[120] D. McDuff *et al.*, “Non-contact imaging of peripheral hemodynamics during cognitive and psychological stressors,” *Scientific Reports*, vol. 10, no. 1, pp. 1–13, 2020.
[121] M. Villarroel *et al.*, “Continuous non-contact vital sign monitoring in neonatal intensive care unit,” *Healthcare technology letters*, vol. 1, no. 3, pp. 87–91, 2014.
[122] J. Jorge *et al.*, “Non-contact monitoring of respiration in the neonatal intensive care unit,” in *2017 12th IEEE International Conference on Automatic Face & Gesture Recognition (FG 2017)*, 2017, pp. 286–293.

[123] J. Allen, “Photoplethysmography and its application in clinical physiological measurement,” *Physiol. Meas.*, vol. 28, no. 3, pp. R1–R39, Mar. 2007, doi: 10.1088/0967-3334/28/3/R01.
[124] P.-C. Hung, K.-Z. Lee, and L.-W. Tsai, “Contact-free heart rate measurement using multiple video data,” in *AIP Conference Proceedings*, 2013, vol. 1559, no. 1, pp. 57–66.
[125] C. Lueangwattana, T. Kondo, and H. Haneishi, “A comparative study of video signals for non-contact heart rate measurement,” in *2015 12th International Conference on Electrical Engineering/Electronics, Computer, Telecommunications and Information Technology (ECTI-CON)*, 2015, pp. 1–5.
[126] K. Mannapperuma, B. D. Holton, P. J. Lesniewski, and J. C. Thomas, “Performance limits of ICA-based heart rate identification techniques in imaging photoplethysmography,” *Physiological measurement*, vol. 36, no. 1, p. 67, 2014.
[127] E. Christinaki *et al.*, “Comparison of blind source separation algorithms for optical heart rate monitoring,” in *2014 4th International Conference on Wireless Mobile Communication and Healthcare-Transforming Healthcare Through Innovations in Mobile and Wireless Technologies (MOBIHEALTH)*, 2014, pp. 339–342.
[128] W. J. Jiang, S. C. Gao, P. Wittek, and L. Zhao, “Real-time quantifying heart beat rate from facial video recording on a smart phone using Kalman filters,” in *2014 IEEE 16th International Conference on e-Health Networking, Applications and Services (Healthcom)*, 2014, pp. 393–396.
[129] T. Pursche, J. Krajewski, and R. Moeller, “Video-based heart rate measurement from human faces,” in *2012 IEEE international conference on consumer electronics (ICCE)*, 2012, pp. 544–545.
[130] H. Monkaresi, R. A. Calvo, and H. Yan, “A machine learning approach to improve contactless heart rate monitoring using a webcam,” *IEEE journal of biomedical and health informatics*, vol. 18, no. 4, pp. 1153–1160, 2013.
[131] A. M. Unakafov, S. Möller, I. Kagan, A. Gail, S. Treue, and F. Wolf, “Using imaging photoplethysmography for heart rate estimation in non-human primates,” *PLoS One*, vol. 13, no. 8, p. e0202581, 2018.
[132] S. Tulyakov, X. Alameda-Pineda, E. Ricci, L. Yin, J. F. Cohn, and N. Sebe, “Self-Adaptive Matrix Completion for Heart Rate Estimation from Face Videos under Realistic Conditions,” in *2016 IEEE Conference on Computer Vision and Pattern Recognition (CVPR)*, Jun. 2016, pp. 2396–2404. doi: 10.1109/CVPR.2016.263.
[133] P. Viola, M. Jones, and others, “Robust real-time object detection,” *International journal of computer vision*, vol. 4, no. 34–47, p. 4, 2001.
[134] C. Tomasi and T. Kanade, “Detection and tracking of point,” features. Technical Report CMU-CS-91-132, Carnegie, Mellon University, 1991.
[135] B. D. Lucas, T. Kanade, and others, “An iterative image registration technique with an application to stereo vision,” 1981.
[136] Jianbo Shi and Tomasi, “Good features to track,” in *Proceedings of IEEE Conference on Computer Vision and Pattern Recognition CVPR-94*, Seattle, WA, USA, 1994, pp. 593–600. doi: 10.1109/CVPR.1994.323794.
[137] Y. Wu and Q. Ji, “Facial landmark detection: A literature survey,” *International Journal of Computer Vision*, vol. 127, no. 2, pp. 115–142, 2019.

[138] S. Tan, D. Chen, C. Guo, and Z. Huang, "Extra facial landmark localization via global shape reconstruction," *Computational intelligence and neuroscience*, vol. 2017, 2017.
[139] J. Lv, X. Shao, J. Xing, C. Cheng, and X. Zhou, "A deep regression architecture with two-stage re-initialization for high performance facial landmark detection," in *Proceedings of the IEEE conference on computer vision and pattern recognition*, 2017, pp. 3317–3326.
[140] M. Koestinger, P. Wohlhart, P. M. Roth, and H. Bischof, "Annotated facial landmarks in the wild: A large-scale, real-world database for facial landmark localization," in *2011 IEEE international conference on computer vision workshops (ICCV workshops)*, 2011, pp. 2144–2151.
[141] P. N. Belhumeur, D. W. Jacobs, D. J. Kriegman, and N. Kumar, "Localizing parts of faces using a consensus of exemplars," *IEEE transactions on pattern analysis and machine intelligence*, vol. 35, no. 12, pp. 2930–2940, 2013.
[142] C. Sagonas, G. Tzimiropoulos, S. Zafeiriou, and M. Pantic, "300 faces in-the-wild challenge: The first facial landmark localization challenge," in *Proceedings of the IEEE International Conference on Computer Vision Workshops*, 2013, pp. 397–403.
[143] C. Sagonas, G. Tzimiropoulos, S. Zafeiriou, and M. Pantic, "A semi-automatic methodology for facial landmark annotation," in *Proceedings of the IEEE conference on computer vision and pattern recognition workshops*, 2013, pp. 896–903.
[144] J. Ahlberg, "An active model for facial feature tracking," *EURASIP Journal on Advances in Signal Processing*, vol. 2002, no. 6, pp. 1–6, 2002.
[145] N. Ibrahim, R. Tomari, W. N. W. Zakaria, and N. Othman, "Non-contact heart rate monitoring analysis from various distances with different face regions," *International Journal of Electrical and Computer Engineering*, vol. 7, no. 6, p. 3030, 2017.
[146] N. Ibrahim, R. Tomari, W. N. W. Zakaria, and N. Othman, "Analysis of Non-invasive Video Based Heart Rate Monitoring System obtained from Various Distances and Different Facial Spot," in *Journal of Physics: Conference Series*, 2018, vol. 1049, no. 1, p. 012003.
[147] Z. Yu, X. Li, and G. Zhao, "Remote photoplethysmograph signal measurement from facial videos using spatio-temporal networks," *arXiv preprint arXiv:1905.02419*, 2019.
[148] A. Bulat and G. Tzimiropoulos, "How far are we from solving the 2d & 3d face alignment problem?(and a dataset of 230,000 3d facial landmarks)," in *Proceedings of the IEEE International Conference on Computer Vision*, 2017, pp. 1021–1030.
[149] L. A. Jeni, J. F. Cohn, and T. Kanade, "Dense 3D face alignment from 2D videos in real-time," in *2015 11th IEEE international conference and workshops on automatic face and gesture recognition (FG)*, 2015, vol. 1, pp. 1–8.
[150] J. Shen, S. Zafeiriou, G. G. Chrysos, J. Kossaifi, G. Tzimiropoulos, and M. Pantic, "The first facial landmark tracking in-the-wild challenge: Benchmark and results," in *Proceedings of the IEEE international conference on computer vision workshops*, 2015, pp. 50–58.
[151] S. Zafeiriou, G. G. Chrysos, A. Roussos, E. Ververas, J. Deng, and G. Trigeorgis, "The 3D Menpo Facial Landmark Tracking Challenge," Oct. 2017.

[152] A. Zadeh, Y. Chong Lim, T. Baltrusaitis, and L.-P. Morency, "Convolutional experts constrained local model for 3d facial landmark detection," in *Proceedings of the IEEE International Conference on Computer Vision Workshops*, 2017, pp. 2519–2528.
[153] V. Blanz and T. Vetter, "A morphable model for the synthesis of 3D faces," in *Proceedings of the 26th annual conference on Computer graphics and interactive techniques*, 1999, pp. 187–194.
[154] Y. Kartynnik, A. Ablavatski, I. Grishchenko, and M. Grundmann, "Real-time facial surface geometry from monocular video on mobile gpus," *arXiv preprint arXiv:1907.06724*, 2019.
[155] Y. Gerhana, W. Zulfikar, A. Ramdani, and M. A. Ramdhani, "Implementation of Nearest Neighbor using HSV to Identify Skin Disease," in *IOP Conference Series: Materials Science and Engineering*, 2018, vol. 288, no. 1, p. 012153.
[156] B. Muhammad and S. A. R. Abu-Bakar, "A hybrid skin color detection using HSV and YCgCr color space for face detection," in *2015 IEEE International Conference on Signal and Image Processing Applications (ICSIPA)*, 2015, pp. 95–98.
[157] S. Roy and S. K. Bandyophadyay, "Face detection using a hybrid approach that combines HSV and RGB," *International Journal of Computer Science and Mobile Computing*, vol. 2, no. 3, pp. 127–136, 2013.
[158] C. Gelinas, C. Arbour, C. Michaud, L. Robar, and J. Côté, "Patients and ICU nurses' perspectives of non-pharmacological interventions for pain management," *Nursing in critical care*, vol. 18, no. 6, pp. 307–318, 2013.
[159] A. Malliani, M. Pagani, F. Lombardi, and S. Cerutti, "Cardiovascular neural regulation explored in the frequency domain.," *Circulation*, vol. 84, no. 2, pp. 482–492, 1991.
[160] C. Horton, R. Srinivasan, and M. D'Zmura, "Envelope responses in single-trial EEG indicate attended speaker in a 'cocktail party,'" *Journal of neural engineering*, vol. 11, no. 4, p. 046015, 2014.
[161] J. Kropotov, "Alpha Rhythms. Functional neuromarkers for psychiatry," *Appl Diagnosis Treatment*, vol. 2016, pp. 89–105, 2016.
[162] M. S. Lee, B. H. Bae, H. Ryu, J.-H. Sohn, S. Y. Kim, and H.-T. Chung, "Changes in alpha wave and state anxiety during ChunDoSunBup Qi-training in trainees with open eyes," *The American journal of Chinese medicine*, vol. 25, no. 03n04, pp. 289–299, 1997.
[163] J. Lagopoulos *et al.*, "Increased theta and alpha EEG activity during nondirective meditation," *The Journal of Alternative and Complementary Medicine*, vol. 15, no. 11, pp. 1187–1192, 2009.
[164] R. Hebert, D. Lehmann, G. Tan, F. Travis, and A. Arenander, "Enhanced EEG alpha time-domain phase synchrony during Transcendental Meditation: Implications for cortical integration theory," *Signal Processing*, vol. 85, no. 11, pp. 2213–2232, 2005.
[165] M. Vaghefi, A. M. Nasrabadi, S. M. R. H. Golpayegani, M.-R. Mohammadi, and S. Gharibzadeh, "Spirituality and brain waves," *Journal of medical engineering & technology*, vol. 39, no. 2, pp. 153–158, 2015.
[166] M. Gola, M. Magnuski, I. Szumska, and A. Wróbel, "EEG beta band activity is related to attention and attentional deficits in the visual performance of elderly

subjects," *International Journal of Psychophysiology*, vol. 89, no. 3, pp. 334–341, 2013.
[167] L. M. Ward, "Synchronous neural oscillations and cognitive processes," *Trends in cognitive sciences*, vol. 7, no. 12, pp. 553–559, 2003.
[168] L. Aftanas, A. Varlamov, S. Pavlov, V. Makhnev, and N. Reva, "Event-related synchronization and desynchronization during affective processing: emergence of valence-related time-dependent hemispheric asymmetries in theta and upper alpha band," *International journal of Neuroscience*, vol. 110, no. 3–4, pp. 197–219, 2001.
[169] L. Aftanas, A. Varlamov, S. Pavlov, V. Makhnev, and N. Reva, "Affective picture processing: event-related synchronization within individually defined human theta band is modulated by valence dimension.," *Neuroscience letters*, vol. 303, no. 2, pp. 115–118, 2001.
[170] V. Nguyen, A. Q. Javaid, and M. A. Weitnauer, "Spectrum-averaged Harmonic Path (SHAPA) algorithm for non-contact vital sign monitoring with ultra-wideband (UWB) radar," in *2014 36th Annual International Conference of the IEEE Engineering in Medicine and Biology Society*, 2014, pp. 2241–2244.
[171] N. Singh and A. B. Raj, "Estimation of Heart Rate and Respiratory Rate using Imaging Photoplethysmography Technique," in *2020 International Conference on System, Computation, Automation and Networking (ICSCAN)*, 2020, pp. 1–5.
[172] D. S. Seidman *et al.*, "A prospective randomized controlled study of phototherapy using blue and blue-green light-emitting devices, and conventional halogen-quartz phototherapy," *Journal of perinatology*, vol. 23, no. 2, pp. 123–127, 2003.
[173] W. R. McCluney, *Introduction to radiometry and photometry*. Artech House, 2014.
[174] W. Verkruysse, L. O. Svaasand, and J. S. Nelson, "Remote plethysmographic imaging using ambient light.," *Optics express*, vol. 16, no. 26, pp. 21434–21445, 2008.
[175] A. Saeed, A. Al-Hamadi, and A. Ghoneim, "Head pose estimation on top of haar-like face detection: A study using the kinect sensor," *Sensors*, vol. 15, no. 9, pp. 20945–20966, 2015.
[176] B. V. Thiyagarajan, "Face Detection and Facial Feature Points' Detection with the help of KLT Algorithm," *IJARCSMS*, vol. 2, no. 8, 2014.
[177] Q.-V. Tran, S.-F. Su, C.-C. Chuang, V.-T. Nguyen, and N.-Q. Nguyen, "Real-time non-contact breath detection from video using adaboost and Lucas-Kanade algorithm," in *2017 Joint 17th World Congress of International Fuzzy Systems Association and 9th International Conference on Soft Computing and Intelligent Systems (IFSA-SCIS)*, 2017, pp. 1–4.
[178] "Facemesh." https://cdn.jsdelivr.net/npm/@tensorflow-models/Facemesh
[179] "Face landmarks detection with MediaPipe Facemesh." https://towardsdatascience.com/face-landmarks-detection-with-mediapipe-facemesh-555fa2e10b06
[180] J. Zhao, M. Zhang, C. He, and K. Zuo, "Data-driven research on the matching degree of eyes, eyebrows and face shapes," *Frontiers in psychology*, vol. 10, p. 1466, 2019.
[181] T. Baltrušaitis, P. Robinson, and L. Morency, "OpenFace: An open source facial behavior analysis toolkit," in *2016 IEEE Winter Conference on Applications of Computer Vision (WACV)*, Mar. 2016, pp. 1–10. doi: 10.1109/WACV.2016.7477553.

[182] A. Sarsenov and K. Latuta, “Face Recognition Based on Facial Landmarks,” in *2017 IEEE 11th International Conference on Application of Information and Communication Technologies (AICT)*, pp. 1–5.
[183] Z. Deng, K. Li, Q. Zhao, and H. Chen, “Face landmark localization using a single deep network,” in *Chinese Conference on Biometric Recognition*, pp. 68–76.
[184] V. Le, J. Brandt, Z. Lin, L. Bourdev, and T. S. Huang, “Interactive facial feature localization,” in *European conference on computer vision*, pp. 679–692.
[185] S. Al-Maadeed, S. F. Peer, and N. Subramanian, “Data Collection and Image Processing System for Ancient Arabic Manuscripts,” in *2018 IEEE 2nd International Workshop on Arabic and Derived Script Analysis and Recognition (ASAR)*, pp. 124–128.
[186] “dlib library.” http://dlib.net/files/shape_predictor_68_face_landmarks.dat.bz2
[187] “My imutils package: A series of OpenCV convenience functions - PyImageSearch.” https://www.pyimagesearch.com/2015/02/02/just-open-sourced-personal-imutils-package-series-opencv-convenience-functions/ (accessed Aug. 27, 2019).
[188] “imutils/imutils at master · jrosebr1/imutils · GitHub.” https://github.com/jrosebr1/imutils/tree/master/imutils (accessed Aug. 20, 2019).
[189] C. Wang, T. Pun, and G. Chanel, “A comparative survey of methods for remote heart rate detection from frontal face videos,” *Frontiers in bioengineering and biotechnology*, vol. 6, p. 33, 2018.
[190] N. Wang, X. Gao, D. Tao, H. Yang, and X. Li, “Facial feature point detection: A comprehensive survey,” *Neurocomputing*, vol. 275, pp. 50–65, Jan. 2018, doi: 10.1016/j.neucom.2017.05.013.
[191] “Dlib 68 points Face landmark Detection with OpenCV and Python.” https://www.studytonight.com/post/dlib-68-points-face-landmark-detection-with-opencv-and-python
[192] G. Lorenzi-Filho, H. R. DAJANI, R. S. Leung, J. S. Floras, and T. D. Bradley, “Entrainment of blood pressure and heart rate oscillations by periodic breathing,” *American journal of respiratory and critical care medicine*, vol. 159, no. 4, pp. 1147–1154, 1999.
[193] J. M. Bland and D. G. Altman, “Agreement between methods of measurement with multiple observations per individual,” *Journal of biopharmaceutical statistics*, vol. 17, no. 4, pp. 571–582, 2007.
[194] J. M. Bland and D. Altman, “Statistical methods for assessing agreement between two methods of clinical measurement,” *The lancet*, vol. 327, no. 8476, pp. 307–310, 1986.

VITA

Student Name: Dibyajyoti Biswal

Educational Institutions: August 2013 - August 2015 National Institute of Technology (NIT), Rourkela, Odisha, India, Master of Technology in Biomedical Engineering

Professional Positions:

November 2021 - Present, Principal Engineer, Machine Intelligence, Oshkosh Corporation

February 2021 - October 2021, R & D Machine Learning Scientist, Eurofins Professional Solutions Services (PSS), Eurofins Lancaster Laboratories

August 2016 - May 2021, Research Assistant, Department of Biomedical Engineering, University of Kentucky

August 2018 - December 2020, Teaching Assistant, FYE (first year engineering), College of Engineering, University of Kentucky

Journal Papers:

MJ Mollakazemi, **D Biswal**, S Sunderam, A Patwardhan, "EEG segments synchronized to be temporally farthest from the R-waves in ECG are more informative during listening to music", *Biomedical Signal Processing and Control*

MJ Mollakazemi, **D Biswal**, SC Elayi, S Thyagarajan, J Evans, A Patwardhan, "Synchronization of Autonomic and Cerebral Rhythms During Listening to Music: Effects of Tempo and Cognition of Songs", *Journal of Physiological Research*

Scholastic and Professional Honors:

2018 University of Kentucky, Graduate School, Max Steckler Fellowship 2018 University of Kentucky,

Office of International Affairs, International Student Tuition Scholarship 2019 University of Kentucky